NASA Contractor Report 189041

Traction Free Finite Elements With the Assumed Stress Hybrid Model

K. Kafie
Massachusetts Institute of Technology
Cambridge, Massachusetts

November 1991

Prepared for
Lewis Research Center
Under Grant NAG3–33

NASA
National Aeronautics and
Space Administration

TRACTION FREE FINITE ELEMENTS

WITH THE ASSUMED STRESS HYBRID MODEL

by

Kurosh Kafie
Massachusetts Institute of Technology
Cambridge, Massachusetts 02139

ABSTRACT

An effective approach in finite element analysis of the stress field at the traction free boundary of a solid continuum was studied. Conventional displacement and Assumed Stress Hybrid finite elements were used in determination of stress concentrations around circular and elliptical holes. Specialized Hybrid elements were then developed to improve satisfaction of prescribed traction boundary conditions. Results of the stress analysis indicated that finite elements which exactly satisfy the free stress boundary conditions are most accurate and efficient in such problems. A general approach for Hybrid finite elements which incorporate traction free boundaries of arbitrary geometry was formulated.

TABLE OF CONTENTS

PAGE

CHAPTER 1

Introduction

The "Finite Element Method" has proven to be an effective and convenient approach to solution of problems of continuum mechanics. Originally conceptualized in the 1950s as a tool in solving problems of elasticity and structural mechanics [1], the finite element method has been increasingly used in many different fields of engineering, applied mathematics, and physics. Rigorous mathematical formulation of the method based on different variational principles has afforded scientists greater flexibilities in the selection of the problem, formulation of the solution, and implementation of the method. Today finite elements are used in problems of heat transfer and fluit flow, as well as the traditional structural mechanics for which they were developed.

The well known assumed displacement approach, based on the principle of minimum potential energy [2], [3] is widely used in finite element formulations of structural mechanics. Although a successful method in many applications, inherent drawbacks of the formulation do exist. In the assumed displacement formulation the requirement of displacement compatibility is identically satisfied throughout the element, by selection of an appropriate set of displacement interpolations. This selection process is not always guaranteed and in fact has posed difficulties in construction of conventional plate bending elements. In the displacement model, equilibrium of applied forces and the resultant stresses is in general not satisfied except in the limiting case where

more and more degrees of freedom are used in modeling the structure until monotonic convergence is achieved with compatible elements. Since in the assumed displacement formulation stresses are obtained by differentiation of the displacements, any error of the displacement solution is amplified in this process and will hence introduce distortion or noise in the stress or strain solution. It is for this reason that when stress concentrations exist in the vicinity of structural discontinuities or supports, a finer mesh of elements is always used. The compatible assumed displacement approach will in principle underestimate the displacement solution by overestimating the stiffness of the structure.

On the other hand, finite elements can be formulated based on the principle of minimum complementary energy [3]. In this approach the stresses satisfy the equilibrium conditions and become the unknown variables directly solved for. In principle the minimum complementary energy formulation will overestimate the displacement solution by underestimating the structural stiffness. Since the condition of displacement continuity along interelement boundaries is not satisfied, the formulation will generate incompatible finite elements.

As introduced by Pian [4][5], the assumed stress hybrid formulation relaxes displacement interpolation requirements critical to the assumed displacement model, while assuring the interelement compatibility condition not achieved by the equilibrium model. Rigorously formulated by Tong and Pian [6], the hybrid model is based on a modified complementary energy principle in which stresses are the variables

directly solved for.

1.1 Objective

For an accurate estimation of the stress field at the streee free boundary of a solid continuum, it is desirable to choose finite elements that satisfy the prescribed stress boundary conditions. For such problems, hybrid stress formulation becomes a more logical alternative because requirements of stress equilibrium and free boundary traction can be simultaneously satisfied.

To assess the effectiveness of assumed stress hybrid elements under prescribed free traction conditions, stress concentrations around circular and elliptical holes subjected to unidirectional tension were examined. For the purpose of this investigation, three distinct hybrid elements are studied. The first study examines the effectiveness of regular isoparametric hybrid elements that do not meet the condition of free boundary traction. The performance of these elements are then judged against conventional displacement based isoparametric elements with regard to solution accuracy and efficiency. Next a second class of hybrid elements that approximately satisfy the prescribed free-traction boundary condition, via the boundary point matching technique, is considered. Finally, the advantage of using hybrid elements that identically satisfy the traction-free boundary condition is examined in the special case of a circular boundary. In each case finite element stress solutions are obtained for a comparative study against the analytical solution. A general formulation for assumed stress hybrid

finite elements that incorporate a traction-free boundary of arbitrary geometry is presented.

CHAPTER 2

The Assumed Stress Hybrid Element

Formulation of the assumed stress hybrid element is in general based on either the stationary value of the modified complementary energy π_{MC}, or of the Hellinger-Reissner principle π_R [3]. It can be shown that for a given set of assumed stresses these formulations produce identical results [5]. Thus depending on the problem at hand, ease of implementation or economical considerations may prove one formulation advantageous to the other.

2.1 The Modified Complementary Energy Principle

In the modified complementary energy principle, stationary value of the functional π_{MC} is established [3];

$$\pi_{MC} = \sum_{n} \left\{ \frac{1}{2} \int_{V_n} \underset{\sim}{\sigma}^T \underset{\sim}{S}\, \underset{\sim}{\sigma}\, dV - \int_{\partial V_n} \underset{\sim}{T}^T \underset{\sim}{u}\, dS + \int_{S_{\sigma_n}} \underset{\sim}{\bar{T}}^T \underset{\sim}{u}\, dS \right\} \tag{2.1}$$

where:

$n \equiv$ Number of elements.

$V_n \equiv$ Spatial domain of element n.

$\partial V_n \equiv$ Boundary of V_n.

$S_\sigma \equiv$ Portion of ∂V_n where tractions are prescribed.

$\underset{\sim}{\sigma} \equiv$ Self equilibrating stresses.

$\underset{\sim}{S} \equiv$ Compliance matrix.

$\underset{\sim}{T} \equiv$ Traction matrix.

$\underset{\sim}{u}$ ≡ Displacement matrix.

$\underset{\sim}{\bar{T}}$ ≡ Prescribed tractions.

Although in the general formulation body forces are also accounted for, their presence is intentionally neglected in equation (2.1). The existence of body forces will be considered in the Reissner formulation in a much simpler manner identical to that of the assumed displacement model.

In the Finite Element formulation the stresses $\underset{\sim}{\sigma}$ are assumed over the entire domain, and the displacements $\underset{\sim}{u}$ are interpolated from the nodal values along the boundaries of the element only.

$$\underset{\sim}{\sigma} = \underset{\sim}{P}\underset{\sim}{\beta} \tag{2.2}$$

$$\underset{\sim}{u} = \underset{\sim}{L}\underset{\sim}{q} \tag{2.3}$$

where:

$\underset{\sim}{P}$ ≡ Matrix of assumed polynomials.

$\underset{\sim}{\beta}$ ≡ Undetermined coefficients.

$\underset{\sim}{L}$ ≡ Interpolation functions.

$\underset{\sim}{q}$ ≡ Nodal displacements.

In Equation (2.1) the product of the traction vector $\underset{\sim}{T}$ and the displacement vector $\underset{\sim}{u}$ is integrated along the boundary of the element. On any

boundary the traction vector can be determined directly from the assumed stresses $\underset{\sim}{\sigma}$;

$$\underset{\sim}{T} = \underset{\sim}{\nu}^T \underset{\sim}{\sigma} = \underset{\sim}{\nu}^T \underset{\sim}{P} \underset{\sim}{\beta} \tag{2.4}$$

where:

$\underset{\sim}{\nu}$ ≡ Matrix of direction cosines.

Substitution of equations (2.2), (2.3) and (2.4) into equation (2.1) will discretize the functional π_{MC} :

$$\pi_{MC} = \sum_n \left\{ \frac{1}{2} \underset{\sim}{\beta}^T \int_{V_n} \underset{\sim}{P}^T \underset{\sim}{S} \underset{\sim}{P} \, dV \, \underset{\sim}{\beta} \right. \tag{2.5}$$

$$\left. - \underset{\sim}{\beta}^T \int_{\partial V_n} \underset{\sim}{P}^T \underset{\sim}{\gamma} \underset{\sim}{L} \, dS \, \underset{\sim}{f} + \int_{S_{\sigma_n}} \underset{\sim}{\bar{T}}^T \underset{\sim}{L} \, dS \, \underset{\sim}{f} \right\}$$

Redefining the integrals of equation (2.5);

$$\underset{\sim}{H} = \int_{V_n} \underset{\sim}{P}^T \underset{\sim}{S} \underset{\sim}{P} \, dV \tag{2.6}$$

$$\underset{\sim}{G} = \int_{\partial V_n} \underset{\sim}{P}^T \underset{\sim}{\gamma} \underset{\sim}{L} \, dS \tag{2.7}$$

$$Q^T = \int_{S_{\sigma_n}} \underset{\sim}{T}^T \underset{\sim}{L} \, dS$$

$$\pi_{MC} = \sum_n \left\{ \frac{1}{2} \underset{\sim}{\beta}^T \underset{\sim}{H} \underset{\sim}{\beta} - \underset{\sim}{\beta}^T \underset{\sim}{G} \underset{\sim}{f} + \underset{\sim}{Q}^T \underset{\sim}{f} \right\} \tag{2.8}$$

2.2 The Hellinger-Reissner Principle

Assuming satisfaction of displacement boundary conditions, the Hellinger-Reissner principle requires the stationary value of the functional π_R [3];

$$\pi_R = \sum_n \left\{ -\int_{V_n} \left[\underset{\sim}{\sigma}^T \underset{\sim}{S} \underset{\sim}{\sigma} - \underset{\sim}{\sigma}^T (\underset{\sim}{D}\,\underset{\sim}{u}) + \underset{\sim}{f}^T \underset{\sim}{u} \right] dV - \int_{S_{\sigma_n}} \underset{\sim}{T}^T \underset{\sim}{u}\, dS \right\} \quad (2.9)$$

where $\underset{\sim}{f}$ is now the matrix of prescribed body forces. Here the integration of the stresses is performed in the spatial domain and matrices $\underset{\sim}{\sigma}$ and $\underset{\sim}{S}$ are identical to those defined for equation (2.1). The essential difference between the π_R and π_{MC} approach is in the interpolation of displacements. Where in the π_{MC} approach displacements are interpolated only along the boundaries (2.3), in the π_R formulation they are interpolated over the entire domain;

$$\underset{\sim}{u} = \underset{\sim}{A}\,\underset{\sim}{q} \quad (2.10)$$

and matrix $\underset{\sim}{D}$ is a differential operator which by operating on the displacements gives the strain matrix;

$$\underset{\sim}{D}\,\underset{\sim}{u} = \underset{\sim}{\epsilon} = \underset{\sim}{D}(\underset{\sim}{A}\,\underset{\sim}{q}) = \underset{\sim}{B}\,\underset{\sim}{q} \quad (2.11)$$

Substitution of equations (2.2) and (2.11) into equation (2.9) will discretize the functional π_R ;

$$\pi_R = \sum_n \left\{ -\frac{1}{2} \underset{\sim}{\beta}^T \int_{V_n} \underset{\sim}{P}^T \underset{\sim}{S} \underset{\sim}{P} \, dV \, \underset{\sim}{\beta} + \underset{\sim}{\beta}^T \int_{V_n} \underset{\sim}{P}^T \underset{\sim}{B} \, dV \, \underset{\sim}{q} \right.$$

$$\left. - \int_{V_n} \underset{\sim}{f}^T \underset{\sim}{A} \, dV \, \underset{\sim}{q} - \int_{S_{\sigma_n}} \underset{\sim}{\bar{T}}^T \underset{\sim}{A} \, dS \, \underset{\sim}{q} \right\} \tag{2.12}$$

Redefining the last three integrals of equation (2.12)

$$\underset{\sim}{G} = \int_{V_n} \underset{\sim}{P}^T \underset{\sim}{B} \, dV \tag{2.13}$$

$$\underset{\sim}{Q}^T = \int_{V_n} \underset{\sim}{f}^T \underset{\sim}{A} \, dV - \int_{S_{\sigma_n}} \underset{\sim}{\bar{T}}^T \underset{\sim}{A} \, dS$$

$$\pi_R = \sum_n \left\{ -\frac{1}{2} \underset{\sim}{\beta}^T \underset{\sim}{H} \underset{\sim}{\beta} + \underset{\sim}{\beta}^T \underset{\sim}{G} \underset{\sim}{q} - \underset{\sim}{Q}^T \underset{\sim}{q} \right\} \tag{2.14}$$

Hence equivalence of the two functionals (2.8) and (2.14) is apparent. By virtue of their mathematical equivalence, body forces present in the π_{MC} formulation can be accounted for in matrix $\underset{\sim}{Q}$, exactly analogous to that of the π_R formulation [5].

2.3 Solution of the Discretized Equations

In both the modified complementary Energy and the Hellinger-Reissner formulation, the functional was seen to reduce to the form;

$$\pi_H = \sum_n \left\{ \mp \frac{1}{2} \underset{\sim}{\beta}^T \underset{\sim}{H} \underset{\sim}{\beta} \mp \underset{\sim}{\beta}^T \underset{\sim}{G} \underset{\sim}{q} \pm \underset{\sim}{Q}^T \underset{\sim}{q} \right\} \tag{2.15}$$

The functional has to assume a stationary value with respect to the independent variable ;

$$\frac{\partial \pi_H}{\partial \underset{\sim}{\beta}} = 0$$

$$\underset{\sim}{\beta} = \underset{\sim}{H}^{-1} \underset{\sim}{G}\, \underset{\sim}{q} \tag{2.16}$$

Substitution of equation (2.16) into (2.15) gives;

$$\pi_H = \sum_n \left\{ \mp \frac{1}{2} \underset{\sim}{q}^T (\underset{\sim}{G}^T \underset{\sim}{H}^{-1} \underset{\sim}{G}) \pm \underset{\sim}{Q}^T \underset{\sim}{q} \right\}$$

Variation of π_H with respect to $\underset{\sim}{q}$ gives;

$$(\underset{\sim}{G}^T \underset{\sim}{H}^{-1} \underset{\sim}{G})\, \underset{\sim}{q} = \underset{\sim}{Q}^T \tag{2.17}$$

Comparison of equation (2.17) with the familiar assumed displacement results;

$$\underset{\sim}{k}\, \underset{\sim}{q} = \underset{\sim}{Q}^T$$

establishes the equivalent stiffness matrix obtained by the Assumed Stress Hybrid method

$$\underset{\sim}{k} = \underset{\sim}{G}^T \underset{\sim}{H}^{-1} \underset{\sim}{G} \tag{2.18}$$

Matrix $\underset{\sim}{G}$ of the above equation, depending on the formulation used, is defined by either equation (2.7) or equation (2.13).

2.4 Constraint Conditions on the Assumed Stresses

The assumed stresses as defined by equation (2.2) are not entirely arbitrary and have to satisfy some minimum requirements.

1) The assumed stresses have to satisfy the homogeneous equations of equilibrium, that is the equations of equilibrium for no applied forces. In most problems of continuum mechanics the satisfaction of the equilibrium conditions can be achieved by extraction of the stresses from an assumed stress function.

2) Another condition imposed on the assumed stresses is the minimum number of betas required to avoid introduction of spurious energy modes. If N is the number of degrees of freedom present in the element, and M the number of rigid body motions the element can undergo, then at least N-M betas have to be used in the formulation of the stiffness matrix.

2.5 Computation of the Stresses

Stresses can be calculated directly from equation (2.2);

$$\underset{\sim}{\sigma} = \underset{\sim}{P}\,\underset{\sim}{\beta}$$

where $\underset{\sim}{\beta}$ is given by equation (2.16)

$$\underset{\sim}{\beta} = \underset{\sim}{H}^{-1}\underset{\sim}{G}\,\underset{\sim}{q}$$

$$\underset{\sim}{\sigma} = \underset{\sim}{P}\,\underset{\sim}{H}^{-1}\underset{\sim}{G}\,\underset{\sim}{q} \qquad (2.19)$$

The matrix product $\underset{\sim}{H}^{-1}\underset{\sim}{G}$ will be computed during the element stiffness computation (equation 2.18), and can be stored for the stress calculation, after the displacement solution $\underset{\sim}{q}$ is obtained.

2.6 Implementation Considerations

It is evident from equation (2.6) that the size of the matrix $\underset{\sim}{H}$ is directly related to the number of betas used in the assumed stress matrix; for example, the size of matrix $\underset{\sim}{H}$ will be n x n if n betas are utilized. Since matrix $\underset{\sim}{H}$ has to be inverted (equation 2.18) for the determination of the element stiffness matrix, it is desirable to keep the number of betas to a minimum for computational efficiency. However, when polynomials are used in the expression of the assumed stresses, a complete polynomial is in general more desirable than an incomplete expression randomly truncated for efficiency sake. This is due to the fact that a complete polynomial will render an invariant element stiffness matrix, while an incomplete polynomial will obviously affect the element stiffness matrix based on its orientation relative to the Global system of coordinates. This problem is of course alleviated if a local system of coordinates is used for the stiffness computation,

although a transformation of the stiffness matrix from the local to the global system of coordinates would then be necessary. In plane elasticity problems it is possible to impose further restrictions on the assumed stresses so that they also satisfy the compatibility conditions throughout the element [7]. The constraints reduce the number of betas used in a set of complete polynomials and maintain element invariance at the same time. This approach is also deemed desirable since the element will then satisfy both the condition of stress equilibrium and compatibility, but is in general not easily applicable especially in three dimensional solid elements.

The difference between π_{HC} and π_R based hybrid element amounts to the difference in the computation of the matrix $\underset{\sim}{G}$ (equation 2.7 and 2.13). Since equations (2.7) and (2.13) are in general integrated numerically, it would appear that the π_R model would be more efficient since the integration is only performed around the boundaries of the element. However, the comparison also requires an investigation of the order of terms being integrated. In the π_R formulation the matrix $\underset{\sim}{\beta}$ (equation 2.13) is obtained by differentiating the displacements (equation 2.11) and therefore the product $\underset{\sim}{P}^T\underset{\sim}{\beta}$ is lower in order than the product $\underset{\sim}{P}^T\underset{\sim}{\gamma}\underset{\sim}{L}$ for the same matrix $\underset{\sim}{P}$. The most efficient approach will thus depend on the number of degrees of freedom of the element and the highest order of powers appearing in the assumed stresses. Another consideration may arise from the construction of the matrix of direction cosines $\underset{\sim}{\gamma}$. In some general three dimensional elements with

boundaries of arbitrary geometry it may be very difficult to establish $\underset{\sim}{\gamma}$ while this problem is nonexistent in the π_R formulation.

Finally, it should be noted that the only rigorous requirement on the displacement interpolation matrix $\underset{\sim}{A}$ of equation (2.10) is that it reduce to the proper interpolation of the displacements along the boundaries of the element, and is otherwise arbitrary. This could somewhat relax the determination of the interpolation functions for an element with uneven distribution of nodes.

CHAPTER 3

Example Problem

To determine the performance of Assumed Stress Hybrid finite elements a plate of finite width with a circular or elliptical hole is analyzed. The plate is subjected to uniaxial tension and hence a condition of stress concentration is developed at the hole, across from the center of the hole directly perpendicular to the direction of the applied load. Analytically obtained values of the stress concentration factor are known from the plane elasticity solutions with both circular and elliptical holes [8].

Figure 1 shows the dimensions of the plate with a circular hole subjected to tensile stress p_o . A stress concentration factor of 4.32 exists at points A and B on the circular hole. Figure 2 shows the dimensions of the plate with the elliptical hole subjected to the same tensile stress p_o . For this configuration a stress concentration factor of 9.50 is present at points A and B shown on the ellipse. The length of the plates compared to the dimensions of the holes were judged long enough to simulate a uniform tensile pressure acting at infinity.

The two dimensional continuum nature of the problem selected for analysis is important since the results will have a direct bearing on similar analyses done with three dimensional continuum elements. The solid three dimensional continuum element can in fact be regarded as a natural extension of its two dimensional continuum counterpart.

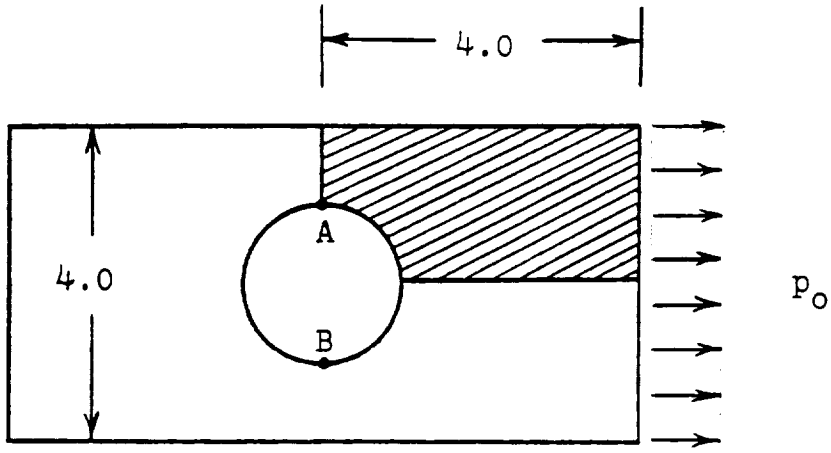

Circle; $x^2+y^2=1.0$

Figure-1 Plate With A Circular Hole

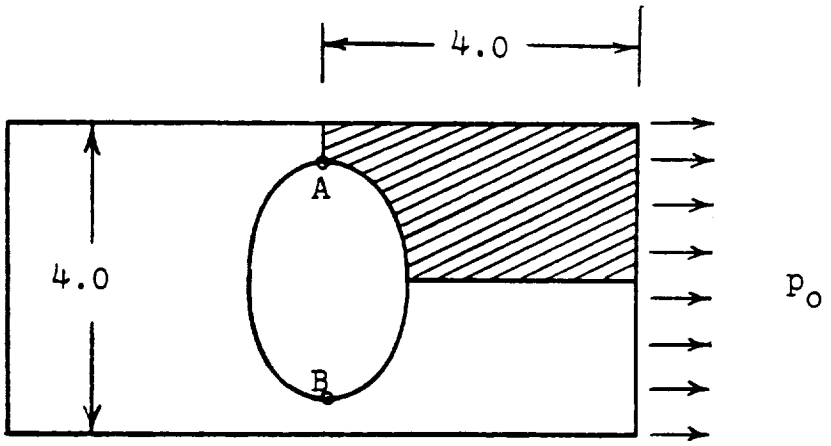

Ellipse; $x^2+(\frac{y}{1.5})^2=1.0$

Figure-2 Plate With An Elliptical Hole

Due to the symmetric nature of the problem only a quarter of the plates were used for analysis, namely the shaded regions of Figures 1 and 2. On the boundaries where the plates were artificially cut, zero displacements were prescribed in directions perpendicular to each respective boundary.

For the finite Element Analysis of the plates, the coarse mesh of Figure 3, labelled Mesh-1, was first used. In Mesh-1 the hole is divided into two sections by a line from the center of either the circle or the ellipse intersecting at 45 degrees. Stresses were computed at locations A shown in Figures 3a and 3b, and were compared against the expected results. It should be noted that Mesh-1 incorporates a total of three elements and in general is not expected to render accurate results.

A finer mesh can be obtained by subdividing Mesh-1. This is achieved by connecting the mid-boundaries of all the elements in Mesh-1, which in effect replaces each element with four subelements. This mesh is labelled Mesh-2 and is shown in Figure 4. Mesh-2 incorporates a total of twelve elements and should in principle yield a better solution compared to Mesh-1.

The Finite Element Analysis Basic Library (FEABL) of the Aeroelastic and Structures Research Laboratory of the Massachusetts Institute of Technology [9] was used for assemblage of the elements and solution of the equations.

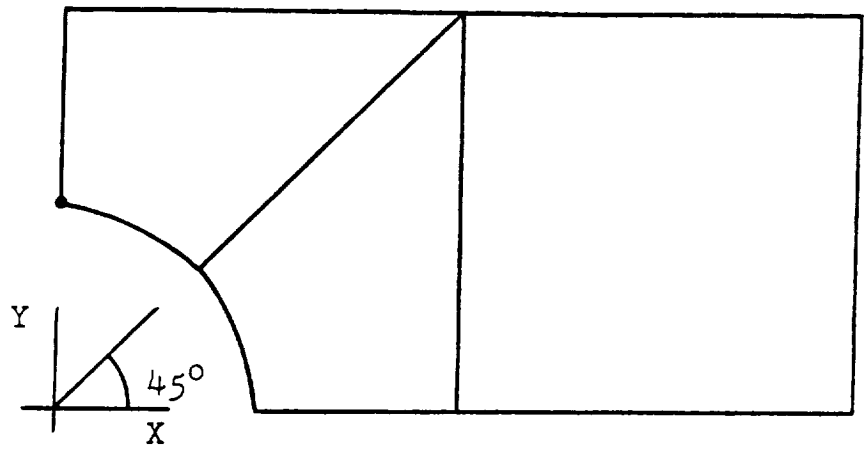

Figure-3a Mesh-1 ; Quarter Plate With Circular Hole

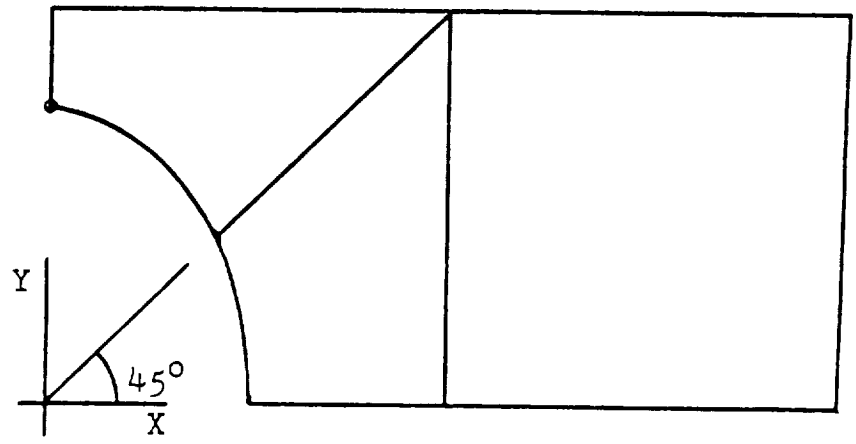

Figure-3b Mesh-1 ; Quarter Plate With Elliptical Hole

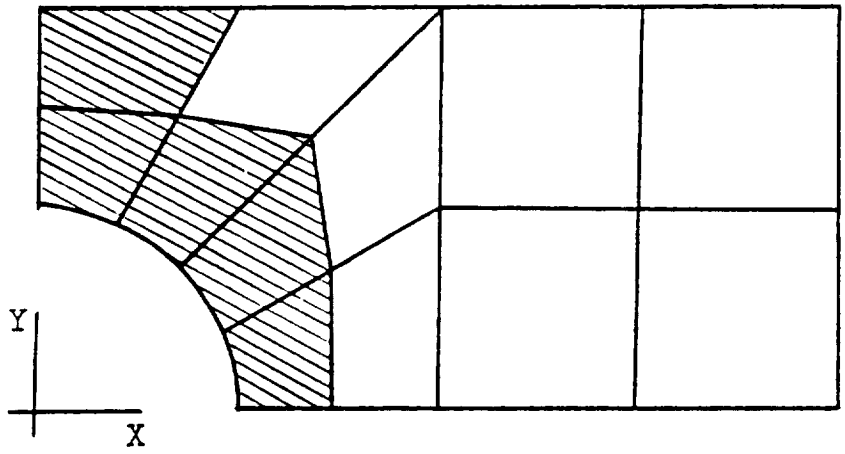

Figure-4a Mesh-2 ; Quarter Plate With Circular Hole

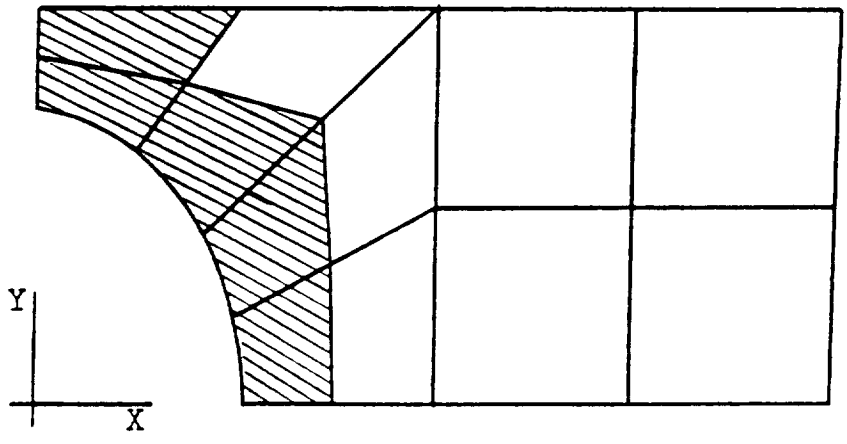

Figure-4b Mesh-2 ; Quarter Plate With Elliptical Hole

CHAPTER 4

A 4-8 Variable Node Hybrid Isoparametric Quadrilateral Element

4.1 Objective

The displacement based eight node isoparametric element has proven very effective in two dimensional continuum problems such as plane stress or plane strain. The availability of the eight node plane element in most of today's advanced Finite Element Library codes confirms its extensive acceptability. To this end it is therefore logical that for analysis of the problems described in Chapter 3, with Finite Element codes utilized by the industry, the eight node displacement based element would be the effective option.

Development of an eight node hybrid isoparametric element will provide a rational alternative for comparison against the eight node displacement based element. The Hybrid Isoparametric Quadrilateral element developed (called HISQUE) is formulated such that any number of the mid-nodes can be removed. The number of stress terms (i.e., the number of betas) programmed in the element is also user defined as an added flexibility for an optimum selection based on the number of nodes employed. The element HISQUE can employ up to a complete cubic set of assumed stresses in the XY plane.

4.2 Formulation of Element HISQUE

4.2.1 The Assumed Stresses

Element HISQUE is formulated based on the Hellinger-Reissner principle:

$$\underset{\sim}{H} = \int_{V_n} \underset{\sim}{P}^T \underset{\sim}{S} \underset{\sim}{P} \, dV \tag{2.6}$$

$$\underset{\sim}{G} = \int_{V_n} \underset{\sim}{P}^T \underset{\sim}{\beta} \, dV \tag{2.13}$$

The matrix of assumed stresses is defined:

$$\underset{\sim}{\sigma} = \begin{Bmatrix} \sigma_{xx} \\ \sigma_{yy} \\ \sigma_{xy} \end{Bmatrix} \tag{4.1}$$

and can be determined from the Airy stress function

$$\sigma_{xx} = \frac{\partial^2 \phi}{\partial y^2} \tag{4.2a}$$

$$\sigma_{yy} = \frac{\partial^2 \phi}{\partial x^2} \tag{4.2b}$$

$$\sigma_{xy} = -\frac{\partial^2 \phi}{\partial x \partial y} \tag{4.2c}$$

As defined by equations (4.2), the stresses obtained will satisfy the homogeneous equations of equilibrium in Cartesian coordinates:

$$\frac{\partial \sigma_{xy}}{\partial x} + \frac{\partial \sigma_{yy}}{\partial y} = 0$$

$$\frac{\partial \sigma_{xx}}{\partial x} + \frac{\partial \sigma_{xy}}{\partial y} = 0$$

If an infinite series of polynomials in ascending powers of x and y is used for the stress function ϕ, where the individual terms of the series are weighted by arbitrary constants α_i:

$$\phi = \alpha_0 + \alpha_1 x + \alpha_2 y + \alpha_3 x^2 + \alpha_4 xy + \alpha_5 y^2 + \ldots \qquad (4.3)$$

then substitution of equation (4.3) into equations (4.2) will determine the stress vector (4.1). The coefficients α_i are then renamed β_j such that β_1 corresponds to the lowest coefficient α_i appearing in the series. Since the element HISQUE can have a maximum number of eight nodes with two degrees of freedom at each node, and also since the element can undergo three rigid body motions, it follows that a minimum of 13 terms are required in the assumed stresses (Chapter 2). The stresses obtained from the Airy stress function (4.3),

$$\begin{aligned}\sigma_{xx} = {} & \beta_1 + y\beta_4 + x\beta_6 + y^2\beta_8 + x^2\beta_{10} \qquad (4.4a)\\ & + 2xy\beta_{11} + y^3\beta_{13} + x^3\beta_{15} + xy^2\beta_{16}\\ & + x^2y\beta_{17} + \ldots\end{aligned}$$

$$\sigma_{yy} = \beta_2 + x\beta_5 + y\beta_7 + x^2\beta_9 + y^2\beta_{10} + 2xy\beta_{12} + x^3\beta_{14} + 3xy^2\beta_{15} + \frac{y^3}{3}\beta_{17} + x^2y\beta_{18} + \cdots \tag{4.4b}$$

$$\sigma_{xy} = \beta_3 - y\beta_6 - x\beta_7 - 2xy\beta_{10} - y^2\beta_{11} - x^2\beta_{12} - 3x^2y\beta_{15} - \frac{y^3}{3}\beta_{16} - xy^2\beta_{17} - \frac{1}{3}x^2\beta_{18} + \cdots \tag{4.4c}$$

or in matrix form,

$$\begin{Bmatrix} \sigma_{xx} \\ \sigma_{yy} \\ \sigma_{xy} \end{Bmatrix} = \begin{bmatrix} & \underset{\sim}{P} & \end{bmatrix} \begin{Bmatrix} \beta_1 \\ \beta_2 \\ \vdots \\ \beta_{18} \end{Bmatrix} \tag{4.4d}$$

From equations (4.4) it is shown that the highest power appearing in the stresses depends on the number of betas retained. As seen in equations (4.4), using eighteen betas will result in a complete cubic expression of the stresses.

4.2.2 The Strain Matrix

The strain matrix $\underset{\sim}{B}$ of equation (2.13) is obtained by the differentiation of the displacements

$$\underset{\sim}{u} = \begin{Bmatrix} u_x \\ u_y \end{Bmatrix} = \underset{\sim}{A}\,\underset{\sim}{q} \tag{4.5}$$

$$\underset{\sim}{\epsilon} = \begin{Bmatrix} \epsilon_{xx} \\ \epsilon_{yy} \\ \epsilon_{xy} \end{Bmatrix} = \begin{bmatrix} \partial/\partial x & 0 \\ 0 & \partial/\partial y \\ \partial/\partial y & \partial/\partial x \end{bmatrix} \begin{Bmatrix} u_x \\ u_y \end{Bmatrix} = \underset{\sim}{D}\,\underset{\sim}{u}$$

$$\underset{\sim}{\epsilon} = \underset{\sim}{D}\,\underset{\sim}{A}\,\underset{\sim}{q} = \underset{\sim}{B}\,\underset{\sim}{q} \tag{4.6}$$

The matrix $\underset{\sim}{A}$ of equation (4.5) is the matrix of the interpolation functions. In the isoparametric transformation of the coordinates the following relations hold:

$$x = \sum_i h_i\, x_i \tag{4.7a}$$

$$y = \sum_i h_i\, y_i \tag{4.7b}$$

where:

h_i = Interpolation functions.

(x_i, y_i) = Nodal coordinates.

or in matrix notation:

$$\begin{Bmatrix} x \\ y \end{Bmatrix} = \begin{bmatrix} & \underset{\sim}{H} & \end{bmatrix} \begin{Bmatrix} x_1 \\ y_1 \\ \vdots \\ y_n \end{Bmatrix} \tag{4.7c}$$

Since in the isoparametric transformation the displacements are interpolated identically:

$$u_x = \sum_i h_i u_i$$

$$u_y = \sum_i h_i v_i$$

where u_i and v_i are nodal displacements of node i in x and y directions respectively. It follows directly that matrix $\underset{\sim}{H}$ of equation (4.7c) is identical to matrix $\underset{\sim}{A}$ of equation (4.5).

For the eight node isoparametric element shown in Figure 5, the interpolation functions h_i are [10]:

$$\begin{aligned}
h_1 &= \tfrac{1}{4}(1+\xi)(1+\eta) - \tfrac{1}{2}\delta_5 h_5 - \tfrac{1}{2}\delta_8 h_8 \\
h_2 &= \tfrac{1}{4}(1-\xi)(1+\eta) - \tfrac{1}{2}\delta_5 h_5 - \tfrac{1}{2}\delta_6 h_6 \\
h_3 &= \tfrac{1}{4}(1-\xi)(1-\eta) - \tfrac{1}{2}\delta_6 h_6 - \tfrac{1}{2}\delta_7 h_7 \\
h_4 &= \tfrac{1}{4}(1+\xi)(1-\eta) - \tfrac{1}{2}\delta_7 h_7 - \tfrac{1}{2}\delta_8 h_8 \\
h_5 &= \frac{\delta_5}{2}(1-\xi^2)(1+\eta) \\
h_6 &= \frac{\delta_6}{2}(1-\xi)(1-\eta^2) \\
h_7 &= \frac{\delta_7}{2}(1-\xi^2)(1-\eta) \\
h_8 &= \frac{\delta_8}{2}(1+\xi)(1-\eta^2)
\end{aligned} \tag{4.8}$$

where:

$$\delta_i = \begin{cases} 1 & \text{if node } i \text{ present} \\ 0 & \text{if node } i \text{ absent} \end{cases}$$

By employing the on/off switches δ_i, any combination of the nodes numbered 5, 6, 7 and 8 can be removed (Figure 5) while an appropriate displacement interpolation is preserved.

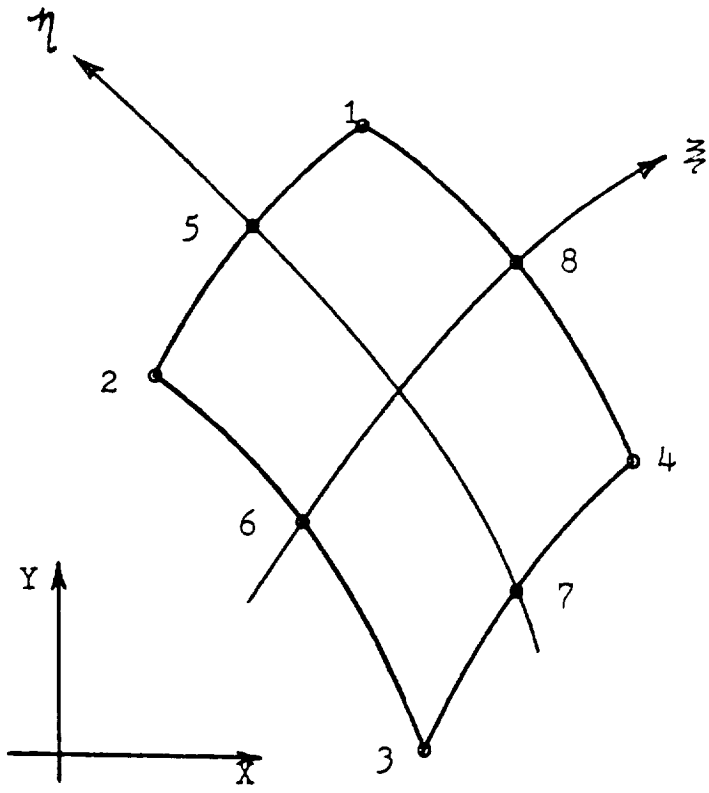

Figure-5 The Nodes Of Element HISQUE

The interpolation functions h_i are functions of ξ and η which in turn means that the displacements as expressed by equation (4.5) are also functions of ξ and η. Derivatives of the displacements with respect to the x, y coordinates can be determined as follows:

$$\frac{\partial u_i}{\partial \xi} = \frac{\partial u_i}{\partial x}\frac{\partial x}{\partial \xi} + \frac{\partial u_i}{\partial y}\frac{\partial y}{\partial \xi}$$

$$\frac{\partial u_i}{\partial \eta} = \frac{\partial u_i}{\partial x}\frac{\partial x}{\partial \eta} + \frac{\partial u_i}{\partial y}\frac{\partial y}{\partial \eta}$$

or,

$$\begin{Bmatrix} \frac{\partial}{\partial \xi} \\ \frac{\partial}{\partial \eta} \end{Bmatrix} u_i = \begin{bmatrix} \underset{\sim}{J} \end{bmatrix} \begin{Bmatrix} \frac{\partial}{\partial x} \\ \frac{\partial}{\partial y} \end{Bmatrix} u_i$$

where $\underset{\sim}{J}$ is the two by two Jacobian matrix, the entries of which can be easily obtained by differentiation of equations (4.7a) and 4.7b).

From equation (4.9) it follows:

$$\begin{Bmatrix} \frac{\partial}{\partial x} \\ \frac{\partial}{\partial y} \end{Bmatrix} u_i = \begin{bmatrix} \underset{\sim}{J} \end{bmatrix}^{-1} \begin{Bmatrix} \frac{\partial}{\partial \xi} \\ \frac{\partial}{\partial \eta} \end{Bmatrix}$$

where:

$$\begin{bmatrix} \underset{\sim}{J} \end{bmatrix}^{-1} = \frac{1}{|\underset{\sim}{J}|} \begin{bmatrix} J_{22} & -J_{12} \\ -J_{12} & J_{11} \end{bmatrix}$$

The $\underset{\sim}{B}$ matrix can then be written as:

$$\underset{\sim}{B} = \begin{bmatrix} \frac{\partial h_1}{\partial x} & 0 & \frac{\partial h_2}{\partial x} & 0 & \cdots & 0 \\ 0 & \frac{\partial h_1}{\partial y} & 0 & \frac{\partial h_2}{\partial y} & \cdots & \frac{\partial h_8}{\partial y} \\ \frac{\partial h_1}{\partial y} & \frac{\partial h_1}{\partial x} & \frac{\partial h_2}{\partial y} & \frac{\partial h_2}{\partial x} & \cdots & \frac{\partial h_8}{\partial x} \end{bmatrix} \qquad (4.11)$$

where [from equation (4.10)]:

$$\frac{\partial h_i}{\partial x} = \frac{1}{|\underset{\sim}{J}|}\left(J_{22}\frac{\partial h_i}{\partial \xi} - J_{12}\frac{\partial h_i}{\partial \eta}\right)$$

$$\frac{\partial h_i}{\partial y} = \frac{1}{|\underset{\sim}{J}|}\left(-J_{12}\frac{\partial h_i}{\partial \xi} + J_{11}\frac{\partial h_i}{\partial \eta}\right)$$

4.2.3 Numerical Integration and Implementation

The matrices $\underset{\sim}{H}$ and $\underset{\sim}{G}$ of equations (2.6) and (2.13) are determined by the Gauss-Quadrature numerical integration scheme [11]:

$$I = \int_V F(x,y)\,dV = t\iint_A F(x,y)\,dA \qquad (4.11)$$

t ≡ Element thickness; assumed constant.

dA ≡ Differential area of the element.

Equation (4.11) becomes:

$$I = t\int_{-1}^{+1}\int_{-1}^{+1} F(\xi,\eta)\,|\underset{\sim}{J}|\,d\xi\,d\eta$$

$$I = t\sum_{i=1}^{M}\sum_{j=1}^{N} F(\xi_i,\eta_j)\,|\underset{\sim}{J}|\,W_i W_j \qquad (4.12)$$

(ξ_i, η_j) = Gauss Integration stations.

where:

W_i, W_j = Gauss weighting factors.

Using n points in the Gauss integration scheme of equation (4.12) (i.e., M = N = n), a polynomial of order 2n - 1 can be integrated exactly. The highest power of x or y that appears in equation (2.6) will depend on the number of betas used in the stress terms. If the complete cubic expression of equations (4.4) with eighteen betas is used, the product $\underset{\sim}{\rho}^T \underset{\sim}{S} \underset{\sim}{\rho}$ will contain polynomial terms of sixth order and hence a 4x4 Gauss quadrature scheme would seem adequate. For an accurate integration of the product $\underset{\sim}{\rho}^T \underset{\sim}{B}$, the number of nodes need to be considered. Equations (4.8) show that the interpolation functions h_i are in general second order in ξ and η. From equation (4.11) it is seen that typical terms appearing in $\underset{\sim}{B}$ are of the form:

$$\left(\frac{\partial h_i}{\partial \zeta}\right)\left(\frac{\partial h_j}{\partial \zeta}\right)$$

where ζ replaces either ξ or η.

When all nodes are present, the matrix will contain fourth powers of ξ and/or η. With a complete cubic distribution of the stresses it is again seen that a four by four Gauss integration will be sufficient to accurately integrate $\underset{\sim}{G}$. Naturally the required number of integration points will change if a lower order of stresses is used or the mid-nodes of the element are completely eliminated.

Matrices $\underset{\sim}{H}$ and $\underset{\sim}{S}$ are hence determined as follows:

$$\underset{\sim}{H} = \sum_i \sum_j \left[\left(\underset{\sim}{P}^T \underset{\sim}{S} \underset{\sim}{P} \right) |\underset{\sim}{J}| \right]_{\xi_i, \eta_j} W_i W_j \tag{4.13}$$

$$\underset{\sim}{G} = \sum_i \sum_j \left[\left(\underset{\sim}{P}^T \underset{\sim}{B} \right) \right]_{\xi_i, \eta_j} W_i W_j \tag{4.14}$$

In equation (4.13), $\underset{\sim}{S}$ is the compliance matrix of an isotropic homogeneous material in plane stress:

$$\underset{\sim}{S} = \frac{1}{E} \begin{bmatrix} 1 & -\nu & 0 \\ -\nu & 1 & 0 \\ 0 & 0 & 2(1+\nu) \end{bmatrix}$$

In equation (4.14), the determinant of the Jacobian matrix $\underset{\sim}{J}$ resulting from the coordinate transformation is eliminated, because as seen in equation (4.11) the matrix $\underset{\sim}{B}$ has the reciprocal of this determinant as a scalar multiplier.

The rationalization of the required number of integration points was arrived at experimentally. It was observed that, for example, using a 5 x 5 or 7 x 7 Gauss integration scheme, makes insignificant changes to the stiffness matrix of the eight node element with complete cubic stress distribution. This deduction is substantiated in a report by Spilker [7] for an eight node hybrid isoparametric element. It should be noted that for strictly two dimensional analysis, imposing the condition of stress compatibility:

$$\nabla^4 \phi = \nabla^2 (\sigma_{xx} + \sigma_{yy}) = 0 \tag{4.15}$$

will not only improve the efficiency of the element by reducing the number of betas, but will also produce a stiffness matrix that models the physical problem more accurately [7]. However, in three dimensional analysis the conditions of stress compatibility do not appear as simple constraint conditions on the stresses and in general are very difficult to meet. For this reason, performance of the eight node element with the assumed stresses of equations (4.4) would be a better judge of the solid isoparametric element.

The stiffness matrix of the element is then determined from equation (2.18):

$$\underset{\sim}{K} = \underset{\sim}{G}^T \underset{\sim}{H}^{-1} \underset{\sim}{G}$$

Since the inversion of matrix $\underset{\sim}{H}$ can add considerable computation time, the most efficient approach should be considered. Many efficient routines are developed that factorize the matrix into triangular matrices and then invert it by backward and forward substitution. For element HISQUE, the subroutine DSINV, of the Scientific Subroutine Package (SSP) programmed by IBM, was used to invert $\underset{\sim}{H}$. This subroutine operates in double precision accuracy and requires storage for only the upper half of the symmetric matrix $\underset{\sim}{H}$, for inverting it by the Cholesky Factorization method.

The stiffness matrix was observed to have three zero eigenvalues corresponding to the three rigid body motions and hence free of spurious energy mode.

4.3 Results and Discussion

4.3.1 Plate with Circular Hole

Stress solutions were obtained with a displacement based eight node isoparametric element (ELEM8)[12] at the point of stress concentration with both Mesh-1 and Mesh-2. Satisfactory stresses (±5%) were obtained in both cases, compared to the expected solution of 4.32 at the point of stress concentration. The results are shown in Figure 6, where modeled with eight node elements Mesh-1 incorporates 36 degrees of freedom, and Mesh-2 106. The precedure was repeated with element HISQUE and the results are also shown in Figure 6. The error in the stresses is summarized in the table below:

TYPE	% error	
	Mesh-1	Mesh-2
ELEM8	-2.38	3.26
HISQUE	-29.4	-.81

An alternative to modeling the problem entirely with displacement or hybrid elements is to use the hybrid element only where the stresses are critical. This treatment of hybrid elements as specialized elements is important from both solution efficiency and dependability aspects. Since the hybrid approach does not differentiate the displacements for the stress solution, it can be argued that where stress determination is the paramount objective, its utilization will become advantageous.

A solution was obtained with Mesh-2, with element HISQUE used in the shaded section of Figure 4a, and element ELEM8 in the remaining part of the quarter plate. The percent error in the maximum stress for this

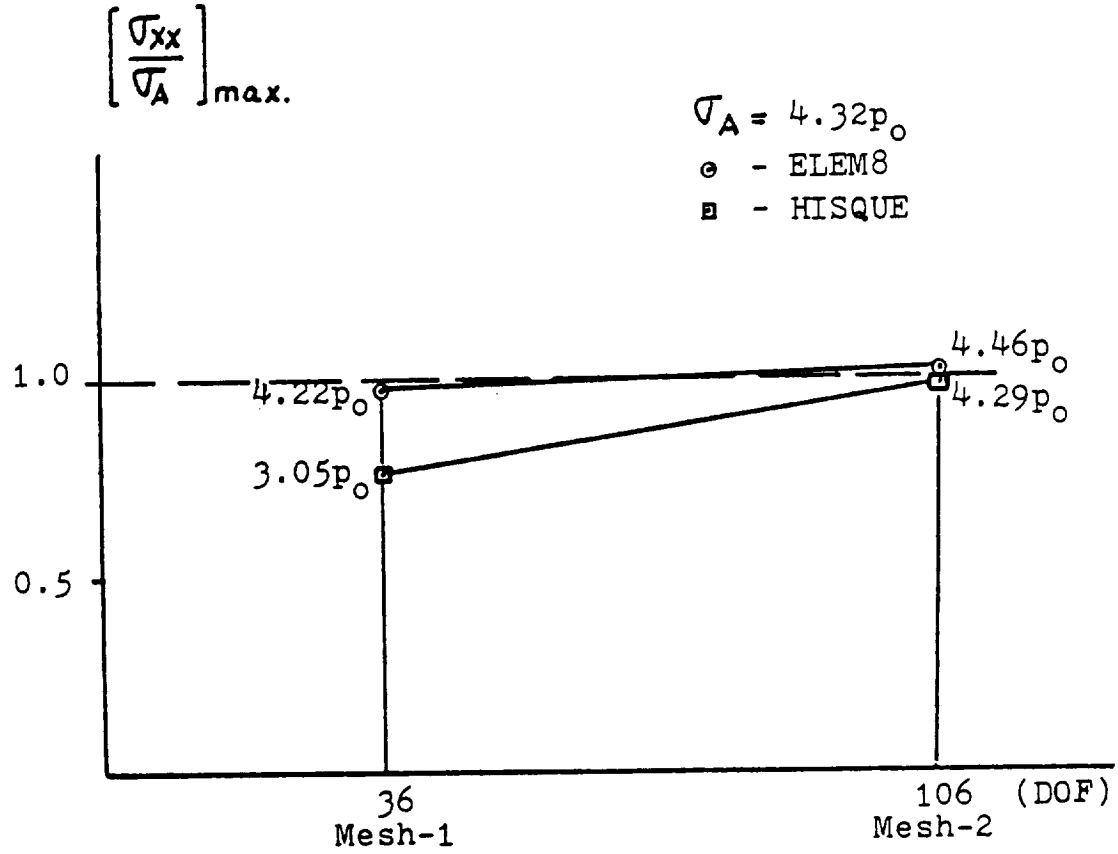

Figure-6 Maximum Stress σ_{xx} In Plate With A Circular Hole

case was -.9%. The difference in the error between this and the two previous cases, where complete hybrid and complete displacement elements were used, appears too academic.

Indeed, except for the appearance of monotonic convergence of the hybrid stress solution versus the oscillating displacement based stress solution, Figure 6, use of the hybrid element HISQUE does not seem justified in the case of the circular hole. Nevertheless, with the finer mesh, better than 2% improvement is observed in the stress solution when element HISQUE is used. Closer examination of the stress equilibrium at the left boundary of the quarter plate, Figure 7, reveals that the resultant stress on this section is closer to the applied force when a complete hybrid, or partially hybrid - partially displacement based model is used. With Mesh-2 the following values were obtained for the resultant stress N:

$$N = \int_S \sigma_{xx}\, dy \qquad (4.16)$$

$S \equiv$ *left boundary of quarter plate*

$N_D = 0.981\, p_o$ (ALL ELEMS)

$N_H = 1.008\, p_o$ (ALL HISQUE)

$N_{H\text{-}D} = 1.008\, p_o$ (MIXED MODEL)

From Figure 7, it is also seen that, at the boundary, the stress solutions of the complete hybrid and the mixed model are indistinguishable.

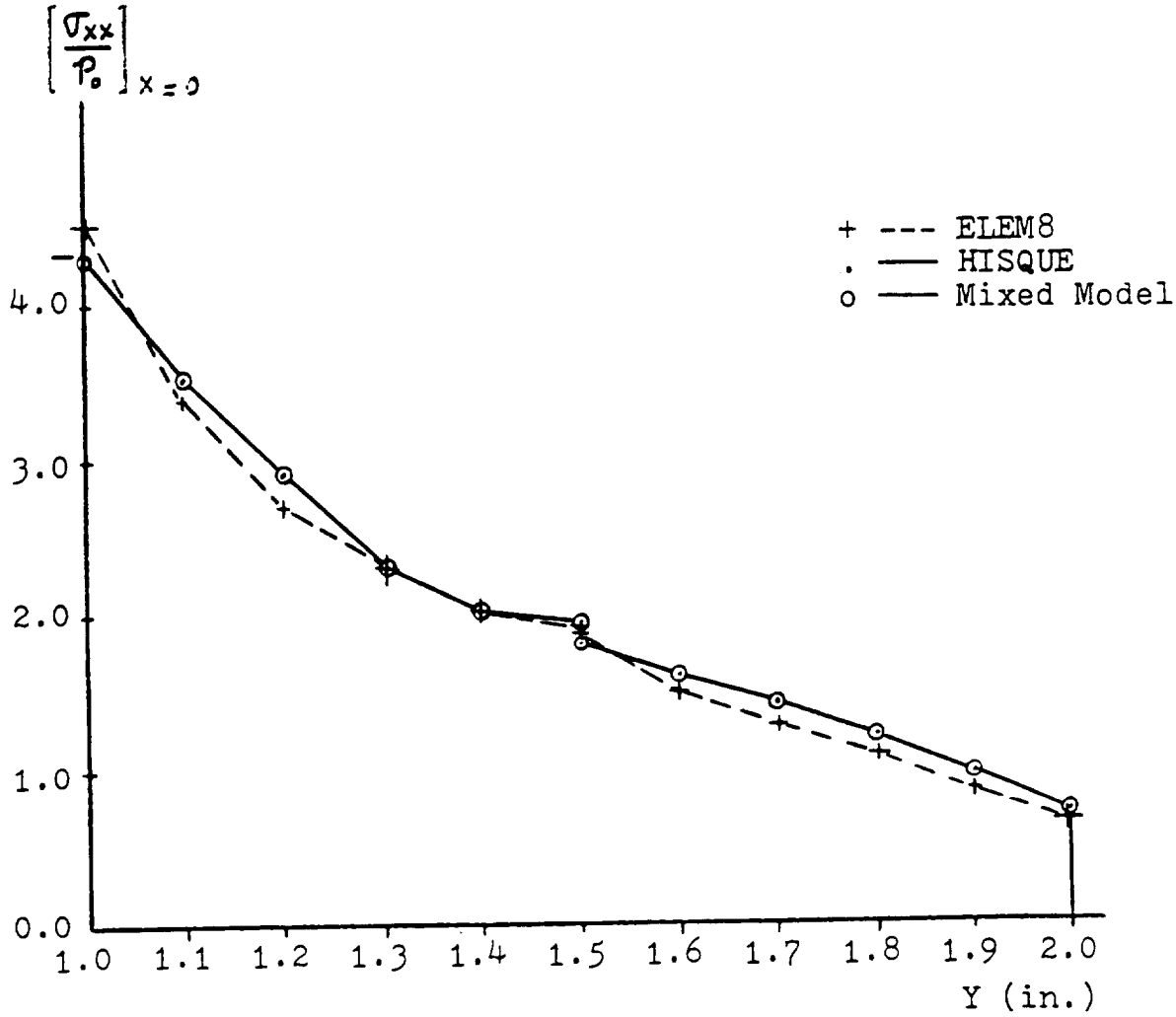

Figure-7 Stress Profile At The Left Edge With Eight-Node Isoparametric Elements

4.3.2 Plate with Elliptical Hole

Stress solutions were obtained at the point of maximum stress of the plate with elliptical hole shown in Figure 2. Modeled according to Figures 2b and 4b, labeled Mesh-1 and Mesh-2, respectively, elements HISQUE and ELEM8 were both used in analysis.

Analysis with the displacement based element ELEM8 did not produce acceptable results ($\pm$5%) with either mesh. As noted earlier, Mesh-1 is really too coarse to realistically model the problem within finite element approximation, and its inclusion is merely intended to provide a convergence trend. With Mesh-1, ELEM8 predicted a stress concentration factor of $7.29\rho_o$, an underestimation with more that 23% error compared to the expected value of $9.50\rho_o$. With Mesh-2, a stress concentration of $8.57\rho_o$ was found which carries an error of -9.8%.

Analysis with element HISQUE converged with Mesh-2 and the results are summarized in the following table:

Element Type	% error	
	Mesh-1	Mesh-2
ELEM8	-23.3	-9.78
HISQUE	-41.9	-4.52

The stresses obtained are shown in Figure 8.

As done in the case of the circular hole, this plate was also analyzed with a combination of the two elements. Here, element HISQUE was used in the shaded region of Figure 4b, and the rest of the plate was modeled with displacement based elements ELEM8. A stress concentra-

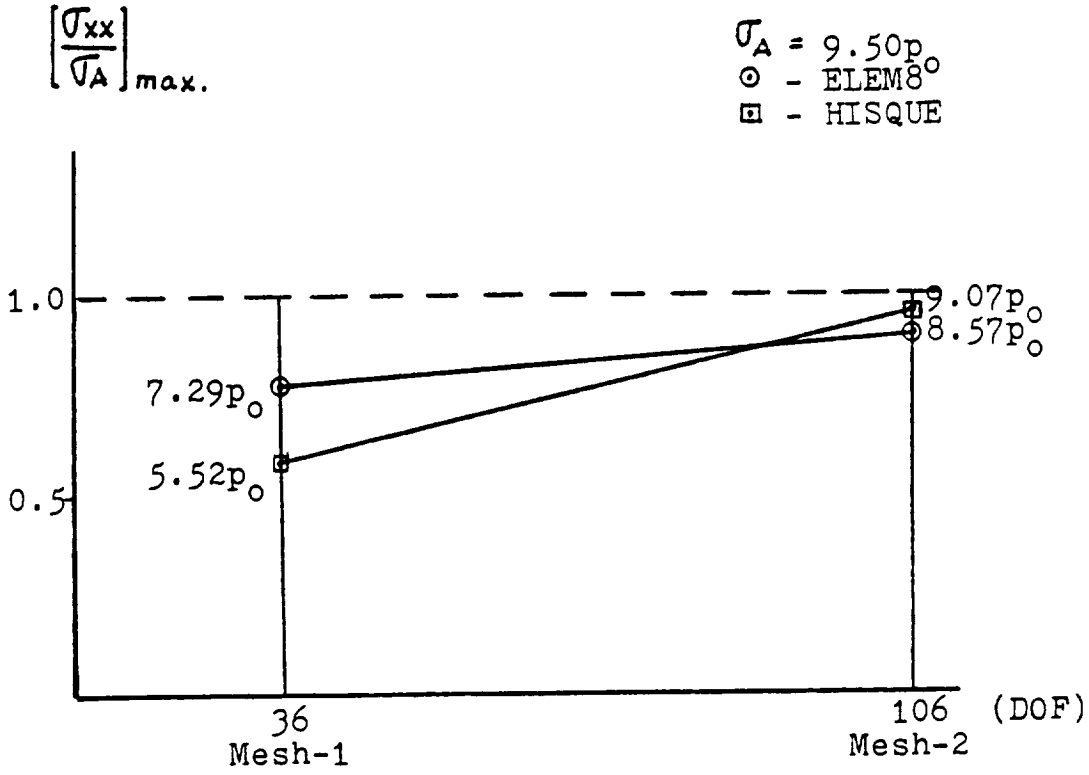

Figure-8 Maximum Stress σ_{xx} In Plate With An Elliptical Hole

tion factor of 9.04 was obtained in this analysis, which only carries an error of 4.84%.

It is seen that employment of the hybrid element provides considerable improvement over the strict displacement based element in the analysis of the elliptical hole problem. Considering that the next refinement of the model would require 48 elements, the introduction of only five hybrid elements around the hole and on the left boundary becomes justifiable. So long as the cost of five hybrid elements equals that of 41 displacement based elements, the reduced burden of modeling the plate with a fine mesh alone would rationalize the proposition. A more accurate comparison should also include the resulting increase in the global stiffness and band-width, and hence the additional storage and solution cost. Although the ratio of required CPU (Central Processing Unit) time for analysis with elements HISQUE and ELEM8 is well below 8:1, there is much room in both for further improvements and a numerical comparison would not be a creditable representative.

Figure 9 shows a plot of the stress distribution in Mesh-2, along the left boundary, for all three cases. Again the indistinguishable results between the complete hybrid model and the mixed hybrid displacement model is emphasized. The reaction equilibrium can be determined from the resultant stress N of equation (4.16):

$$N_D = 1.01\, p_o \qquad \text{(ALL ELEM8)}$$

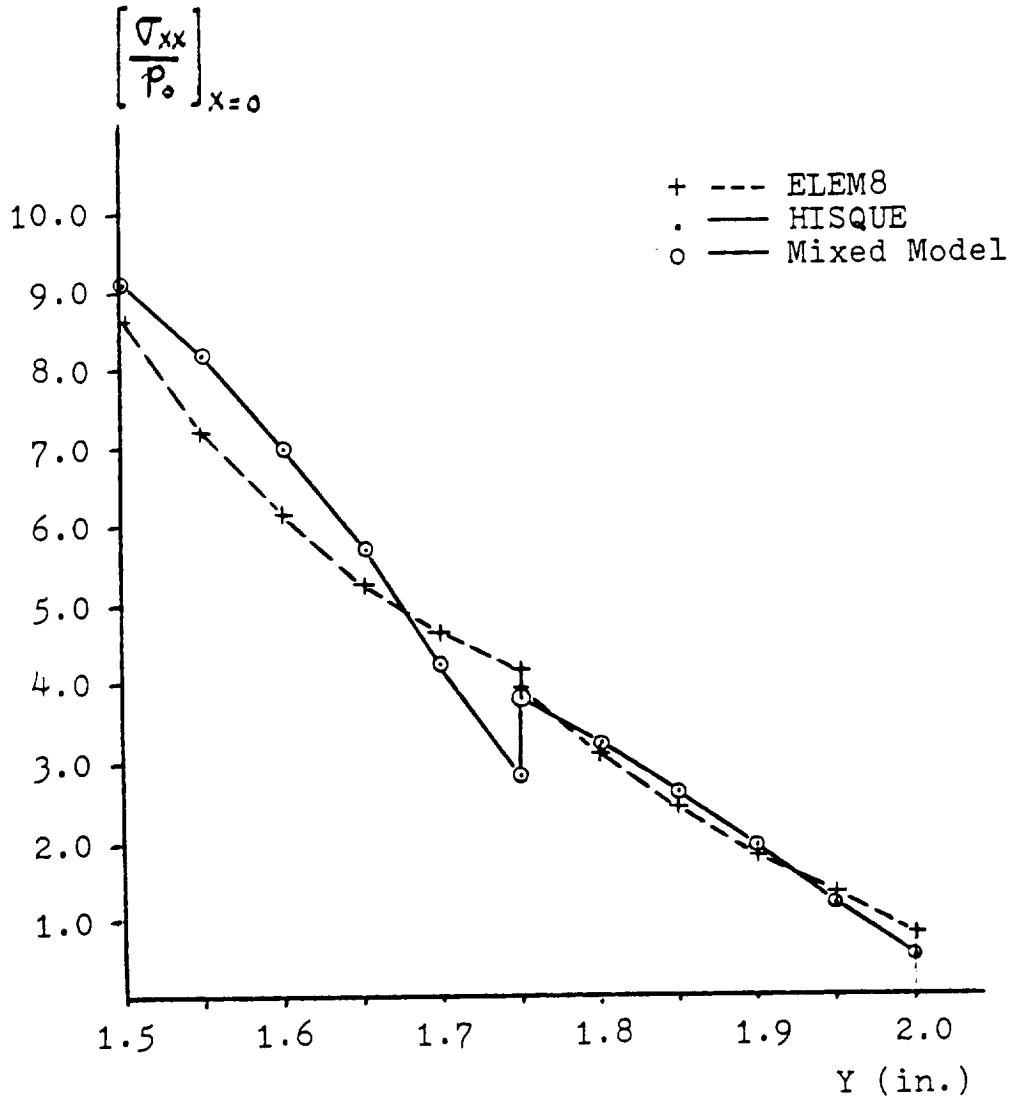

Figure-9 Stress Profile Of Plate With Elliptical Hole

$$N_H = 1.06\ p_o \qquad \text{(ALL HISQUE)}$$

$$N_{H\text{-}D} = 1.05\ p_o \qquad \text{(MIXED MODEL)}$$

The fact that on the left edge, equilibrium is almost exactly satisfied and the stress distribution is nearly continuous across the two elements may erroneously suggest that the displacement solution of the stress field has attained convergence.

A close examination of the normal stresses around the hole will provide an explanation of the more accurate hybrid analysis. The stress normal to the elliptical hole can be determined by transforming stress components along directions normal and tangent to the ellipse. The angle of the normal α, is given by:

$$\alpha = 180^\circ + \tan^{-1}\left[\frac{\tan\theta}{(1.5)^2}\right]$$

where:

$\theta \equiv$ Angle of point (x, y) on the ellipse, in polar coordinates.

Since the hole is not subjected to any external loads, a zero normal stress condition is in effect prescribed at the hole. Figure 10a shows a plot of the normal stresses obtained with the hybrid and the displacement analysis. The results obtained with the mixed model are again indistinguishable from the complete hybrid analysis and hence are not shown. It is evident from Figure 10a that the hybrid element approximates the stress boundary condition more accurately than the displacement element.

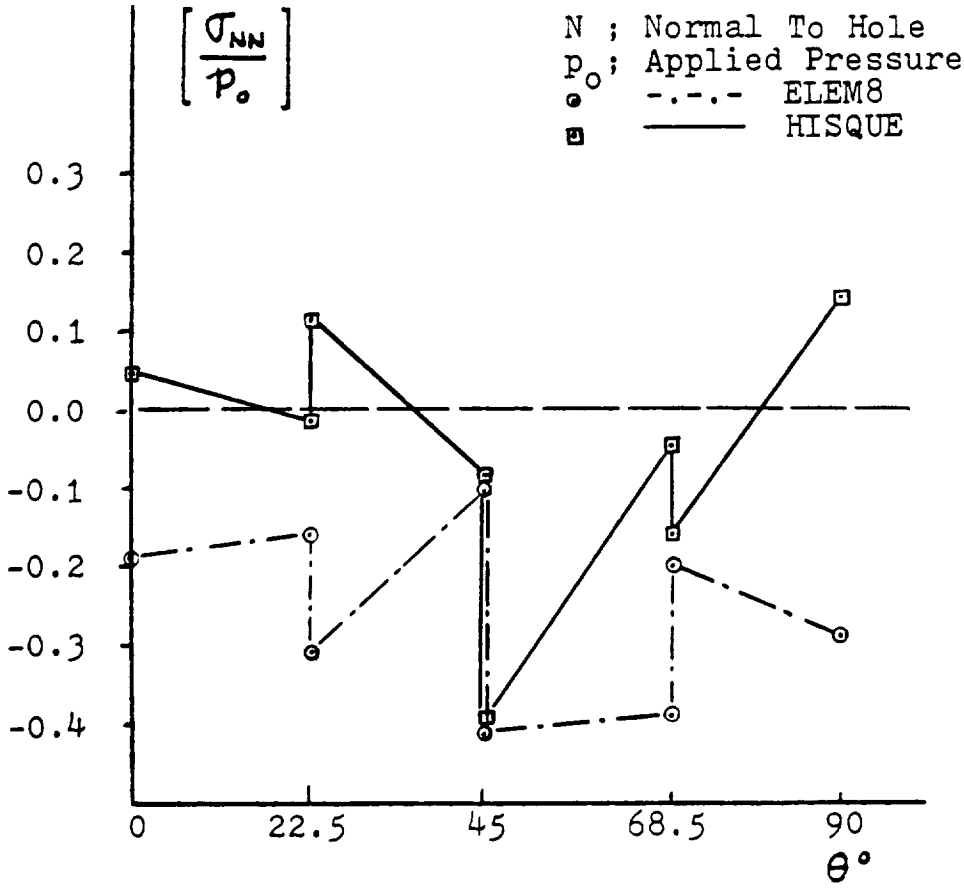

Figure-10a Distribution Of The Normal Stress At The Elliptical Hole

In terms of the absolute value of the stress deviation from zero, the displacement based results are at best 21% worse than the hybrid result, and over 700% at $\theta = 22.5^{o}$. Figure 10b shows the normal stresses to the elliptical boundary normalized by the hoop stress.

4.4 Concluding Remarks

The ability of the hybrid element HISQUE to better satisfy stress boundary conditions around a hole, compared to the displacement based element ELEM8, is seen to produce better stress results in the cases of circular and elliptical holes.

The most dependable, accurate and economical model in the finite element analysis of these problems is judged to be one that employs hybrid elements where accurate stress predictions are critical. The mixed model employs displacement based elements for the rest of the structure.

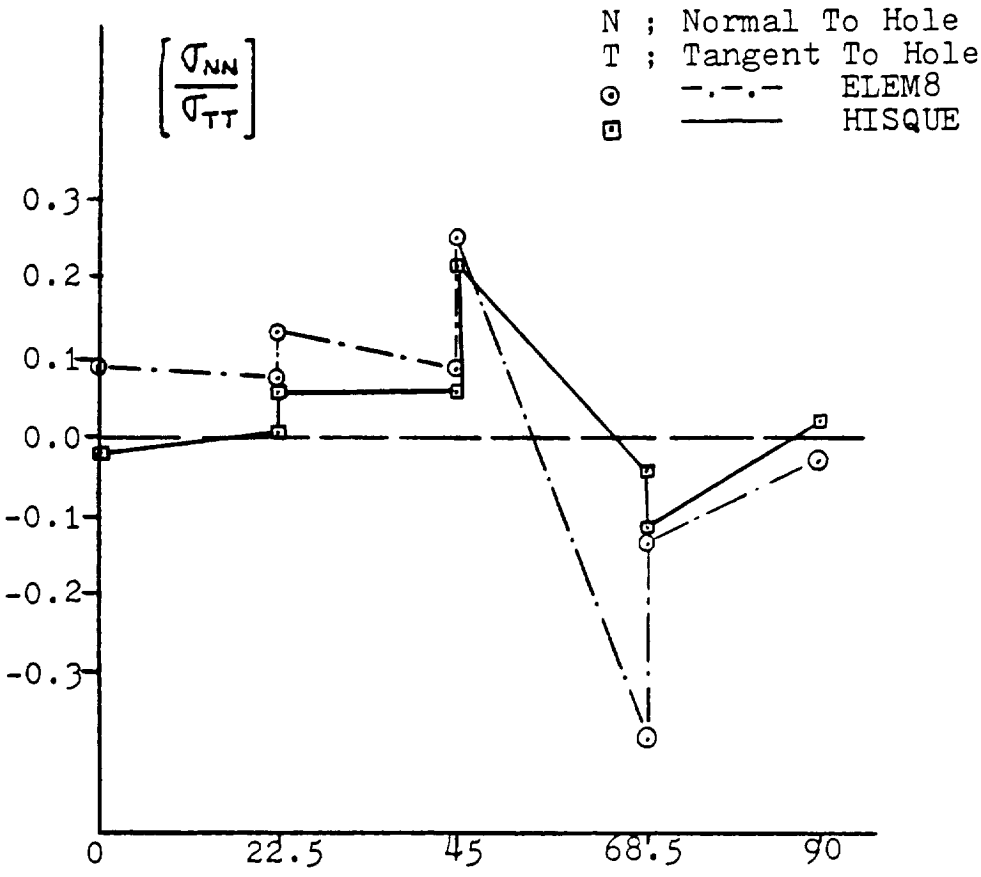

Figure-10b Distribution Of $(\sigma_{NN}/\sigma_{TT})$ At The Elliptical Hole

CHAPTER 5

A-7-10 Variable Node Hybrid Isoparametric Quadrilateral Element

5.1 Introduction and Objective

Comparison of results obtained with eight node isoparametric elements indicates that satisfaction of the free traction boundary condition is essential in successful stress concentration analysis around holes. For this purpose, the formulation of a specialized hybrid isoparametric element, HEL710, based on the collocation method suggested by Atluri [13], is presented. This approach led to introduction of two additional nodes on one boundary of the element HISQUE. For preservation of compatibility in analysis with other elements the mid-nodes of the other three edges of the element are removable. The optimum stress distribution for this element was found to be a complete quartic.

The objective is improvement of solution accuracy and efficiency compared to that obtained with a mixed model employing hybrid and displacement based eight node isoparametric elements. Element HEL710 is shown in Figure 11 in the Cartesian global coordinates.

5.2 The Boundary Point Matching Technique

As developed by Atluri and Rhee [13], the boundary point matching technique works by introducing the Lagrange multiplier $\bar{u}$ in the variational formulation to enforce traction equilibrium. The Lagrange multiplier $\bar{u}$ is then the compatible interelement boundary displacement.

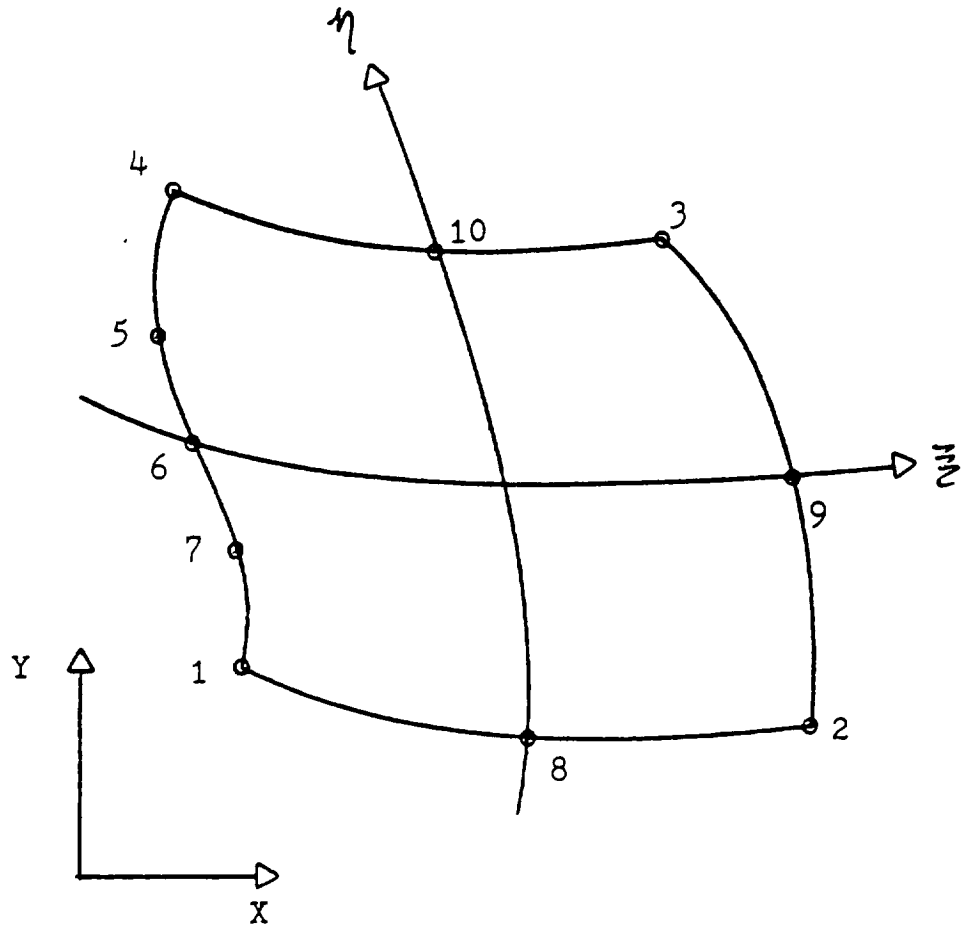

Figure-11 The Nodes Of Element HEL710

$$\pi_H = -\frac{1}{2}\int_V \underset{\sim}{\sigma}^T \underset{\sim}{S}\,\underset{\sim}{\sigma}\, dV + \int_{\partial V} \underset{\sim}{T}\,\underset{\sim}{u}\, dS + \int_{S_\sigma} (\underset{\sim}{T}-\bar{\underset{\sim}{T}})^T \bar{\underset{\sim}{u}}\, dS \qquad (5.1)$$

$\pi_H \equiv$ The hybrid stress functional.

$\bar{u} \equiv$ Compatible interelement boundary displacements.

$S_\sigma \equiv$ Portions of boundary where tractions are prescribed.

$\bar{T} \equiv$ Prescribed tractions.

Comparison with equation (2.1) shows that the last integral is added to satisfy the traction equilibrium. If the following assumptions are made:

$$\underset{\sim}{\sigma} = \underset{\sim}{P}\,\underset{\sim}{\beta} \qquad (2.2)$$

$$\underset{\sim}{u} = \underset{\sim}{L}\,\underset{\sim}{q} \qquad (2.3)$$

$$\bar{\underset{\sim}{u}} = \underset{\sim}{F}\,\underset{\sim}{\alpha} \qquad (5.2)$$

Then one can write the traction vector in terms of the stresses:

$$\underset{\sim}{T} = \underset{\sim}{R}\,\underset{\sim}{\beta} = \underset{\sim}{\nu}^T \underset{\sim}{P}\,\underset{\sim}{\beta} \qquad (2.4)$$

In equation (5.2) $\underset{\sim}{\alpha}$ are undetermined coefficients and $\underset{\sim}{F}$ are arbitrary order polynomials.

Substitution of equations (2.2), (2.3), (2.4) and (5.2) into equation (5.1) gives:

$$\pi_H = -\frac{1}{2}\underset{\sim}{\beta}^T\underset{\sim}{H}\underset{\sim}{\beta} + \underset{\sim}{\beta}^T\underset{\sim}{G}\underset{\sim}{q} + \underset{\sim}{\beta}^T\underset{\sim}{C}^T\underset{\sim}{\alpha} - \underset{\sim}{Q}^T\underset{\sim}{\alpha} \tag{5.3}$$

The functional π_H should attain a stationary value with respect to the two independent variables $\underset{\sim}{\alpha}$ and $\underset{\sim}{\beta}$.

$$\underset{\sim}{H}\underset{\sim}{\beta} - \underset{\sim}{G}\underset{\sim}{q} - \underset{\sim}{C}^T\underset{\sim}{\alpha} = 0 \tag{5.4a}$$

$$\underset{\sim}{C}\underset{\sim}{\beta} - \underset{\sim}{Q} = 0 \tag{5.4b}$$

where:

$$\underset{\sim}{Q} = \int_{S_\sigma} \underset{\sim}{F}^T\underset{\sim}{\bar{T}}\, dS$$

and $\underset{\sim}{C}$ is determined by substituting coordinates of points on the boundary in the $\underset{\sim}{\rho}$ matrix. From equation (5.4a):

$$\underset{\sim}{\beta} = \underset{\sim}{H}^{-1}\underset{\sim}{G}\underset{\sim}{q} + \underset{\sim}{H}^{-1}\underset{\sim}{C}^T\underset{\sim}{\alpha} \tag{5.5}$$

Therefore, from equation (5.4b):

$$\underset{\sim}{Q} = \underset{\sim}{C}\underset{\sim}{H}^{-1}\underset{\sim}{G}\underset{\sim}{q} + \underset{\sim}{C}\underset{\sim}{H}^{-1}\underset{\sim}{C}^{T}\underset{\sim}{\alpha}$$

$$\underset{\sim}{\alpha} = -(\underset{\sim}{C}\underset{\sim}{H}^{-1}\underset{\sim}{C}^{T})^{-1}\underset{\sim}{C}\underset{\sim}{H}^{-1}\underset{\sim}{G}\underset{\sim}{q} + (\underset{\sim}{C}\underset{\sim}{H}^{-1}\underset{\sim}{C}^{T})^{-1}\underset{\sim}{Q} \qquad (5.6)$$

Substituting (5.6) into (5.5):

$$\underset{\sim}{\beta} = \underset{\sim}{H}^{-1}\underset{\sim}{G}\underset{\sim}{q} - \underset{\sim}{H}^{-1}\underset{\sim}{C}^{T}(\underset{\sim}{C}\underset{\sim}{H}^{-1}\underset{\sim}{C}^{T})^{-1}\underset{\sim}{C}\underset{\sim}{H}^{-1}\underset{\sim}{G}\underset{\sim}{q}$$
$$+ \underset{\sim}{H}^{-1}\underset{\sim}{C}^{T}(\underset{\sim}{C}\underset{\sim}{H}^{-1}\underset{\sim}{C}^{T})^{-1}\underset{\sim}{Q} \qquad (5.7)$$

By substitution of (5.6) and (5.7) into (5.3) and comparison with the assumed displacement functional

$$\pi_{0} = \frac{1}{2}\underset{\sim}{q}^{T}\underset{\sim}{K}\underset{\sim}{q}$$

the element stiffness matrix $\underset{\sim}{k}$ is obtained:

$$\underset{\sim}{k} = \underset{\sim}{G}^{T}\underset{\sim}{H}^{-1}\underset{\sim}{G} - \underset{\sim}{G}^{T}\underset{\sim}{H}^{-1}\underset{\sim}{C}^{T}(\underset{\sim}{C}\underset{\sim}{H}^{-1}\underset{\sim}{C}^{T})^{-1}\underset{\sim}{C}\underset{\sim}{H}^{-1}\underset{\sim}{G} \qquad (5.8)$$

However, if an element with n nodes is considered at m nodes of which (n > m) zero traction is prescribed, then the general stiffness matrix of this element

$$\underset{\sim}{k} = \underset{\sim}{G}^T \underset{\sim}{H}^{-1} \underset{\sim}{G} \tag{2.18}$$

can be rewritten as:

$$\underset{\sim}{k} = \begin{bmatrix} \underset{\sim}{G}_A^T \\ \underset{\sim}{G}_B^T \end{bmatrix} \underset{\sim}{H}^{-1} \begin{bmatrix} \underset{\sim}{G}_A \\ \underset{\sim}{G}_B \end{bmatrix} \tag{5.9}$$

Where $\underset{\sim}{G}_B$ is that portion of $\underset{\sim}{G}$ corresponding to the m nodes at which tractions are prescribed to be zero. From equation (5.9) the stiffness matrix is seen to partition accordingly:

$$\underset{\sim}{k} = \begin{bmatrix} \underset{\sim}{k}_{AA} & \underset{\sim}{k}_{AB} \\ \underset{\sim}{k}_{BA} & \underset{\sim}{k}_{BB} \end{bmatrix}$$

Here $\underset{\sim}{k}_{BB}$ is a matrix of order (m x m). Since no loads are applied at nodes B then:

$$\underset{\sim}{k} \begin{Bmatrix} \underset{\sim}{f}_A \\ \underset{\sim}{f}_B \end{Bmatrix} = \begin{Bmatrix} \underset{\sim}{Q}_A \\ \underset{\sim}{0} \end{Bmatrix}$$

Static condensation of the $\underset{\sim}{f}_B$ degrees of freedom gives:

$$\underset{\sim}{k}_r \underset{\sim}{f}_A = \underset{\sim}{Q}_A$$

where:

$$\underset{\sim}{K}_r = \underset{\sim}{G}_A \underset{\sim}{H}^{-1} \underset{\sim}{G}_A - \underset{\sim}{G}_A^T \underset{\sim}{H}^{-1} \underset{\sim}{G}_B \left(\underset{\sim}{G}_B^T \underset{\sim}{H}^{-1} \underset{\sim}{G}_B \right)^{-1} \underset{\sim}{G}_B^T \underset{\sim}{H}^{-1} \underset{\sim}{G}_A \qquad (5.10)$$

The equivalence of equations (5.8) and (5.10) is seen when

$$\underset{\sim}{C} = \underset{\sim}{G}_B^T$$

In other words the method of boundary point matching is equivalent to introducing additional nodes on a traction free edge and then statically condensing these nodes in obtaining a reduced stiffness matrix.

Although very flexible, the boundary point matching technique has inherent drawbacks. The major cost-related criticism directed at the assumed strees hybrid formulation is the necessity of a matrix inversion for stiffness matrix evaluation. As is seen from equation (5.8) the boundary point matching requires a second matrix inversion, namely of the matrix product ($\underset{\sim}{C} \underset{\sim}{H}^{-1} \underset{\sim}{C}^T$). Furthermore, the size of this matrix is directly related to the number of collocation points used to satisfy the boundary traction condition; hence, the more accurate a solution desired, the higher a price for the element.

To avoid costly inversions, element HEL710 employs only two additional nodes on one boundary ($\xi = -1$), compared to the eight node element HISQUE. Since addition of two nodes per element used on the hole surface does not increase the total global degrees of freedom significantly, no static condensation is performed by element HEL710.

5.3 Formulation of Element HEL710

5.3.1 The Assumed Stresses

With all the nodes present, element HEL710 possesses 20 degrees of freedom and therefore requires 17 betas in the assumed stresses to exclude spurious zero energy modes. For completeness, the cubic assumed stresses of element HISQUE, equations (4.4), with 18 betas were used. Since element HEL710 incorporates five nodes on one edge, it takes advantage of a quartic displacement interpolation on this edge and hence for a better balance a complete quartic stress distribution, employing 25 betas, was also tried. A complete quartic stress distribution is obtained by addition of the following terms to equations (4.4):

$$\begin{aligned}
\sigma_{xx} &= x^4\beta_{19} + x^3y\beta_{20} + x^2y^2\beta_{21} + xy^3\beta_{22} + y^4\beta_{23} \\
\sigma_{yy} &= 6x^2y^2\beta_{19} + xy^3\beta_{20} + \frac{y^4}{6}\beta_{21} + 4x^3y\beta_{24} + x^4\beta_{25} \qquad (5.11) \\
\sigma_{xy} &= -4x^3y\beta_{19} - \frac{3}{2}x^2y^2\beta_{20} - \frac{2}{3}xy^3\beta_{21} - 4y^4\beta_{22} - x^4\beta_{24}
\end{aligned}$$

5.3.2 Interpolation Functions and the Strain Matrix

The strain matrix is determined in a completely analogous manner to that of element HISQUE, with the only difference existing in the interpolation functions. The interpolation functions h_i were constructed such that the displacement distributions on any boundary of the element were compatible with the number of nodes present on that boundary. Another requirement satisfied by the interpolation functions is:

$$\sum_i h_i = 1$$

The following interpolation functions were obtained for the isoparametric element:

$$h_1 = \frac{1}{3}(\eta+\tfrac{1}{2})\eta(\eta-\tfrac{1}{2})(\eta-1)(1-\xi^2) - \frac{1}{2}\delta_8 h_8$$

$$h_2 = \frac{1}{4}(1-\eta)(1+\xi^2) - \frac{1}{2}\delta_8 h_8 - \frac{1}{2}\delta_7 h_7$$

$$h_3 = \frac{1}{4}(1+\xi^2)(1+\eta) - \frac{1}{2}\delta_9 h_9 - \frac{1}{2}\delta_{10} h_{10}$$

$$h_4 = \frac{1}{3}(\eta+1)(\eta+\tfrac{1}{2})\eta(\eta-\tfrac{1}{2})(1-\xi^2) - \frac{1}{2}\delta_{10} h_{10}$$

$$h_5 = \frac{4}{3}(\eta+1)(\eta+\tfrac{1}{2})\eta(\eta-\tfrac{1}{2})(\xi^2-1)$$

$$h_6 = -2(\eta+1)(\eta+\tfrac{1}{2})(\eta-\tfrac{1}{2})(\eta-1)(\xi^2-1)$$

$$h_7 = \frac{4}{3}(\eta+1)(\eta)(\eta-\tfrac{1}{2})(\eta-1)(\xi^2-1)$$

$$h_8 = \frac{1}{2}\delta_8(1-\xi^2)(1-\eta)$$

$$h_9 = \frac{1}{2}\delta_9(1-\eta^2)(1+\xi^2)$$

$$h_{10} = \frac{1}{2}\delta_{10}(1-\xi^2)(1+\eta)$$

where: $\delta_i = \begin{cases} 1 & \text{if node } i \text{ present} \\ 0 & \text{if node } i \text{ absent} \end{cases}$

It is seen that by employing the δ_{ij} function, any combination of nodes numbered 8, 9 and 10, Figure 11, can be removed without disintegration of interelement compatibility. This characteristic will allow element HEL710 to be used in analysis with four and/or eight node elements.

5.3.3 Implementation

A 5 x 5 Gauss numerical integration was found to be the minimum order for an adequate integration of matrices $\underset{\sim}{H}$ and $\underset{\sim}{G}$. Very insignificant changes of the stiffness matrix resulted when higher order integration was used. Otherwise, the implementation of element HEL710 is identical to that of element HISQUE, presented in Chapter 4.

5.4 Results and Discussion

5.4.1 Plate with Circular Hole

The plate was modeled entirely with displacement based eight node elements ELEM8, except around the hole where elements HEL710 were used. Two sets of stress solutions were obtained. The first set of results acquired using complete cubic assumed stresses was completely unacceptable. Stress concentrations of $1.80\,p_o$ and $3.43\,p_o$ were obtained at the point of maximum stress, with Mesh-1 and Mesh-2, respectively. With a complete quartic stress distribution the stress solutions were somewhat improved, and stress concentrations of $3.03\,p_o$ and $4.21\,p_o$ were computed. The percent error in the stress solutions are summarized below:

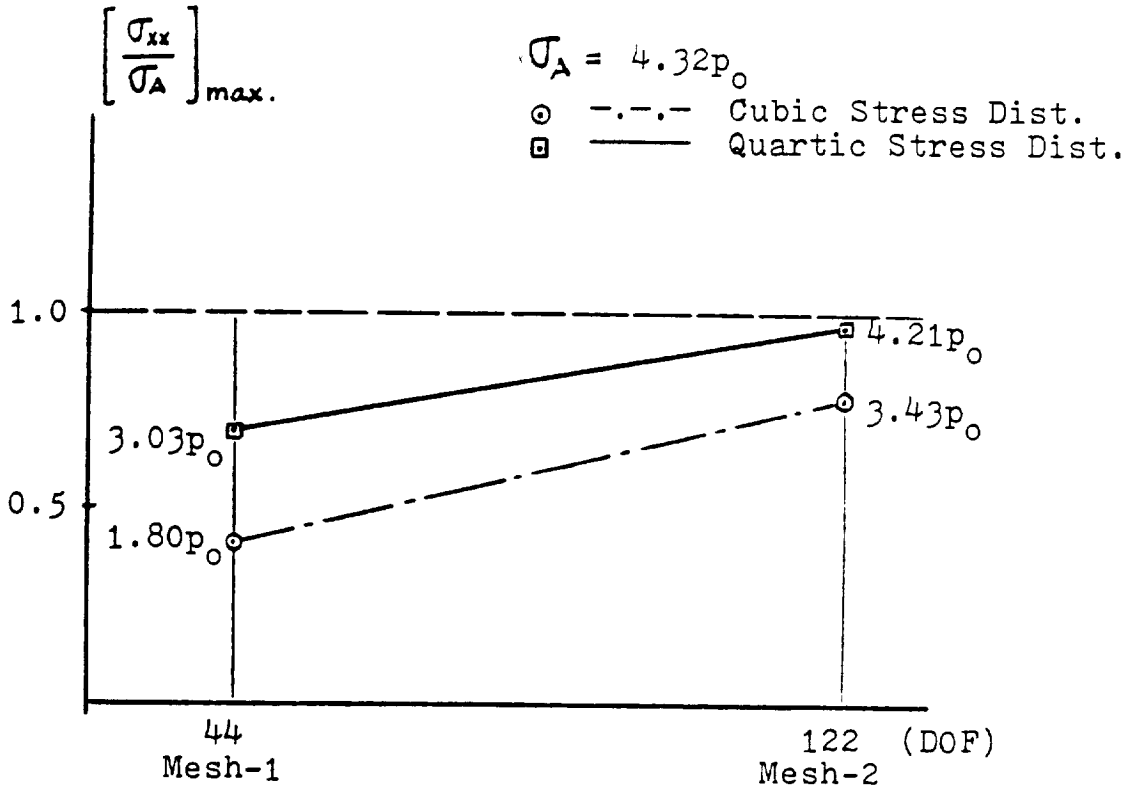

Figure-12 Maximum Stress By HEL710 In Plate With Circular Hole

Element Stress	% error	
	Mesh-1	Mesh-2
Cubic	-58.3	-20.6
Quartic	-29.9	-2.55

Although not as accurate as element HISQUE, with Mesh-2 and a complete quartic stress distribution the computed stress concentration factor converged within the $\pm 5\%$ acceptable margin. The convergence of the stress solution is shown in Figure 12 for both cases. It is clear that element HISQUE with cubic assumed stresses is not effective in analysis and was therefore not used for the elliptical hole.

5.4.2 Plate with Elliptical Hole

Again element HEL710 was used around the hole while the rest of the plate was modeled with ELEM8. Stress concentrations of $4.76\,p_o$ and $8.47\,p_o$ were computed at the point of maximum stress with Mesh-1 and Mesh-2, respectively. The analysis did not converge to the correct solution of $9.50\,p_o$ and proved element HEL710 unsuccessful, in all respects. Firstly, element HEL710 employs 25 betas resulting in a matrix of order (25 x 25). Inversion of this matrix makes element HEL710 almost twice as expensive as element HISQUE. Secondly, element HEL710 employs four degrees of freedom more than element HISQUE, resulting in a larger global stiffness matrix and hence additional computational cost.

5.5 Concluding Remarks

The normal stresses around the boundary of the elliptical hole, as

determined by element HEL710 with Mesh-2, are plotted in Figure 13, against the polar coordinate location of the hole θ. As angle θ increases, the ellipse exhibits more pronounced curvature variations; subsequently element HEL710 is unable to contain the magnitude of the normal stress close to zero. Elements inaccuracy is also partially due to the unbalanced nature of this element. Introduction of additional nodes will increase the cost of the element and further deteriorate any possible ability to compete against element HISQUE on economical grounds.

Development of a more balanced element (i.e., comparable number of nodes on boundaries) which identically satisfies the traction free condition at the hole is judged most effective for analysis.

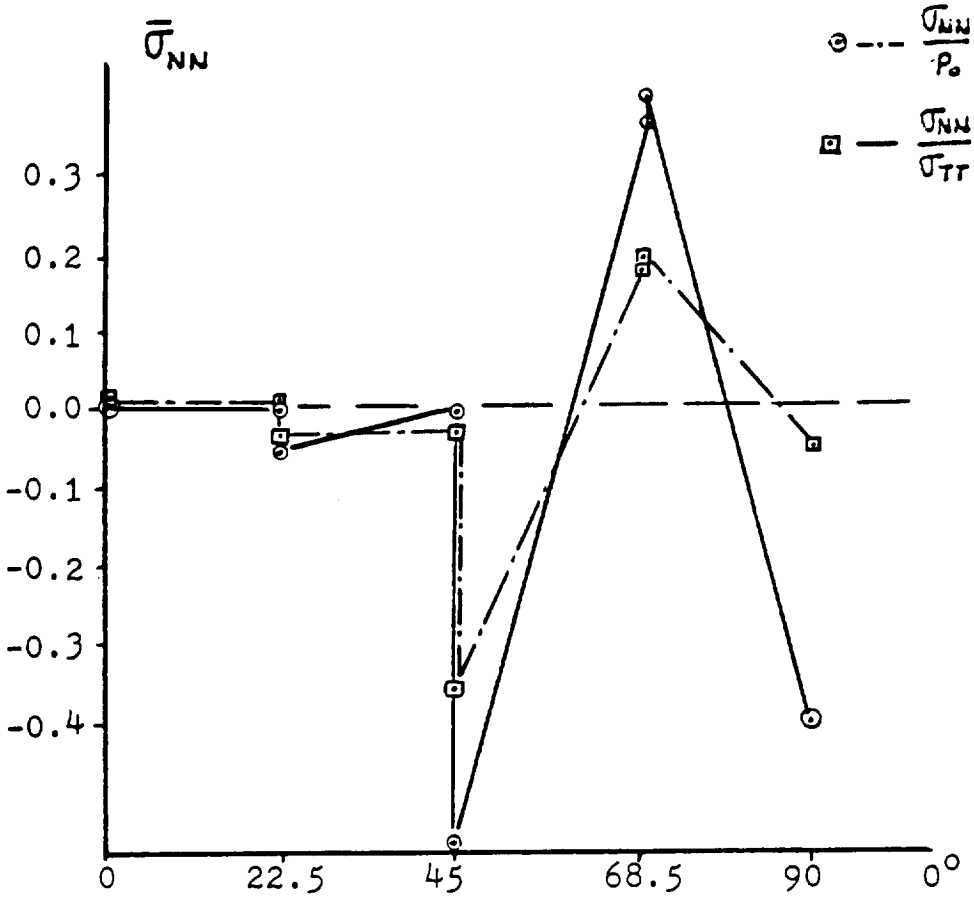

Figure-13 Distribution Of The Normal Stress At The Elliptical Hole By HEL710

CHAPTER 6

A Four-Node Element With a Circular Traction Free Edge

6.1 Introduction and Objective

Instead of pointwise satisfaction of the free traction condition at the hole, via boundary point matching or other similar techniques, it is possible to formulate an element which will exactly satisfy this stress boundary condition at a circular hole. To this end a four-node element which incorporates a built-in traction free circular edge is formulated in polar coordinates. Although restricted to analysis of circular holes, the four-node polar element, named PET4, will serve as a model element for comparative evaluation.

Element PET4 is formulated with two different sets of assumed stresses. The first set of stresses satisfies the equilibrium conditions while the second set satisfies the stress compatibility conditions in addition to equilibrium. The objective is again for the improvement of solution accuracy, and efficiency, compared to other efficient alternatives, namely the mixed model approach of Chapter 4.

6.2 Formulation of Element PET4

The formulation of element PET4 is based on the modified complementary energy functional π_{MC}. In the π_{MC} formulation the matrix $\underset{\sim}{G}$ is determined by integrating the product of boundary tractions and inter-element displacements, around the element boundary (equation 2.7). Since element PET4 has prescribed zero tractions on the circular edge, evalua-

tion of matrix $\underset{\sim}{G}$ is needed on the remaining three edges only. Figure 14 shows the nodes of element PET4.

6.2.1 The Assumed Stresses

If the origin of the system of coordinates is located at the center of the circular hole, then the condition of zero traction at the hole reduces to simple constraints imposed on the stresses in polar coordinates:

$$\sigma_{rr}\Big|_{r=a} = \sigma_{r\theta}\Big|_{r=a} = 0 \tag{6.1}$$

where:

$a \equiv$ Radius of the circular hole.

A set of assumed stresses that identically satisfy the equations of equilibrium can be obtained from the Airy stress function ϕ[14].

$$\begin{aligned} \sigma_{rr} &= \frac{1}{r}\frac{\partial \phi}{\partial r} + \frac{1}{r^2}\frac{\partial^2 \phi}{\partial \theta^2} \\ \sigma_{\theta\theta} &= \frac{\partial^2 \phi}{\partial r^2} \\ \sigma_{r\theta} &= -\frac{\partial}{\partial r}\left(\frac{1}{r}\frac{\partial \phi}{\partial r}\right) \end{aligned} \tag{6.2}$$

Assuming the Airy stress function to be of the form

$$\phi = \sum_{k}\sum_{n} A_{kn} r^{n} \left\{ \cos k\theta \; ; \; \sin k\theta \right\} \tag{6.3}$$

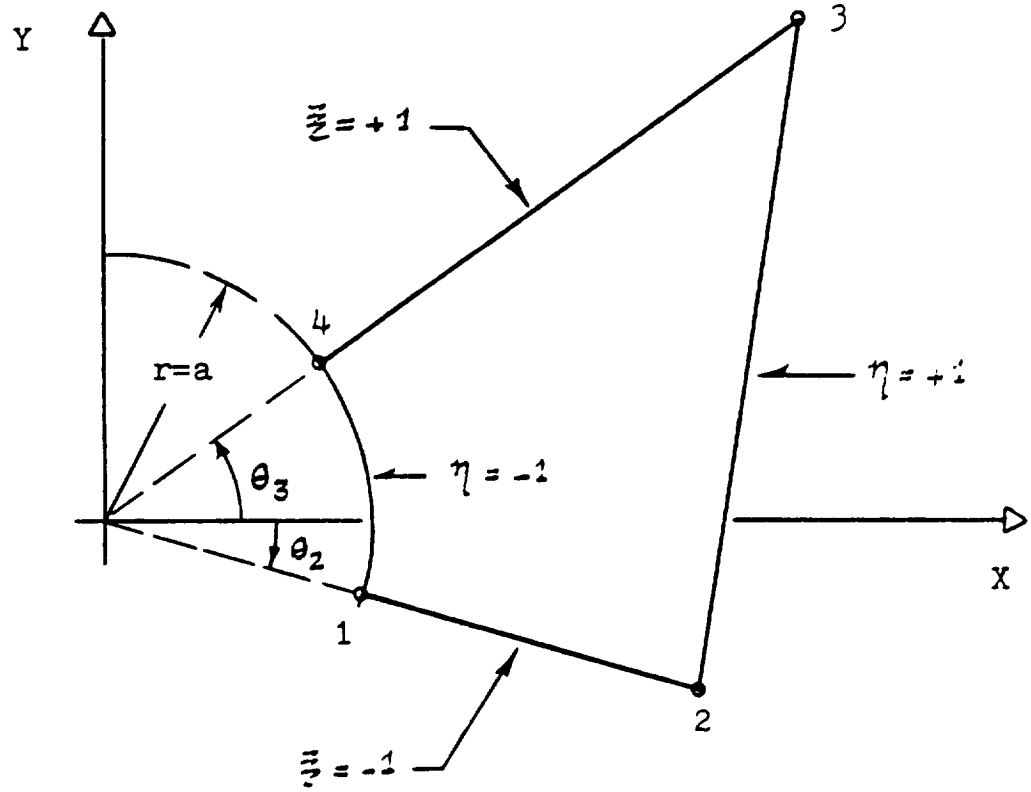

Figure-14 The Polar Traction-Free Element PET4

then substitution of equation (6.3) into equations (6.2) yields:

$$\sigma_{rr} = \sum_k \sum_n A_{kn} (n-k^2) r^{n-2} \left\{ \cos k\theta \; ; \; \sin k\theta \right\}$$
$$\sigma_{\theta\theta} = \sum_k \sum_n A_{kn} n(n-1) r^{n-2} \left\{ \cos k\theta \; ; \; \sin k\theta \right\} \qquad (6.4)$$
$$\sigma_{r\theta} = \sum_k \sum_n A_{kn} (1-n) r^{n-2} \left\{ -\sin k\theta \; ; \; \cos k\theta \right\}$$

Expanding equations (6.4) with both terms $\cos k\theta$ and $\sin k\theta$ will provide a set of stresses weighted with respect to the coefficients A_{kn}. Imposing the zero traction condition of equation (6.1) will reduce the number of constant coefficients and hence will in general provide an infinite series of polynomials in r and transcendental circular functions of θ. An expansion of the terms with:

$$k = 0, 1$$
$$n = 0, 1, 2, 3, 4, 5$$

resulted in a twelve-term set of stresses. After rearranging the terms in increasing powers of r and redefining the coefficients A_{kn} as β_i, the following result is obtained:

$$\sigma_{rr} = 2\left(1-\frac{a}{r}\right)\beta_1 + \left(1-\frac{a^2}{r^2}\right)\cos\theta\,\beta_2 + \left(1-\frac{a^2}{r^2}\right)\sin\theta\,\beta_3$$
$$+ 3\left(r-\frac{a^2}{r}\right)\beta_4 + 2\left(r-\frac{a^3}{r^2}\right)\cos\theta\,\beta_5 + 2\left(r-\frac{a^3}{r^2}\right)\sin\theta\,\beta_6$$
$$+ 4\left(r^2-\frac{a^3}{r}\right)\beta_7 + 3\left(r^2-\frac{a^4}{r^2}\right)\cos\theta\,\beta_8 + 3\left(r^2-\frac{a^4}{r^2}\right)\sin\theta\,\beta_9$$
$$+ 5\left(r^3-\frac{a^4}{r}\right)\beta_{10} + 4\left(r^3-\frac{a^5}{r^2}\right)\cos\theta\,\beta_{11} + 4\left(r^3-\frac{a^5}{r^2}\right)\sin\theta\,\beta_{12}$$

$$
\begin{aligned}
\sigma_{\theta\theta} &= 2\beta_1 + 2\cos\theta\,\beta_2 + 2\sin\theta\,\beta_3 + 6r\beta_4 \\
&+ 6r\cos\theta\,\beta_5 + 6r\sin\theta\,\beta_6 + 12r^2\beta_7 \\
&+ 12r^2\cos\theta\,\beta_8 + 12r^2\sin\theta\,\beta_9 + 20r^3\beta_{10} \\
&+ 20r^3\cos\theta\,\beta_{11} + 20r^3\sin\theta\,\beta_{12}
\end{aligned}
\tag{6.5}
$$

$$
\begin{aligned}
\sigma_{r\theta} &= \left(1 - \frac{a^2}{r^2}\right)\sin\theta\,\beta_2 + \left(\frac{a^2}{r^2} - 1\right)\cos\theta\,\beta_3 \\
&+ 2\left(r - \frac{a^3}{r^2}\right)\sin\theta\,\beta_5 + 2\left(\frac{a^3}{r^2} - r\right)\cos\theta\,\beta_6 \\
&+ 3\left(r^2 - \frac{a^4}{r^2}\right)\sin\theta\,\beta_8 + 3\left(\frac{a^4}{r^2} - r^2\right)\cos\theta\,\beta_9 \\
&+ 4\left(r^3 - \frac{a^5}{r^2}\right)\sin\theta\,\beta_{11} + 4\left(\frac{a^5}{r^2} - r^3\right)\cos\theta\,\beta_{12}
\end{aligned}
$$

or in matrix form:

$$
\underset{\sim}{\sigma} = \begin{Bmatrix} \sigma_{rr} \\ \sigma_{\theta\theta} \\ \sigma_{r\theta} \end{Bmatrix} = \underset{\sim}{P}\,\underset{\sim}{\beta} \tag{6.6}
$$

Equations (6.5) show that retaining all 12 betas in the assumed stresses will result in a cubic distribution, while truncating the series after β_9 will render a quadratic distribution of the stresses. The full set of stresses of equations (6.5), with twelve betas, was used in element PET4/12, and the truncated series with nine betas was used in element PET4/9. Equation (2.6) will then determine matrix $\underset{\sim}{H}$.

6.2.2 Displacement Interpolations

The displacement interpolations are required along the boundary for evaluation of the $\underset{\sim}{G}$ matrix. Along the edges connecting nodes 1-2, 2-3, and 3-4 (Figure 14), a linear interpolation between the nodal displacements will ensure interelement compatibility.

Along any straight edge i connecting nodes i and i + 1 (Figure 15):

$$u_i = \begin{Bmatrix} u_x \\ u_y \end{Bmatrix} = \underset{\sim}{L}_i \underset{\sim}{q}_i \tag{6.7}$$

It should be noted that displacements are interpolated in the Cartesian coordinates to finally render the stiffness matrix in the Cartesian rather than polar system of coordinates. Therefore it follows that at edge i:

$$u = \frac{\zeta}{2}(u_{i+1} - u_i) + \frac{1}{2}(u_{i+1} + u_i) \tag{6.8}$$

where: $\zeta = \frac{2}{\ell}\left(s - \frac{\ell}{2}\right)$

$s \equiv$ length along side i from node i.

Equation (6.8) applies to displacements u_x and u_y both. If the matrix $\underset{\sim}{q}$ is defined:

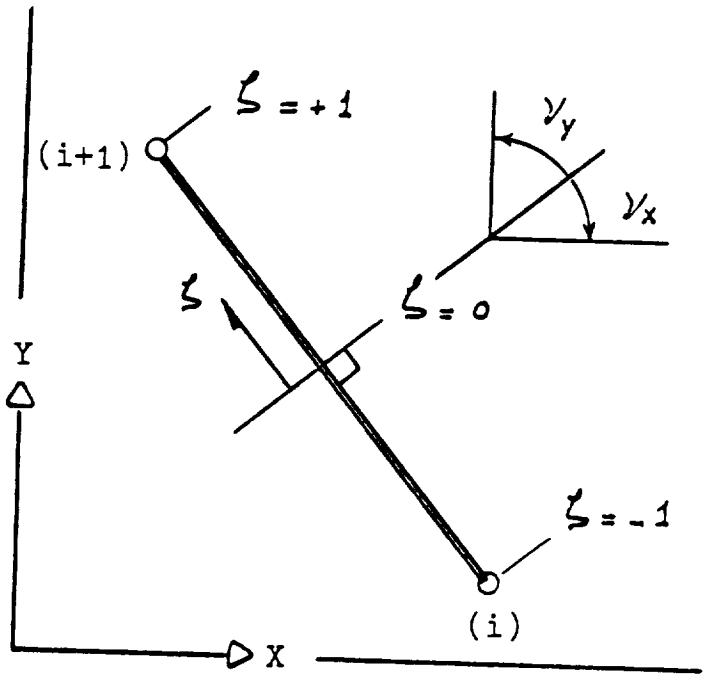

Figure-15 Boundary Interpolation And Direction Cosines Of Edge i

$$\underset{\sim}{q} = \begin{Bmatrix} u_1 \\ v_1 \\ u_2 \\ v_2 \\ \vdots \\ v_4 \end{Bmatrix} \tag{6.9}$$

Then from equations (6.7), (6.8) and (6.9) it follows for side i:

$$\begin{aligned} L_{1,2i-1} &= \tfrac{1}{2}(1-\zeta) \\ L_{1,2i+1} &= \tfrac{1}{2}(1+\zeta) \\ L_{2,2i} &= \tfrac{1}{2}(1-\zeta) \\ L_{2,2i+2} &= \tfrac{1}{2}(1+\zeta) \qquad ; \quad i = 1,2,3 \end{aligned} \tag{6.10}$$

Again, no interpolation along the circular edge (4-1) is needed since no integration is required at this edge.

The $\underset{\sim}{G}$ matrix is then determined from:

$$\underset{\sim}{G} = \int_{\partial V} \underset{\sim}{\rho}^T \underset{\sim}{\gamma}\, \underset{\sim}{L}\, dS \tag{2.7}$$

since $\underset{\sim}{L}$ is the matrix of displacement interpolations in Cartesian coordinates, a transformation of the stresses from their original polar coordinates is necessary:

$$\underset{\sim}{\sigma} = \underset{\sim}{T}\,\bar{\underset{\sim}{\sigma}} = \hat{\underset{\sim}{\rho}}\,\underset{\sim}{\beta} \tag{6.11}$$

$$\underset{\sim}{\sigma} \equiv \text{Cartesian based stresses}$$

$$\underset{\sim}{T} \equiv \text{Transformation matrix} \tag{6.11}$$

$$\underset{\sim}{\bar{\sigma}} \equiv \text{Polar based stresses} = \underset{\sim}{\rho}/\underset{\sim}{\beta}$$

hence:

$$\underset{\sim}{\hat{\rho}} = \underset{\sim}{T}\,\underset{\sim}{\rho} \tag{6.12}$$

Where $\underset{\sim}{T}$ is the familiar transformation matrix due to rotation of the axes:

$$\underset{\sim}{T} = \begin{bmatrix} m^2 & n^2 & -2mn \\ n^2 & m^2 & 2mn \\ mn & -mn & m^2-n^2 \end{bmatrix} \tag{6.13}$$

$m = \cos\theta$

$n = \sin\theta$

$\theta \equiv$ Angle of rotation

In equation (2.7), $\underset{\sim}{\gamma}$ is defined as the matrix of direction cosines of Figure 15:

$$\underset{\sim}{\gamma} = \begin{bmatrix} \gamma_x & 0 & \gamma_y \\ 0 & \gamma_y & \gamma_x \end{bmatrix} \tag{6.14}$$

which when multiplied by the stresses produce the traction vector.

From (2.7):

$$\underset{\sim}{G} = \int_{\partial V} \underset{\sim}{\hat{P}}^{T} \underset{\sim}{\gamma} \underset{\sim}{L} \, dS$$

From (6.12):

$$\underset{\sim}{G} = \int_{\partial V} \underset{\sim}{P}^{T} \underset{\sim}{T}^{T} \underset{\sim}{\gamma} \underset{\sim}{L} \, dS$$

$$\underset{\sim}{G} = \int_{\partial V} \underset{\sim}{P}^{T} \underset{\sim}{\bar{\gamma}} \underset{\sim}{L} \, dS \qquad (6.15)$$

From equations (6.13) and (6.14) it follows:

$$\underset{\sim}{\bar{\gamma}} = \underset{\sim}{\bar{T}}^{T} \underset{\sim}{\gamma}$$

$$\underset{\sim}{\bar{\gamma}} = \begin{bmatrix} m^2\gamma_x + mn\,\gamma_y & n^2\gamma_y + mn\,\gamma_x \\ n^2\gamma_x - mn\,\gamma_y & m^2\gamma_y - mn\,\gamma_x \\ -2mn\,\gamma_x + \gamma_y(m^2 - n^2) & 2mn\,\gamma_y + \gamma_x(m^2 - n^2) \end{bmatrix} \qquad (6.16)$$

As defined by equation (6.16), the matrix $\underset{\sim}{\bar{\gamma}}$ will transform stresses in polar coordinates to tractions in Cartesian coordinates, at any point ϑ on a boundary. Thus all the matrices of equation (6.15) are defined for integration.

6.2.3 Implementation and Numerical Integration

For a Gauss-quadrature numerical integration of equation (2.6) a coordinate transformation is necessary:

$$\underset{\sim}{H} = t\int_A \underset{\sim}{F}(r,\theta)\, r\, dr\, d\theta = t\int_{-1}^{+1}\int_{-1}^{+1} \underset{\sim}{F}(\xi,\eta)\,|\underset{\sim}{J}|\, d\xi\, d\eta \qquad (6.17)$$

where:

$$\underset{\sim}{F}(r,\theta) \equiv \underset{\sim}{\rho}^T \underset{\sim}{S}\, \underset{\sim}{\rho}$$

$$\underset{\sim}{J} \equiv \text{Jacobian matrix of transformation}$$

For the transformation of equation (6.17) the polar coordinates are to be expressed in the ξ,η system:

$$\theta = f(\xi,\eta) \qquad (6.18)$$

$$r = g(\xi,\eta) \qquad (6.19)$$

From Figure 14 it is seen that if sides connected by nodes 1-2 and 3-4 are radial, and hence functions of r only, then function f of equation (6.18) constitutes a linear interpolation of angles labeled θ_2 and θ_3 in Figure 14.

$$\theta = \underset{\sim}{\xi}\left(\frac{\theta_3 - \theta_2}{2}\right) + \left(\frac{\theta_3 + \theta_2}{2}\right) \qquad (6.20)$$

Where $\underset{\sim}{\xi}$ is the non-dimensional coordinate of equation (6.17) defined to assume values of +1 and -1 at the boundaries 1-2 and 3-4, of Figure 14,

respectively. This assumption forces element PET4 to possess two radial edges, but its adoption results in considerable simplifications and is hence preferable.

With θ interpolation fixed, interpolation in the r direction is straightforward. Defining the non-dimensional coordinate η to be -1 at the circular edge 4-1 and +1 at the straight edge 2-3, then:

$$r = a \quad ; \quad \eta = -1 \tag{6.21a}$$

$$r = h(\theta) \quad ; \quad \eta = +1 \tag{6.21b}$$

$$\text{where;} \quad h(\theta) = \frac{X_2 Y_3 - X_3 Y_2}{(X_2 - X_3)\sin\theta - (Y_2 - Y_3)\cos\theta} \tag{6.22}$$

is the equation of line 2-3 in polar coordinates. In equation (6.22), x_i, y_i are the Cartesian coordinates of node i. The interpolation in the r direction is then simply:

$$r = \frac{1}{2}\left[h(\theta) - a\right]\eta + \frac{1}{2}\left[h(\theta) + a\right] \tag{6.23}$$

It is seen that equation (6.23) reduces to the conditions of equations (6.21).

With functions f and g of equations (6.18) and (6.19) defined the Jacobian of the transformation is given:

$$\underset{\sim}{J} = \begin{bmatrix} \frac{\partial r}{\partial \xi} & \frac{\partial r}{\partial \eta} \\ \frac{\partial \theta}{\partial \xi} & \frac{\partial \theta}{\partial \eta} \end{bmatrix}$$

From equation (6.20), it is clear that θ is independent of η and therefore the determinant of the Jacobian matrix simplifies:

$$det(\underset{\sim}{J}) = \frac{\theta_3 - \theta_2}{\delta} \left\{ [h(\theta) - a]^2 \eta + h^2(\theta) - a^2 \right\} \qquad (6.24)$$

For a numerical integration of the matrix $\underset{\sim}{H}$ as shown in equation (6.17), Gauss integration stations ξ_i and η_j are picked and their corresponding r and θ coordinates are determined from equations (6.20) and (6.23). This in turn enables the evaluation of the stress matrix $\underset{\sim}{\rho}$ at any integration point. Equation (6.17) then reduces to the familiar form:

$$\underset{\sim}{H} = t \sum_i \sum_j \underset{\sim}{F}(\xi_i, \eta_j) \left| \underset{\sim}{J}(\xi_i, \eta_j) \right| W_i W_j \qquad (6.25)$$

where:

W_i = Gauss integration weights.

For the numerical integration of equation (6.15), the linear interpolation of equation (6.8) is used:

$$x(\zeta_n) = \frac{\zeta_n}{2}(x_{i+1} - x_i) + \frac{1}{2}(x_{i+1} + x_i)$$

$$y(\zeta_n) = \frac{\zeta_n}{2}(y_{i+1} - y_i) + \frac{1}{2}(y_{i+1} + y_i) \quad ; \text{edge } (i, i+1)$$

where: $\zeta_n \equiv$ Gauss integration station

therefore: $$r(\zeta_n) = \sqrt{x^2(\zeta_n) + y^2(\zeta_n)}$$

$$\theta = \theta(\zeta_n) = \tan^{-1}\left[\frac{y(\zeta_n)}{x(\zeta_n)}\right]$$

Direction cosines of equation (6.16) are also defined for edge (i, i + 1)

$$\gamma_x = \cos\left\{\tan^{-1}\left(\frac{x_{i+1} - x_i}{y_i - y_{i+1}}\right)\right\}$$

$$\gamma_y = \sin\left\{\tan^{-1}\left(\frac{x_{i+1} - x_i}{y_i - y_{i+1}}\right)\right\}$$

Equation (6.15) can then be broken into three separate integrals along the three straight edges of the element

$$\underset{\sim}{G} = \sum_{i=1}^{3} \underset{\sim}{S}_i \qquad (6.26)$$

where:

$$\underset{\sim}{G}_i = \sum_j \underset{\sim}{F}(\zeta_j) \frac{d\Delta}{d\zeta} W_j \qquad (6.27)$$

From equation (6.15):

$$\underset{\sim}{F}(\zeta_j) = \left[\underset{\sim}{\rho}^T \underset{\sim}{\bar{y}} \underset{\sim}{L} \right]_{\zeta_j}$$

And from equation (6.8):

$$\frac{d\Delta}{d\zeta} = \frac{\ell}{2}$$

Equation (2.18), along with (6.25), (6.26) and (6.27) determine the stiffness matrix $\underset{\sim}{k}$.

In most cases a 5 point Gauss integration was found sufficient for accurate integration of matrices $\underset{\sim}{H}$ and $\underset{\sim}{G}$. For the complete stress distribution of equation (6.5) with 12 betas, 7 points were required to integrate the $\underset{\sim}{G}$ matrix.

6.2.4 Element PET4X5

As previously discussed in Chapter 4, in two dimensional plane analysis, the assumed stresses can be chosen such that the condition of compatibility is also satisfied:

$$\nabla^4 \phi = 0 \qquad (4.15)$$

If the Airy stress function is assumed to be [14][15]:

$$\phi = \phi^{(0)}(r) + \sum_{n=1}^{\infty} \phi^{(n)}(r) \left\{ \begin{matrix} \sin n\theta \\ \cos n\theta \end{matrix} \right\}$$

$$\phi^{(0)}(r) = a_0 + b_0 \ln r + c_0 r^2 + d_0 r^2 \ln r \qquad (6.28)$$

$$\phi^{(n)}(r) = a_n r^n + b_n r^{-n} + c_n r^{2+n} + d_n r^{2-n}$$

then substitution of $\phi^{(0)}$ in equation (6.2) and (6.1) gives:

$$\sigma_{rr}^{(0)} = b_0 \left(\frac{1}{r^2} - \frac{1}{a^2} \right) + 2d_0 (\ln r - \ln a)$$

$$\sigma_{\theta\theta}^{(0)} = -b_0 \left(\frac{1}{r^2} + \frac{1}{a^2} \right) + 2d_0 (1 + \ln r - \ln a) \qquad (6.29)$$

$$\sigma_{r\theta}^{(0)} = 0$$

Similarly by substitution of $\phi^{(n)}$ it follows:

$$\sigma_{rr}^{(n)} = \left\{ \begin{matrix} (n^2-1) c_n a^2 r^{n-2} - (1-n) d_n a^{-2n+2} r^{n-2} \\ -(1+n) c_n a^{2n+2} r^{-n-2} - (1-n^2) d_n a^2 r^{-n-2} \\ + (2+n-n^2) c_n r^n + (2-n-n^2) d_n r^{-n} \end{matrix} \right\} \left\{ \begin{matrix} \sin n\theta \\ \cos n\theta \end{matrix} \right\}$$

$$\sigma_{\theta\theta}^{(n)} = \left\{ \begin{matrix} (1-n^2) c_n a^2 r^{n-2} + (1-n) d_n a^{-2n+2} r^{n-2} \\ + (1+n) c_n a^{2n+2} r^{-2-n} + (1-n^2) d_n a^2 r^{-n-2} \\ + (2+3n+n^2) c_n r^n + (2-3n+n^2) d_n r^{-n} \end{matrix} \right\} \left\{ \begin{matrix} \sin n\theta \\ \cos n\theta \end{matrix} \right\} \qquad (6.30)$$

$$\sigma_{r\theta}^{(n)} = \Big\{ (1-n^2) C_n a^2 r^{n-2} + (1-n) d_n a^{-2n+2} r^{n-2}$$
$$- (1+n) C_n a^{2n+2} r^{-n-2} - (1-n^2) d_n a^2 r^{-n-2}$$
$$+ (n^2+n) C_n r^n + (n-n^2) d_n r^{-n} \Big\} (-\cos n\theta ; \sin n\theta) \qquad (6.30)$$

In condensed matrix notation:

$$\underset{\sim}{\sigma} = \underset{\sim}{\sigma}^{(0)} + \sum_{n}^{\infty} \underset{\sim}{\sigma}^{(n)}$$

If the logarithmic terms appearing in $\underset{\sim}{\sigma}^{(0)}$ are dropped; for n = 1, 2 the following results are obtained:

$$\sigma_{rr} = \left(1 - \frac{a^2}{r^2}\right)\beta_1 + \left(r - \frac{a^4}{r^3}\right)\left\{\cos\theta\beta_2 + \sin\theta\beta_3\right\}$$
$$+ \left(1 + \frac{3a^4}{r^4} - \frac{4a^2}{r^2}\right)\left\{\cos 2\theta\beta_4 + \sin 2\theta\beta_5\right\}$$
$$\sigma_{\theta\theta} = \left(1 + \frac{a^2}{r^2}\right)\beta_1 + \left(3r + \frac{a^4}{r^3}\right)\left\{\cos\theta\beta_2 + \sin\theta\beta_3\right\}$$
$$- \left(1 + \frac{3a^4}{r^4}\right)\left\{\cos 2\theta\beta_4 + \sin 2\theta\beta_5\right\} \qquad (6.31)$$
$$\sigma_{r\theta} = \left(r - \frac{a^4}{r^3}\right)\left\{\sin\theta\beta_2 - \cos\theta\beta_3\right\}$$
$$+ \left(\frac{3a^4}{r^4} - \frac{2a^2}{r^2} - 1\right)\left\{\sin 2\theta\beta_4 - \cos 2\theta\beta_5\right\}$$

where the coefficients C_n and D_n of equations (6.29) and (6.30) are replaced with β's.

Using the assumed stresses of equation (6.31), element PET4 will satisfy conditions of stress equilibrium, compatibility and free traction at the boundary, in addition to interelement compatibility. As shown in equation (6.31) only 5 betas are present in the assumed stresses and therefore the size of the matrix $\underset{\sim}{H}$ is kept to a minimum. The element using the set of stresses of equation (6.31) is named PET4X5 and with the exception of the assumed stresses, its formulation is identical to elements PET4/9 and PET4/12 discussed earlier.

6.3 Results and Discussion

On the finite element model of the plate with circular hole elements PET4 were used at the hole boundary. Since elements PET4 possess two nodes at each edge, a compatible four-node displacement based isoparametric element [12], called ELEM4, was used to model the plate away from the hole.

The plate was analyzed with elements PET4/9 and PET4/12 to determine the optimum set of assumed stresses between the two. Element PET4/12 was found superior in performance although a converged stress solution was not obtained with Mesh-2 in either case. Figure 16 shows a plot of the stresses obtained with the two elements. The percent error of the stresses are summarized in the following table:

Element Type	% error	
	Mesh-1	Mesh-2
PET4/9	-30.7	-12.2
PET4/12	-36.0	-8.31

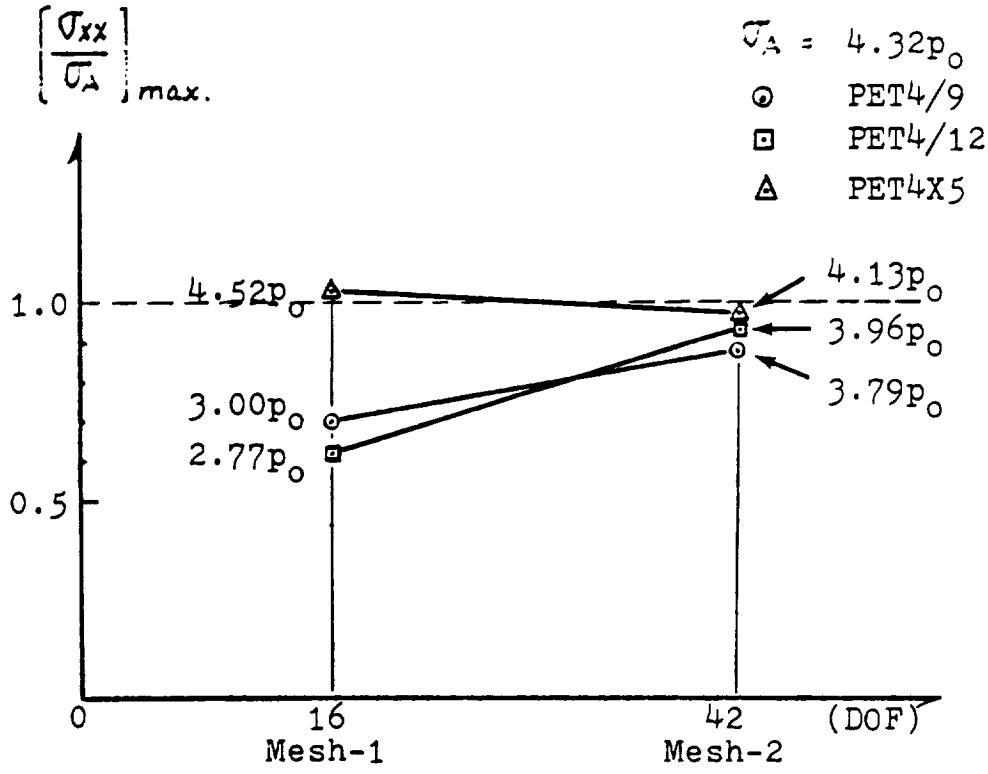

Figure-16 Maximum Stress σ_{xx} In Plate With Circular Hole

Although the results may at first appear unsatisfactory, a closer comparison of Figure 16 and Figure 6 will indicate that analysis with elements PET4 utilizes less than half of the number of degrees of freedom of an equivalent model using eight node elements. Element PET4/12 is in addition much more economical than element HISQUE, when employing 8 nodes and 18 betas. Combined with the four-node displacement based elements ELEM4, a reduction of more than 50% in the total solution time (CPU) resulted in comparison with the eight node analysis of the same mesh.

Element PET4X5 is yet more economical than element PET4/12 in that it only uses 5 betas. With Mesh-1, employing a total of 16 degrees of freedom, PET4X5 produced a stress concentration of $4.52\,p_o$, already within the acceptable margin of $\pm 5\%$. With Mesh-2 a stress concentration of $4.13\,p_o$ (error = -4.4%) was predicted. These results are also plotted in Figure 16. The in plane stress σ_{xx} along the y axis, obtained with PET4X5, is plotted in Figure 17 for Mesh-1 and Mesh-2. Element PET4X5 is judged so far the most efficient and effective finite element in analysis of stress concentration around circular holes.

6.4 Concluding Remarks

Satisfactory stress solutions of element PET4X5 suggest that in addition to assuring the traction free boundary condition at the hole, satisfaction of stress compatibility conditions will further improve the performance of the element. In the case of element PET4/12, where compatibility conditions are not met, the stress solution contained

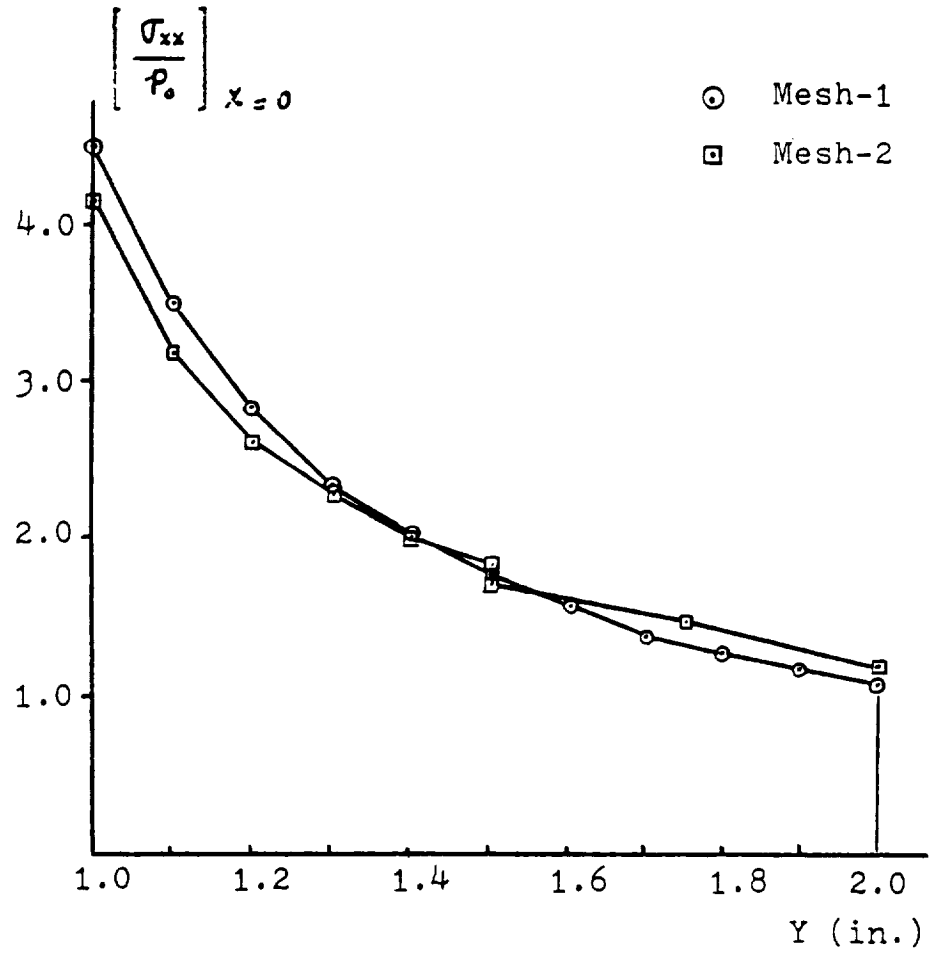

Figure-17 Stress Profile Of Plate With Circular Hole By Element PET4X5

8.3% error when modeled with Mesh-2. In view of the considerable cost reductions achieved with element PET4/12, in addition to the fact that few degrees of freedom (42) were used in analysis, this element presents desirable advantages compared to the eight node hybrid isoparametric element HISQUE. The apparent failure of element PET4/12 is nevertheless more due to the ineffectiveness of the four-node elements in connects than its own capabilities.

CHAPTER 7

Conclusion

7.1 An Eclectic Approach

Use of hybrid isoparametric finite elements was found more desirable than their displacement based counterparts in stress concentration analysis around holes. Although these elements do not strictly satisfy the required traction free boundary condition, they consistently approximated this condition more accurately than the conventional displacement element.

Adoption of the boundary point matching technique was seen to reduce element cost effectiveness without a justifiable proportional increase in element accuracy. However, improvement in solution accuracy and efficiency was achieved when the free traction condition at the hole was exactly satisfied by adoption of an appropriate set of assumed stresses. Here, hybrid formulation provides the only effective means of satisfying stress boundary conditions.

Further improvements resulted when in addition to satisfaction of boundary traction, stress compatibility conditions were also satisfied. This deduction is a natural consequence of satisfying stress equilibrium, compatibility, boundary traction and interelement displacement continuity in such finite elements.

In three dimensional elements, satisfaction of stress compatibility may prove too difficult although other requirements met in two dimen-

sional analysis can be assured. A general formulation of two dimensional hybrid isoparametric elements that incorporate any number of traction free boundaries is provided in Appendix A. This formulation can be extended to solid elements and its generality affords satisfaction of free traction condition on boundaries of arbitrary geometry.

Finally, employment of such specialized hybrid elements leads to an eclectic modeling of the physical problem which in general yields more efficient and accurate solutions. This implies use of specialized elements where stress boundary conditions are prescribed, hybrid elements in regions of high stress gradients, and displacement elements otherwise. Indeed in problems of stress concentration, fracture mechanics, or wave propagation use of hybrid elements will provide noticeable improvements.

7.2 Recommended Research

The twelve node solid element of Figure 18, as well as the two dimensional six node elements it incorporates on each side can be formulated by the approach of Appendix A. Performance of the six node element should be compared with elements HISQUE and PET4 of Chapters 4 and 6. In this element node 5 is introduced on the mid-boundary to provide a traction free edge of flexible geometry, while node 6 is to allow connection with eight node elements for added effectiveness. Satisfactory results with the two dimensional element should justify its extension to a study of the twelve-node solid element.

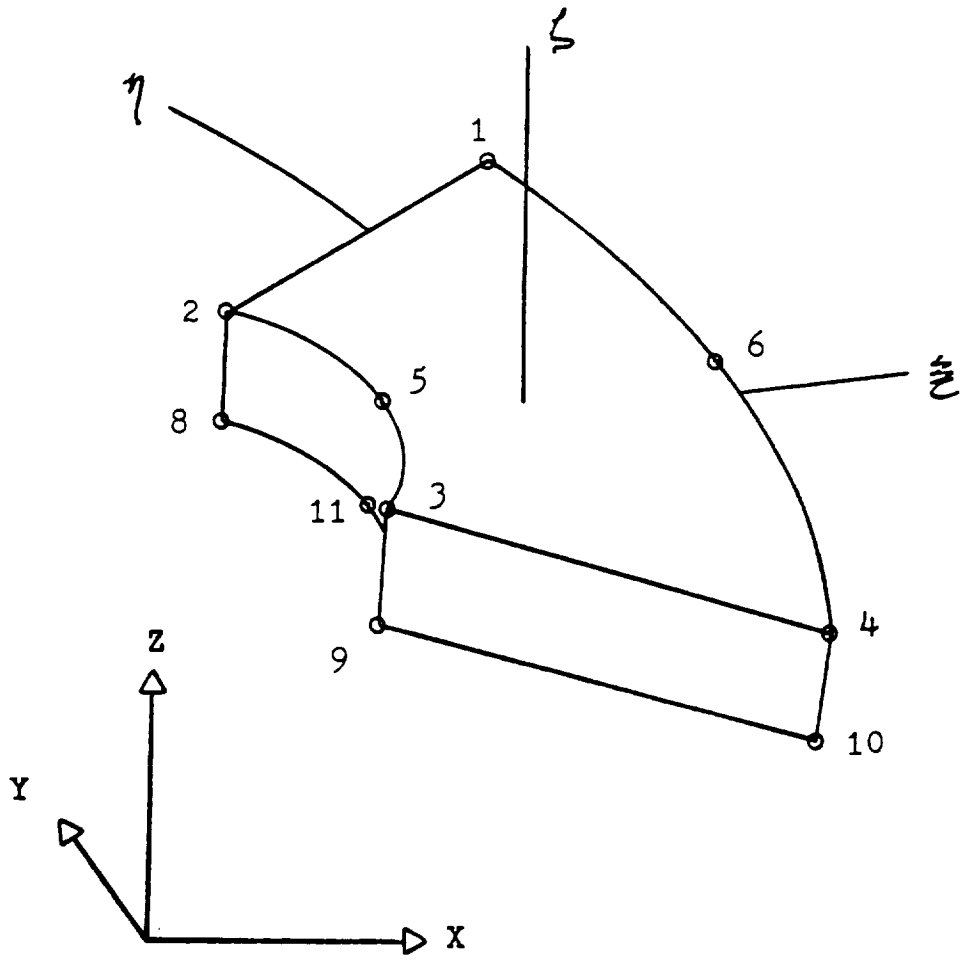

Figure-18 A Twelve-Node Traction-Free Solid Element

APPENDIX A

Satisfaction of Free Traction Boundary Condition in Assumed Stress Hybrid Isoparametric Finite Elements

A.1 Introduction and Objective

In finite element analysis of stress concentrations induced by the presnece of holes in a structure, satisfaction of the free traction boundary condition at the hole becomes a prerequisite for effective stress computation. Since isoparametric finite elements conveniently conform to shapes of arbitrary geometry, formulation of a two dimensional hybrid isoparametric element that identically satisfies the condition of free traction at the boundary is developed. The general characteristic of this formulation makes it applicable to three dimensional solid elements as well.

A.2 Curvilinear Coordinates of Isoparametric Transformation

In isoparametric transformation, Cartesian coordinates X and Y are interpolated by a set of shape function h_i:

$$x = \sum_{i}^{n} x_i h_i \qquad \text{(A-1)}$$

$$y = \sum_{i}^{n} y_i h_i \qquad \text{(A-2)}$$

where:

(X_i, Y_i) ≡ Coordinate of node i.

n ≡ Number of nodes.

Equations (A-1) and (A-2) can be rewritten in summation form:

$$x = x_q h_q \qquad (A\text{-}3)$$

$$; \quad q = 1, 2, \ldots, n$$

$$y = y_q h_q \qquad (A\text{-}4)$$

In equations (A-1) through (A-4), h_i are functions of the isoparametric coordinates ξ^1 and ξ^2. From these equations the covariant base vectors of the isoparametric system are found [16]:

$$\bar{g}_1 = \left(x_q \frac{\partial h_q}{\partial \xi^1} \right) \bar{i}_1 + \left(y_q \frac{\partial h_q}{\partial \xi^1} \right) \bar{i}_2 \qquad (A\text{-}5)$$

$$\bar{g}_2 = \left(x_q \frac{\partial h_q}{\partial \xi^2} \right) \bar{i}_1 + \left(y_q \frac{\partial h_q}{\partial \xi^2} \right) \bar{i}_2 \qquad (A\text{-}6)$$

from which the covariant metric tensor results:

$$g_{11} = \left(x_q \frac{\partial h_q}{\partial \xi^1} \right)^2 + \left(y_q \frac{\partial h_q}{\partial \xi^1} \right)^2 \qquad (A\text{-}7)$$

$$g_{12} = \left(x_q \frac{\partial h_q}{\partial \xi_1}\right)\left(x_q \frac{\partial h_q}{\partial \xi_2}\right) + \left(y_q \frac{\partial h_q}{\partial \xi_1}\right)\left(y_q \frac{\partial h_q}{\partial \xi_2}\right) \tag{A-8}$$

$$g_{22} = \left(x_q \frac{\partial h_q}{\partial \xi_2}\right)^2 + \left(y_q \frac{\partial h_q}{\partial \xi_2}\right)^2 \tag{A-9}$$

$$g = \det(g_{ij})$$

$$g = \left\{\left(x_q \frac{\partial h_q}{\partial \xi_1}\right)\left(y_q \frac{\partial h_q}{\partial \xi_2}\right) - \left(x_q \frac{\partial h_q}{\partial \xi_2}\right)\left(y_q \frac{\partial h_q}{\partial \xi_1}\right)\right\}^2 \tag{A-10}$$

The normal vector to the plane of the element, $\vec{n}_p$ can be determined from:

$$\vec{n}_p = \frac{\bar{g}_1 \times \bar{g}_2}{\sqrt{g}} = \vec{i}_3$$

The contravariant base vectors of a general isoparametric planar element follow:

$$\bar{g}^1 = \frac{\bar{g}_2 \times \vec{n}_p}{\sqrt{g}} = \frac{1}{\sqrt{g}}\left\{\left(y_q \frac{\partial h_q}{\partial \xi_2}\right)\bar{i}_1 - \left(x_q \frac{\partial h_q}{\partial \xi_2}\right)\bar{i}_2\right\} \tag{A-11}$$

$$\bar{g}^2 = \frac{\bar{n}_p \times \bar{g}_1}{\sqrt{g}} = \frac{1}{\sqrt{g}}\left\{-\left(y_q \frac{\partial h_q}{\partial \xi_1}\right)\bar{i}_1 + \left(x_q \frac{\partial h_q}{\partial \xi_1}\right)\bar{i}_2\right\} \tag{A-12}$$

The Christoffel symbols of the transformation are defined:

$$\Gamma^k_{mn} = \bar{g}^k \cdot \frac{\partial \bar{g}_m}{\partial \xi^n} = \Gamma^k_{nm}$$

Defining:

$$f_{,i} = \frac{\partial f}{\partial \xi^i}$$

$$f_{,ij} = \frac{\partial^2 f}{\partial \xi^i \partial \xi^j}$$

$$\Gamma_{11}^1 = \frac{1}{\sqrt{\beta}} \left\{ y_{,2}\, x_{,11} - x_{,2}\, y_{,11} \right\} \tag{A-13}$$

$$\Gamma_{12}^1 = \frac{1}{\sqrt{\beta}} \left\{ y_{,2}\, x_{,11} - x_{,2}\, y_{,12} \right\} \tag{A-14}$$

$$\Gamma_{22}^1 = \frac{1}{\sqrt{\beta}} \left\{ y_{,2}\, x_{,22} - x_{,2}\, y_{,22} \right\} \tag{A-15}$$

$$\Gamma_{11}^2 = \frac{1}{\sqrt{\beta}} \left\{ -y_{,1}\, x_{,11} + x_{,1}\, y_{,11} \right\} \tag{A-16}$$

$$\Gamma_{12}^2 = \frac{1}{\sqrt{\beta}} \left\{ -y_{,1}\, x_{,12} + x_{,1}\, y_{,12} \right\} \tag{A-17}$$

$$\Gamma_{22}^2 = \frac{1}{\sqrt{\beta}} \left\{ -y_{,1}\, x_{,22} + x_{,1}\, y_{,22} \right\} \tag{A-18}$$

A.3 The Boundary Normal and Traction Constraints

Consider the eight node isoparametric element shown in Figure A-1, with vector $\vec{T}$ designated as tangent to boundary $\xi' = -1$. This boundary constitutes a parabola, the equation of which is determined by element shape functions h_2, h_3, and h_6.

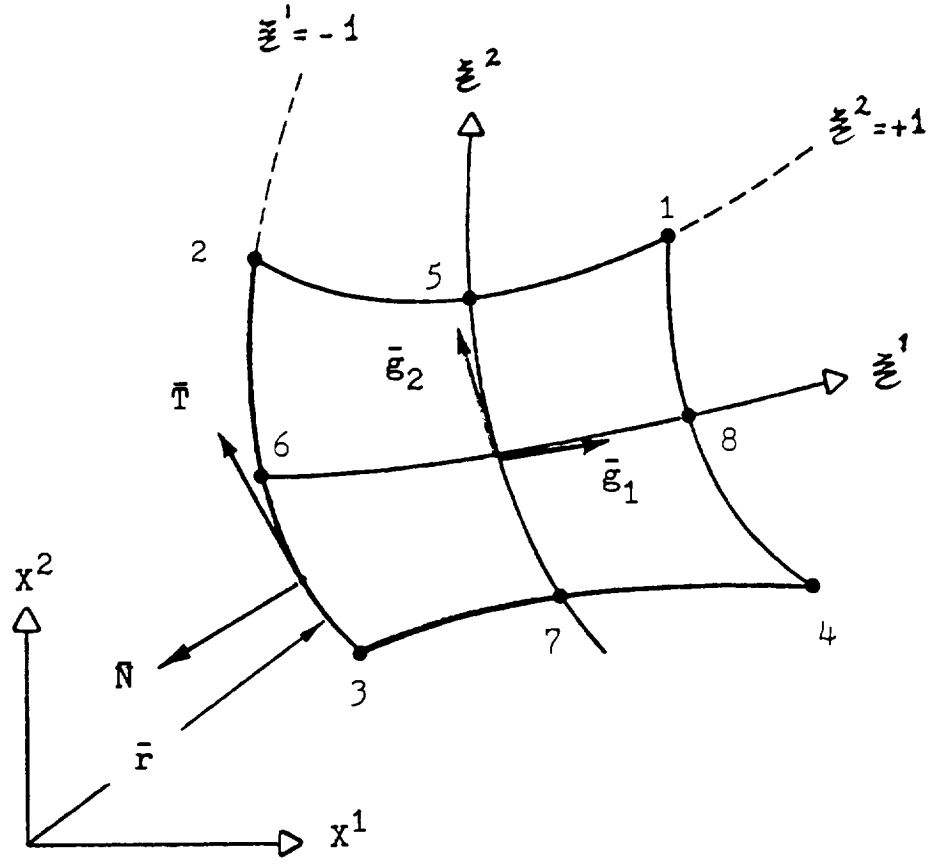

Figure A-1 The Eight-Node Planar Element

$$\vec{r} = (X_2 H_2 + X_3 H_3 + X_6 H_6)\,\vec{i}_1 + (Y_2 H_2 + Y_3 H_3 + Y_6 H_6) \qquad \text{(A-19)}$$

where: $$H_i \equiv h_i \Big|_{\xi' = -1} = H_i(\xi^2)$$

The tangent vector $\vec{T}$ follows directly from (A-19):

$$\vec{T} = \frac{\partial \vec{r}}{\partial \xi^2} = \left(X_2 \frac{\partial H_2}{\partial \xi^2} + X_3 \frac{\partial H_3}{\partial \xi^2} + X_6 \frac{\partial H_6}{\partial \xi^2}\right)\vec{i}_1 + \left(Y_2 \frac{\partial H_2}{\partial \xi^2} + Y_3 \frac{\partial H_3}{\partial \xi^2} + Y_6 \frac{\partial H_6}{\partial \xi^2}\right)\vec{i}_2 \qquad \text{(A-20)}$$

If the tangent vector is defined:

$$\vec{T} = (A\,\vec{i}_1 + B\,\vec{i}_2)$$

then the normal vector to this boundary is:

$$\vec{N} = (B\,\vec{i}_1 - A\,\vec{i}_2) \qquad \text{(A-21)}$$

$$\vec{N} \cdot \vec{T} = 0$$

It should be noted that $\vec{T}$, and $\vec{N}$ are not unit vectors, but can be normalized if needed. From equations (A-20) and (A-21) the normal vector results:

$$\vec{N} = \left(y_2 \frac{\partial H_2}{\partial \xi^2} + y_3 \frac{\partial H_3}{\partial \xi^2} + y_6 \frac{\partial H_6}{\partial \xi^2} \right) \vec{i}_1 - \left(x_2 \frac{\partial H_2}{\partial \xi^2} + x_3 \frac{\partial H_3}{\partial \xi^2} + x_6 \frac{\partial H_6}{\partial \xi^2} \right) \vec{i}_2 \qquad \text{(A-22)}$$

Equation (A-22) is then compared with the first contravariant base bector $\bar{g}^1$ given by equation (A-11). At the boundary $\xi^1 = -1$:

$$\bar{g}^1 = \frac{1}{\sqrt{g}} \left\{ \left(x_q \frac{\partial h_q}{\partial \xi^2} \right) \vec{i}_1 - \left(x_q \frac{\partial h_q}{\partial \xi^2} \right) \vec{i}_2 \right\} \Bigg|_{\xi^1 = -1} \qquad \text{(A-23)}$$

Noting that the shape functions h_g are defined to vanish at nodes $i \neq g$, equation (A-23) reduces to:

$$\bar{g}^1 = \frac{1}{\sqrt{g}} \left\{ \left(y_2 \frac{\partial h_2}{\partial \xi^2} + y_3 \frac{\partial h_3}{\partial \xi^2} + y_6 \frac{\partial h_6}{\partial \xi^2} \right) \vec{i}_1 - \left(x_2 \frac{\partial h_2}{\partial \xi^2} + x_3 \frac{\partial h_3}{\partial \xi^2} + x_6 \frac{\partial h_6}{\partial \xi^2} \right) \vec{i}_2 \right\} \Bigg|_{\xi^1 = -1} \qquad \text{(A-24)}$$

The vectors $\vec{N}$ and $\vec{g}^1$ defined by equations (A-22) and (A-24) are seen to be parallel since:

$$\frac{\partial H}{\partial \xi^2} = \frac{\partial}{\partial \xi^2} \left\{ h_j \Big|_{\xi^1 = -1} \right\} = \frac{\partial h_g}{\partial \xi^2} \Big|_{\xi^1 = -1}$$

<u>Therefore the normal vector at the boundary $\xi^1 = -1$ is parallel to the first contravariant base vector $\bar{g}^1$</u>. As a result of this conclusion it can be shown that if the assumed stresses used in the hybrid formulation

are the contravariant tensor stresses of the isoparametric system, the condition of free boundary traction reduces to simple conditions of constraint on the stresses. Similar conclusion can be drawn by considering the boundary $\xi^1 = +1$.

Along the boundary ξ^1 = constant, components of the traction vector $\bar{t}$ are expressed in terms of the contravariant stress tensor:

$$t^i = \tau^{ij} n_j \tag{A-25}$$

$$t^1 = \tau^{11} n_1 + \tau^{12} n_2 \tag{A-26}$$

$$t^2 = \tau^{21} n_1 + \tau^{22} n_2 \tag{A-27}$$

Where τ^{ij} is the contravariant stress tensor, and n_i are the components of the unit vector $\hat{N}$, normal to the boundary:

$$\hat{N} = \frac{1}{\sqrt{n_1^2 + n_2^2}} \left\{ n_1 \bar{g}^1 + n_2 \bar{g}^2 \right\} \tag{A-28}$$

The normal vector $\hat{N}$ was shown to be parallel to the contravariant base vector $\bar{g}^1$ and therefore:

$$\hat{N} = \frac{1}{\sqrt{g^{11}}} \bar{g}^1 \qquad ; \quad (\xi^1 = \text{constant}) \tag{A-29}$$

Comparison of equations (A-28) and (A-29) gives:

$$n_1 = \frac{1}{\sqrt{g''}}$$

$$n_2 = 0$$

which reduces equations (A-26) and (A-27):

$$t^1 = \tau'' n_1 \tag{A-30}$$

$$t^2 = \tau^{21} n_1 = \tau^{12} n_1 \tag{A-31}$$

The traction vector is resolved into contravariant components along the covariant base vectors:

$$\vec{t} = t^i \vec{g}_i = t^1 \vec{g}_1 + t^2 \vec{g}_2 \tag{A-32}$$

substituting from equations (A-30) and (A-31):

$$\vec{t} = \tau'' n_1 \vec{g}_1 + \tau^{21} n_1 \vec{g}_2 \quad ; (\xi^1 = \text{constant}) \tag{A-33}$$

For zero traction at the boundary ξ^1 = constant:

$$\left[\tau'' = \tau^{12} = 0 \right]_{\xi^1 = \text{constant}} \tag{A-34}$$

Similarly for a prescribed pressure p_o at this boundary;

$$\tau^{11} = p_o \xi^{11}$$
$$\tau^{12} = p_o \xi^{12} \qquad \text{(A-35)}$$

which is seen to reduce to equations (A-34) in the special case of no applied pressure.

Similar conditions are obtained at boundaries $\xi^2 =$ constant. As shown in Figure A-2, the first covariant base vector $\bar{g}_1$ is always tangent to this boundary. From equation (A-12) it follows that the contravariant base vector $\bar{g}^2$ is normal to line $\xi^2 =$ constant. The unit normal is hence obtained:

$$\hat{N} = \frac{1}{\sqrt{g^{22}}} \bar{g}^2 \quad ; \quad (\xi^2 = \text{constant}) \qquad \text{(A-36)}$$

Comparison with equation (A-28) shows that along lines $\xi^2 =$ constant:

$$n_1 = 0 \qquad \text{(A-37)}$$

Substituting (A-37) into (A-26), and (A-27) will in turn simplify equation (A-32):

$$\bar{\tau} = \tau^{12} n_2 + \tau^{22} n_2 \quad ; \quad (\xi^2 = \text{constant})$$

For $\bar{\tau} = 0$ at boundary $\xi^2 =$ constant:

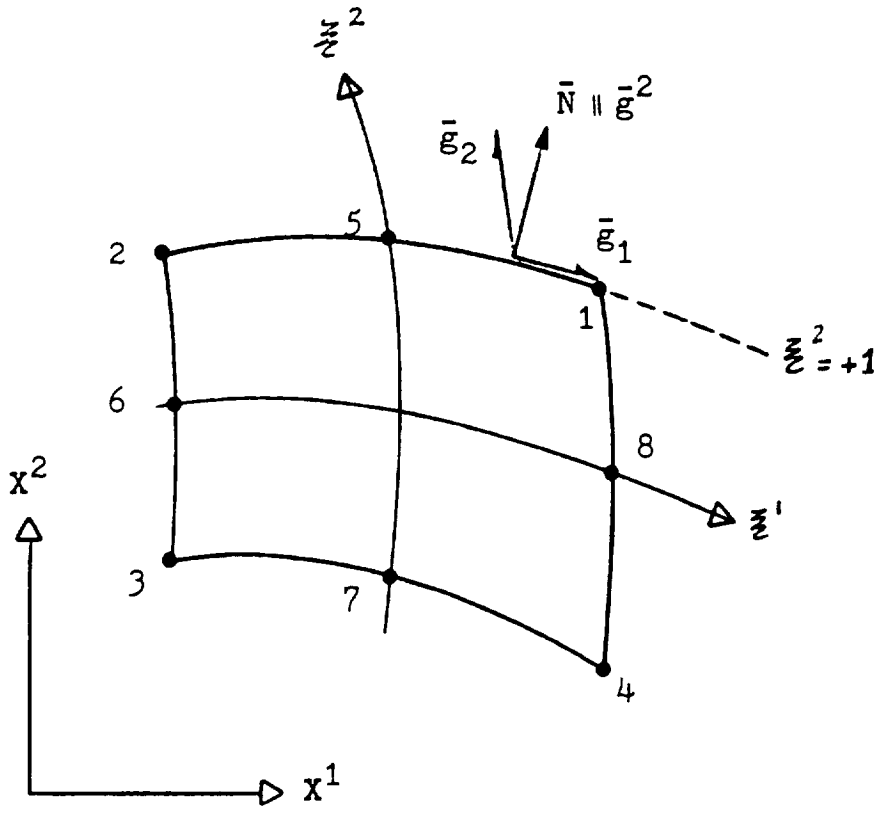

Figure A-2 Normal Vector To Boundary $\xi^2 = 1$

$$\left[\; \tau^{12} = \tau^{22} = 0 \;\right]_{\xi^2 = \text{constant}} \qquad \text{(A-38)}$$

A.4 Implementation

The following formulation illustrates how the aforementioned results can be applied to a two dimensional isoparametric element incorporating a traction free boundary at $\xi^1 = -1$.

A.4.1 The Assumed Stresses

The two dimensional contravariant stress tensor can be obtained from the Airy stress function:

$$\tau^{\alpha\beta} = e^{\alpha\lambda} e^{\beta\delta} \phi_{|\lambda\delta} \qquad \text{(A-39)}$$

where $e^{\alpha\beta}$ is the two dimensional permutation tensor:

$$e^{11} = e^{22} = 0$$

$$e^{12} = -e^{21} = \frac{1}{\sqrt{g}}$$

and g is defined by equation (A-10).

Stresses obtained from euqation (4-39) will necessarily satisfy the homogeneous equations of stress equilibrium:

$$\tau^{\alpha\beta}{}_{|\beta} = 0$$

From equation (A-39) it follows:

$$\tau^{11} = \frac{1}{\beta}\left\{\frac{\partial^2\phi}{(\partial\xi^2)^2} - \frac{\partial\phi}{\partial\xi^1}\Gamma^1_{22} - \frac{\partial\phi}{\partial\xi^2}\Gamma^2_{22}\right\} \qquad \text{(A-40)}$$

$$\tau^{22} = \frac{1}{\beta}\left\{\frac{\partial^2\phi}{(\partial\xi^1)^2} - \frac{\partial\phi}{\partial\xi^1}\Gamma^1_{11} - \frac{\partial\phi}{\partial\xi^2}\Gamma^2_{11}\right\} \qquad \text{(A-41)}$$

$$\tau^{12} = -\frac{1}{\beta}\left\{\frac{\partial^2\phi}{\partial\xi^1\partial\xi^2} - \frac{\partial\phi}{\partial\xi^1}\Gamma^1_{12} - \frac{\partial\phi}{\partial\xi^2}\Gamma^2_{12}\right\} \qquad \text{(A-42)}$$

; $\Gamma^{\gamma}_{\alpha\beta} \equiv$ Christoffel Symbols

For simplicity the Christoffel symbols are redefined:

$$A(\xi,\eta) = \Gamma^1_{22}$$

$$B(\xi,\eta) = \Gamma^2_{22}$$

$$C(\xi,\eta) = \Gamma^1_{12}$$

$$D(\xi,\eta) = \Gamma^2_{12}$$

$$E(\xi,\eta) = \Gamma^1_{11}$$

$$F(\xi,\eta) = \Gamma^2_{11}$$

With ξ and η replacing ξ^1 and ξ^2 respectively. Substituting into equations (A-40), (A-42), and (A-41) gives:

$$\tau^{11} = \frac{1}{\delta}\left\{\phi_{,22} - A(\xi,\eta)\,\phi_{,1} - E(\xi,\eta)\,\phi_{,2}\right\}$$

$$\tau^{12} = \frac{-1}{\delta}\left\{\phi_{,12} - C(\xi,\eta)\,\phi_{,1} - D(\xi,\eta)\,\phi_{,2}\right\}$$

$$\tau^{22} = \frac{1}{\delta}\left\{\phi_{,11} - E(\xi,\eta)\,\phi_{,1} - F(\xi,\eta)\,\phi_{,2}\right\}$$

where $\phi_{,1}$ and $\phi_{,2}$ are partial derivatives of ϕ with respect to ξ and η, respectively.

Assuming the Airy stress function:

$$\phi = \sum_m \sum_n A_{mn}\,\xi^m \eta^n$$

the contravariant stress components become:

$$\tau^{11} = \frac{1}{\delta}\sum_m \sum_n \left\{(n+2)(n+1)\,A_{m,n+2} - (m+1)\,A_{m+1,n}\,A(\xi,\eta) - (n+1)\,A_{m,n+1}\,B(\xi,\eta)\right\}\xi^m \eta^n \qquad \text{(A-43)}$$

$$\tau^{12} = -\frac{1}{\delta}\sum_m \sum_n \left\{(m+1)(n+1)\,A_{m+1,n+1} - (m+1)\,A_{m+1,n}\,C(\xi,\eta) - (n+1)\,A_{m,n+1}\,D(\xi,\eta)\right\}\xi^m \eta^n \qquad \text{(A-44)}$$

$$\tau^{22} = \frac{1}{\beta} \sum_m \sum_n \Big\{ (m+2)(m+1) A_{m+2,n} - (m+1) A_{m+1,n} E(\xi,\eta) - (n+1) A_{m,n+1} F(\xi,\eta) \Big\} \xi^m \eta^n \tag{A-45}$$

To prescribe zero tractions at boundary $\xi = -1$ of the element:

$$\Big[\tau^{11} = \tau^{12} = 0 \Big]_{\xi = -1} \tag{A-34}$$

Substituting equations (A-43), and (A-44) into equation (A-34) introduces constraints among coefficients A_{mn}. Rearranging the indices to unify the coefficients A_{mn} gives:

$$\tau^{11} = \frac{1}{\beta} \sum_{m=0}^{M} \sum_{n=0}^{N} \Big\{ m \xi^{m-1} \eta^n \bar{A} + n \xi^m \eta^{n-1} \bar{B} \Big\} A_{mn} \tag{A-35}$$

$$\tau^{22} = \frac{1}{\beta} \sum_{m=0}^{M} \sum_{n=0}^{N} \Big\{ m(m-1) \xi^{m-2} \eta^n - m \xi^{m-1} \eta^n E(\xi,\eta) - n \xi^m \eta^{n-1} F(\xi,\eta) \Big\} A_{mn} \tag{A-36}$$

$$\tau^{12} = \frac{-1}{\beta} \sum_{m=0}^{M} \sum_{n=0}^{N} \Big\{ m \xi^{m-1} \eta^n \bar{C} + n \xi^m \eta^{n-1} \bar{D} \Big\} A_{mn} \tag{A-37}$$

where the functions $\bar{A}$, $\bar{B}$, $\bar{C}$, and $\bar{D}$ are defined:

$$\bar{G}(\xi,\eta) = G(-1,\eta) - G(\xi,\eta)$$

and therefore vanish at $\xi = -1$. As a consequence τ'' and τ^{12} of equations (A-35) and (A-37) are also identically zero at this boundary. Equations (A-35) through (A-37) can be expanded in as many terms as required. Redefining coefficients A_{mn} as β_i, the stresses are expressable in matrix form:

$$\underset{\sim}{\sigma}(\xi,\eta) = \underset{\sim}{P}(\xi,\eta)\underset{\sim}{\beta} \qquad \text{(A-38a)}$$

An advantage of this approach is immediately obvious from equation (A-38a). Since the assumed stresses are chosen in the isoparametric system, the resulting stiffness matrix is invariant and hence unaffected by element rotation relative to the Cartesian coordinates. This eliminates the need for a complete polynomial of stresses and allows selective adoption of effective terms.

For implementation on the high speed computer equations (A-38) can be rewritten in a much simpler form:

$$\underset{\sim}{\sigma} = \underset{\sim}{\Gamma}\,\underset{\sim}{\bar{P}}\,\underset{\sim}{\beta} \qquad \text{(A-38b)}$$

which compared with equation (A-38a) gives:

$$\underset{\sim}{P} = \underset{\sim}{\Gamma}\,\underset{\sim}{\bar{P}} \qquad \text{(A-38c)}$$

Here $\underset{\sim}{\Gamma}$ is the matrix of Christoffel symbols, the entires of which were previously defined:

$$\underset{\sim}{\Gamma} = \frac{1}{\bar{\rho}\bar{C}} \begin{bmatrix} 0 & \bar{A} & \bar{E} \\ 1 & -\bar{E} & -F \\ 0 & -\bar{C} & -\bar{D} \end{bmatrix} \tag{A-38d}$$

Matrix $\underset{\sim}{\bar{\rho}}$ of equation (A-38c) is simply obtained by expansion of the following series:

$$\underset{\sim}{\bar{\rho}} = \sum_{m=0}^{M} \sum_{n=0}^{N} \begin{Bmatrix} m(m-1)\xi^{m-2}\eta^{n} \\ m\xi^{m-1}\eta^{n} \\ n\xi^{m}\eta^{n-1} \end{Bmatrix} \tag{A-38e}$$

Thus equations (A-38c), (A-38d), and (A-38e) completely define a set of self equilibrating assumed stresses.

In computation of matrix $\underset{\sim}{H}$:

$$\underset{\sim}{H} = \int_{V} \underset{\sim}{\rho}^{T} \underset{\sim}{S} \underset{\sim}{\rho} \, dV \tag{A-39}$$

Gauss integration coordinates become the natural variables and the necessity for evaluation of a Jacobian matrix of transformation is eliminated. The assumed stresses of equation (A-38c) can be easily evaluated at Gaussian integration stations and equation (A-39) becomes:

$$H = t \sum_{i} \sum_{j} (\underset{\sim}{\rho}^{T} \underset{\sim}{S} \underset{\sim}{\rho})_{\xi_i, \eta_j} W_i W_j \tag{A-40}$$

(ξ_i, η_j) = Gauss integration stations.

W_i = Gauss weighting factor.

The compliance matrix $\underset{\sim}{S}$ of equations (A-39) and (A-40) relates the covariant strain tensor to the contravariant stress tensor:

$$\gamma_{mn} = S_{mnpq}\,\tau^{pq} \tag{A-41}$$

For isotropic materials $\underset{\sim}{S}$ is defined [17]:

$$S_{mnpq} = \frac{1+\nu}{E}\left(\delta_{mp}\delta_{nq} + \delta_{mq}\delta_{np}\right) - \frac{\nu}{E}\delta_{mn}\delta_{pq} \tag{A-42}$$

$E \equiv$ Young's Modulus.

$\nu \equiv$ Poisson's Ratio.

In matrix form equation (A-41) becomes:

$$\begin{Bmatrix} \gamma_{11} \\ \gamma_{22} \\ \gamma_{12} \end{Bmatrix} = \begin{bmatrix} S_{1111} & S_{1122} & 2S_{1112} \\ S_{2211} & S_{2222} & 2S_{2212} \\ S_{1211} & S_{1222} & 2S_{1212} \end{bmatrix} \begin{Bmatrix} \tau^{11} \\ \tau^{22} \\ \tau^{12} \end{Bmatrix} \tag{A-43}$$

where:

$$S_{1111} = \frac{1}{E}\delta_{11}^{2}$$

$$S_{1122} = S_{2211} = \frac{1}{E}\left\{(1+\nu)\delta_{12}^{2} - \nu\,\delta_{11}\delta_{22}\right\}$$

$$S_{1112} = S_{1211} = \frac{1}{E}\delta_{11}\delta_{12}$$

$$S_{2222} = \frac{1}{E}\delta_{22}^{2}$$

$$S_{2212} = \frac{1}{E}\delta_{12}\delta_{22} = S_{1222}$$

$$S_{1212} = \frac{1}{2E}\left\{(1+\nu)\delta_{11}\delta_{22} + (1-\nu)\delta_{12}^{2}\right\}$$

A.4.2 The Strain Matrix

Interpolation of the strain matrix $\underset{\sim}{B}$ is required for computation of matrix $\underset{\sim}{G}$. In the Reissner formulation:

$$\underset{\sim}{G} = \int_V \underset{\sim}{P}^T \underset{\sim}{B} \, dV \tag{A-44}$$

To obtain the final stiffness matrix in the Cartesian system of coordinates, displacements are interpolated in Cartesian coordinates and hence transformation of the stresses to the same system becomes necessary:

$$\sigma^{\alpha\beta} = \frac{\partial x^\alpha}{\partial \xi^\gamma} \frac{\partial x^\beta}{\partial \xi^\delta} \tau^{\gamma\delta} \tag{A-45}$$

where: $\tau^{\alpha\beta}$ = contravariant isoparametric stresses

$\sigma^{\alpha\beta}$ = cartesian stresses (X, Y)

In matrix form, equation (A-45) becomes:

$$\begin{Bmatrix} \sigma^{XX} \\ \sigma^{YY} \\ \sigma^{XY} \end{Bmatrix} = \begin{bmatrix} T_{11} & T_{12} & T_{13} \\ T_{21} & T_{22} & T_{23} \\ T_{31} & T_{32} & T_{33} \end{bmatrix} \begin{Bmatrix} \tau^{11} \\ \tau^{22} \\ \tau^{12} \end{Bmatrix} \tag{A-46}$$

where:

$$T_{11} = \left(\frac{\partial x}{\partial \xi}\right)^2$$

$$T_{12} = \left(\frac{\partial x}{\partial \xi}\right)^2$$

$$T_{13} = 2\,\frac{\partial x}{\partial \xi}\,\frac{\partial y}{\partial \xi}$$

$$T_{21} = \left(\frac{\partial x}{\partial \eta}\right)^2$$

$$T_{22} = \left(\frac{\partial y}{\partial \eta}\right)^2$$

$$T_{23} = 2\,\frac{\partial x}{\partial \eta}\,\frac{\partial y}{\partial \eta}$$

$$T_{31} = \frac{\partial x}{\partial \xi}\,\frac{\partial x}{\partial \eta}$$

$$T_{32} = \frac{\partial y}{\partial \xi}\,\frac{\partial y}{\partial \eta}$$

$$T_{33} = 2\,\frac{\partial x}{\partial \xi}\,\frac{\partial y}{\partial \eta}$$

Derivatives of the Cartesian coordinates with respect to ξ and η are determined from the interpolations:

$$x = \sum_i' x_i h_i \qquad \text{(A-1)}$$

$$y = \sum_i' y_i h_i \qquad \text{(A-2)}$$

In isoparametric elements the displacements are interpolated identically:

$$u = \sum_i' u_i h_i \qquad \text{(A-47)}$$

$$v = \sum_i' v_i h_i \qquad \text{(A-48)}$$

From equations (A-47) and (A-48) the strains can be determined:

$$\epsilon_{11} = \epsilon_{xx} = \frac{\partial u}{\partial x}$$

$$\epsilon_{22} = \epsilon_{yy} = \frac{\partial v}{\partial y}$$

$$\epsilon_{12} = \epsilon_{xy} = \frac{\partial u}{\partial y} + \frac{\partial v}{\partial x}$$

These equations in turn determine the matrix $\underset{\sim}{B}$ in terms of the nodal displacements :

$$\underset{\sim}{\epsilon} = \underset{\sim}{B}\,\underset{\sim}{q} \qquad \text{(A-49)}$$

With equations (A-46) and (A-49), matrix $\underset{\sim}{G}$ of equation (A-44) becomes:

$$\underset{\sim}{G} = \int_V \underset{\sim}{T}\,\underset{\sim}{P}\,\underset{\sim}{B}\; dV \qquad \text{(A-50)}$$

where $\underset{\sim}{T}$ is the matrix of transformation, and $\underset{\sim}{P}$ is defined by equation (A-38c). Matrix $\underset{\sim}{G}$ of equation (A-50) can also be integrated by the Gauss quadrature scheme of equation (A-40).

A.5 Extension to Solid Elements

Similar results can be derived for solid isoparametric elements, Figure A-3. The three dimensional components of a traction vector expressed in terms of the contravariant stresses are:

$$t^1 = \tau^{11} n_1 + \tau^{12} n_2 + \tau^{13} n_3$$

$$t^2 = \tau^{21} n_1 + \tau^{22} n_2 + \tau^{23} n_3$$

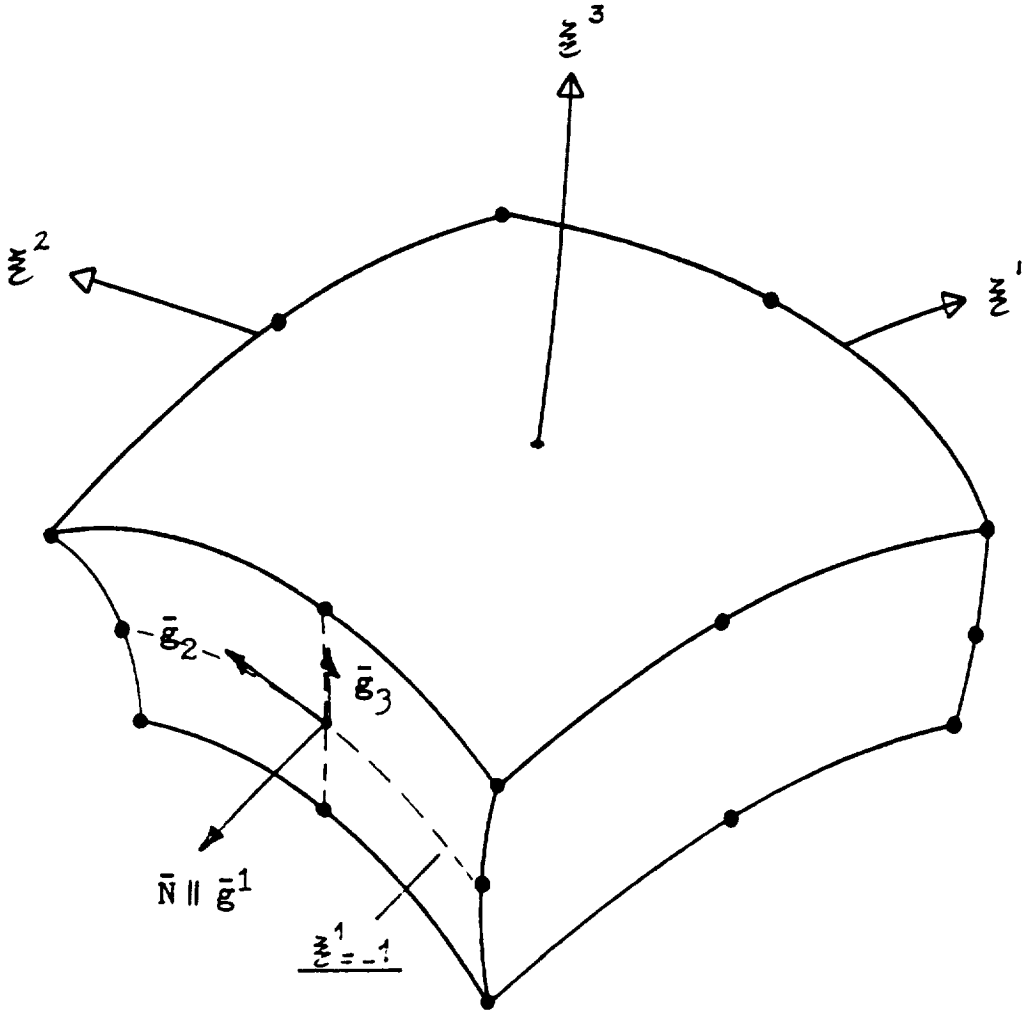

Figure A-3 Normal To Boundary Of A Solid Isoparametric Element

$$t^3 = \tau^{3'} n_1 + \tau^{32} n_2 + \tau^{33} n_3 \qquad \text{(A-51)}$$

where: n_i = Components of unit normal vector $\hat{N}$

At the boundary $\xi' = -1$ of Figure A-3, the contravariant base vector $\bar{g}'$ is along the direction of the normal to this boundary, $\bar{N}$:

$$\hat{N} = \frac{\bar{N}}{|\bar{N}|} = n_1 \bar{g}' \quad ; \quad n_2 = n_3 = 0 \qquad \text{(A-52)}$$

Substitution of equation (A-52) into equations (A-51) gives

$$t' = \tau'' n_1$$
$$t^2 = \tau^{2'} n_2$$
$$t^3 = \tau^{3'} n_3$$

Therefore if the assumed contravariant stresses of a hybrid solid element are chosen such that:

$$\left[\tau'' = \tau^{2'} = \tau^{3'} = 0 \right]_{\xi' = -1}$$

the condition of free traction will be automatically satisfied at boundary $\xi' = -1$ of this element.

APPENDIX B

Computer Programs

The computer programs are all in form of subroutines. This enables use of the programs in Finite Element codes by way of linking a main program to the desired element stiffness matrix subroutine. Each program is followed by another subroutine for computation of the stresses.

All subroutines were programmed and executed on the Digital VAX-11/780 computer. All programs are written in FORTRAN-IV.

B.1 ELEMENT HISQUE

The following variables are required by subroutine HISQUE:

E =Young's modulus

NU =Poisson's ratio

T =Element thickness

X =Vector of nodal coordinates, x

Y =Vector of nodal coordinates, y

Ix =0(1) if node x is absent(present)

NBETA =Number of betas

IO =Output control variable

The following variables are returned by subroutine HISQUE:

HINVG =Product of matrices [H]inv. and [G]

REALK =Element stiffness matrix

Subroutine QUEST computes the stress vector STRESS from the following variables:

XS,YS =Coordinates of point at which stress is desired

Hinvg =Matrix returned by subroutine HISQUE

DISP =Vector of nodal displacements

```
C*********************************************************************
C          KUROSH  KAFIE                          MARCH 1981,  M.I.T.  *
C*********************************************************************

      SUBROUTINE HISQUE(E,NU,T,X,Y,I5,I6,I7,I8,NBETA,IO,HINVG,REALK)


      IMPLICIT REAL*8(A-H,O-Z)
      DOUBLE PRECISION NU,J11,J12,J21,J22
      REAL HINVG(NBETA,1),REALK(2*(4+I5+I6+I7+I8),1)
      CHARACTER*5  ASTRNG
      CHARACTER*13 BSTRNG

      DIMENSION X(1),Y(1),GS(4,4),GW(4,4)
      DIMENSION DUM(3),F(8),DZ(8),DE(8)

      DIMENSION S(3,3),P(3,18),H(18,18)
      DIMENSION BE(3,16),G(18,16)
      DIMENSION HG(18,16),STMTX(16,16)

      DDX(M)=+J22*DZ(M)-J12*DE(M)
      DDY(M)=-J21*DZ(M)+J11*DE(M)

      DATA GS/      0.00D0,                0.00D0,
     1  .000000000000000D0, .000000000000000D0,
     2 -.577350269189626D0, .577350269189626D0,
     2  .000000000000000D0, .000000000000000D0,
     3 -.774596669241483D0, .000000000000000D0,
     3  .774596669241483D0, .000000000000000D0,
     4 -.861136311594053D0,-.339981043584856D0,
     4  .339981043584856D0, .861136311594053D0/

      DATA GW/      2.00D0,                0.00D0,
     1  .000000000000000D0, .000000000000000D0,
     2 1.000000000000000D0,1.000000000000000D0,
     2  .000000000000000D0, .000000000000000D0,
     3  .555555555555556D0, .888888888888889D0,
     3  .555555555555556D0, .000000000000000D0,
     4  .347854845137454D0, .652145154862546D0,
     4  .652145154862546D0, .347854845137454D0/

      NNODES=4+I5+I6+I7+I8
      NDOF  =2*NNODES

      C5    =    I5
      C6    =    I6
      C7    =    I7
      C8    =    I8
```

```
                    NINT=3
      IF(NNODES.GT.4) NINT=4
      IF(NBETA.GT.12) NINT=4

      IF(NNODES.LT.4.OR.NNODES.GT.8)GO TO 1000
      IF((NDOF-3).GT.NBETA)          GO TO 2000
      IF(NBETA.GT.18)                GO TO 3000

      DO 100 IR=1,18
      DO 50 ICH=1,18
   50 H(IR,ICH)=0.D00
      DO 75 ICG=1,16
   75 G(IR,ICG)=0.D00
  100 CONTINUE

      DO 145 IROW=1,3
      DO 125 ICOL=1,18
  125  P(IROW,ICOL)=0.0D00
      DO 135 JCOL=1,16
  135 BE(IROW,JCOL)=0.0D00
  145 CONTINUE

      N5=I5*(5          )
      N6=I6*(5+I5       )
      N7=I7*(5+I5+I6    )
      N8=I8*(5+I5+I6+I7)
      IF (N5.EQ.0) N5=8
      IF (N6.EQ.0) N6=8
      IF (N7.EQ.0) N7=8
      IF (N8.EQ.0) N8=8

       S(1,1)=1.0D00/E
       S(1,2)=-NU/E
       S(1,3)=0.0D0
       S(2,1)=-NU/E
       S(2,2)=1.0D00/E
       S(2,3)=0.0D0
       S(3,1)=0.0D0
       S(3,2)=0.0D0
       S(3,3)=2.D0*(1.D0+NU)/E

  200 DO 500 II=1,NINT
      ZE=GS(II,NINT)
      DO 500 JJ=1,NINT
      ET=GS(JJ,NINT)

      OPZ  =1.D0+ZE
      OMZ  =1.D0-ZE
```

```
      OPE  =1.D0+ET
      OME  =1.D0-ET
      OMZSQ=1.D0-ZE**2
      OMESQ=1.D0-ET**2

      F(N5)=C5*OMZSQ*OPE/2.D0
      F(N6)=C6*OMESQ*OMZ/2.D0
      F(N7)=C7*OMZSQ*OME/2.D0
      F(N8)=C8*OMESQ*OPZ/2.D0

      F(1)=0.25D0*OPZ*OPE-(F(N5)+F(N8))/2.D0
      F(2)=0.25D0*OMZ*OPE-(F(N5)+F(N6))/2.D0
      F(3)=0.25D0*OMZ*OME-(F(N6)+F(N7))/2.D0
      F(4)=0.25D0*OPZ*OME-(F(N7)+F(N8))/2.D0

      XS=0.0D00
      YS=0.0D00

      DO 250 K=1,NNODES
      XS=XS+X(K)*F(K)
      YS=YS+Y(K)*F(K)
  250 CONTINUE

      XSQ=XS*XS
      YSQ=YS*YS
      XCU=XS*XSQ
      YCU=YS*YSQ

      P(1,1)=1.0D00
      P(1,4)=YS
      P(1,6)=XS
      P(1,8)=YSQ
      P(1,10)=XSQ
      P(1,11)=2.D0*XS*YS
      P(1,13)=YCU
      P(1,15)=XCU
      P(1,16)=XS*YSQ
      P(1,17)=XSQ*YS

      P(2,2)=1.0D00
      P(2,5)=XS
      P(2,7)=YS
      P(2,9)=XSQ
      P(2,10)=YSQ
      P(2,12)=P(1,11)
      P(2,14)=XCU
      P(2,15)=3.D0*XS*YSQ
      P(2,17)=YCU/3.D0
      P(2,18)=XSQ*YS
```

```
      P(3,3)=1.0D00
      P(3,6)=-YS
      P(3,7)=-XS
      P(3,10)=-P(1,11)
      P(3,11)=-YSQ
      P(3,12)=-XSQ
      P(3,15)=-3.D0*XSQ*YS
      P(3,16)=-YCU/3.D0
      P(3,17)=-XS*YSQ
      P(3,18)=-XCU/3.D0

      DZ(N5)=-C5*ZE*OPE
      DE(N5)=+C5*OMZSQ/2.D0
      DZ(N6)=-C6*OMESQ/2.D0
      DE(N6)=-C6*OMZ*ET
      DZ(N7)=-C7*ZE*OME
      DE(N7)=-C7*OMZSQ/2.D0
      DZ(N8)=+C8*OMESQ/2.D0
      DE(N8)=-C8*OPZ*ET

      DZ(1)=0.25D0*OPE-(DZ(N5)+DZ(N8))/2.D0
      DE(1)=0.25D0*OPZ-(DE(N5)+DE(N8))/2.D0
      DZ(2)=-.25D0*OPE-(DZ(N5)+DZ(N6))/2.D0
      DE(2)=0.25D0*OMZ-(DE(N5)+DE(N6))/2.D0
      DZ(3)=-.25D0*OME-(DZ(N6)+DZ(N7))/2.D0
      DE(3)=-.25D0*OMZ-(DE(N6)+DE(N7))/2.D0
      DZ(4)=0.25D0*OME-(DZ(N7)+DZ(N8))/2.D0
      DE(4)=-.25D0*OPZ-(DE(N7)+DE(N8))/2.D0

      J11=0.0D00
      J12=0.0D00
      J21=0.0D00
      J22=0.0D00

      DO 350 K=1,NNODES
      J11=DZ(K)*X(K)+J11
      J12=DZ(K)*Y(K)+J12
      J21=DE(K)*X(K)+J21
      J22=DE(K)*Y(K)+J22
  350 CONTINUE

      DETJ=J11*J22-J12*J21

      WTH=GW(II,NINT)*GW(JJ,NINT)*T*DETJ

      DO 400 J=1,NBETA
      DO 370 K=1,3
      DUM(K)=0.0D00
```

```
      DO 370 L=1,3
370   DUM(K)=DUM(K)+S(K,L)*P(L,J)
      DO 390 I=J,NBETA
      HTEMP=0.0D00
      DO 380 L=1,3
380   HTEMP=HTEMP+P(L,I)*DUM(L)
390   H(I,J)=H(I,J)+HTEMP*WTH
400   CONTINUE

      DO 435 I=1,(NDOF-1),2
      BE(1,I)=DDX((I+1)/2)
      BE(3,I)=DDY((I+1)/2)
435   CONTINUE

      DO 445 I=2,NDOF,2
      BE(2,I)=DDY(I/2)
      BE(3,I)=DDX(I/2)
445   CONTINUE


      WTG=GW(II,NINT)*GW(JJ,NINT)*T
      DO 450 I=1,NBETA
      DO 450 J=1,NDOF
      DO 450 K=1,3
450   G(I,J)=G(I,J)+P(K,I)*BE(K,J)*WTG

500   CONTINUE

      CALL MXINV(H,18,IERH,NBETA)

      WRITE(6,550)IERH
550   FORMAT(/,'  Inversion Indicator Returned
     - By SSP(IBM) = ',I3)

      DO 625 I=1,NBETA
      DO 625 J=1,NDOF
      HG(I,J)=0.0D00
      DO 600 K=1,NBETA
600   HG(I,J)=HG(I,J)+H(I,K)*G(K,J)
625   HINVG(I,J)=HG(I,J)

      DO 675 I=1,NDOF
      DO 675 J=1,NDOF
      STMTX(I,J)=0.0D00
      DO 650 K=1,NBETA
650   STMTX(I,J)=STMTX(I,J)+G(K,I)*HG(K,J)
675   REALK(I,J)=STMTX(I,J)

      IF(IO.EQ.0) GO TO 800
```

```
      WRITE(6,700)NNODES,NBETA
  700 FORMAT(/,° [ K ] Matrix Returned By § HISQUE †°/
     -°   SPECIFIED:  Number of Nodes =  °,I1,/
     -°                Number of Betas = °,I2)
      DO 725 KROW=1,NDOF
  725 WRITE(6,775)(REALK(KROW,KCOL),KCOL=1,NDOF)
  775 FORMAT(/,1X,8(E13.7,3X),/,1X,8(E13.7,3X))

  800 RETURN



 1000 ASTRNG=°NODES°
      BSTRNG=°OUT OF RANGE.°
      WRITE(6,5000)ASTRNG,NNODES,BSTRNG
      STOP

 2000 ASTRNG=°BETAS°
      BSTRNG=°INSUFFICIENT.°
      GO TO 4000

 3000 ASTRNG=°BETAS°
      BSTRNG=°OUT OF RANGE.°
 4000 WRITE(6,5000)ASTRNG,NBETA,BSTRNG
 5000 FORMAT(1X,
     -°*********************************************************°,/,
     -° * PROGRAM ABORT ACTIVATED BY § HISQUE † :               *°,/,
     -° * SPECIFIED NUMBER OF °,A5,° [°,I2,°] IS °,A13,°      *°
     -,/,° *********************************************************°)
      STOP
      END
```

```
      SUBROUTINE QUEST(XS,YS,I5,I6,I7,I8,NBETA,HINVG,DISP,STRESS)

      DIMENSION DISP(1),STRESS(1),HINVG(NBETA,1)
      DIMENSION P(3,18),PHINVG(3,16)

      NNODES=4+I5+I6+I7+I8
      NDOF  =2*NNODES

      DO 100 IROW=1,3
      DO 100 ICOL=1,18
  100 P(IROW,ICOL)=0.0D00

      P(1,1)=1.0D00
      P(1,4)=YS
      P(1,6)=XS
      P(1,8)=YS**2
      P(1,10)=XS**2
      P(1,11)=2.D0*XS*YS
      P(1,13)=YS**3
      P(1,15)=XS**3
      P(1,16)=XS*(YS**2)
      P(1,17)=(XS**2)*YS

      P(2,2)=1.0D00
      P(2,5)=XS
      P(2,7)=YS
      P(2,9)=XS**2
      P(2,10)=YS**2
      P(2,12)=2.D0*XS*YS
      P(2,14)=XS**3
      P(2,15)=3.D0*XS*(YS**2)
      P(2,17)=(YS**3)/3.D0
      P(2,18)=(XS**2)*YS

      P(3,3)=1.0D00
      P(3,6)=-YS
      P(3,7)=-XS
      P(3,10)=-2.D0*XS*YS
      P(3,11)=-YS**2
      P(3,12)=-XS**2
      P(3,15)=-3.D0*(XS**2)*YS
      P(3,16)=(YS**3)/(-3.D0)
      P(3,17)=-XS*(YS**2)
      P(3,18)=(XS**3)/(-3.D0)

      DO 200 I=1,3
      DO 200 J=1,NDOF
      PHINVG(I,J)=0.0
      DO 200 K=1,NBETA
```

```
      PHINVG(I,J)=P(I,K)*HINVG(K,J)+PHINVG(I,J)
  200 CONTINUE
      DO 300 I=1,3
      STRESS(I)=  0.0
      DO 300 K=1,NDOF
      STRESS(I)=PHINVG(I,K)*DISP(K)+STRESS(I)
  300 CONTINUE
      RETURN
      END
```

B.2 ELEMENT HEL710

The following variables are required by subroutine HEL710:

E =Young's modulus

NU =Poisson's ratio

T =Element thickness

X =Vector of nodal coordinates, x

Y =Vector of nodal coordinates, y

Ix =0(1) if node x is absent(present)

IO =Output control variable

The following variables are returned by subroutine HEL710:

HINVG =Product of [H]inv. and [G] matrices

REALK =Element stiffness matrix

Subroutine HELSTR computes the stress vector STRESS from the following variables:

XS,YS =Coordinates of point at which stress is desired

HINVG =Matrix returned by subroutine HEL710

DISP =Vector of nodal displacements

```
C*****************************************************************
C     KUROSH  KAFIE                          MARCH 1981,  M.I.T.   *
C*****************************************************************

      SUBROUTINE HEL710(E,NU,T,X,Y,I8,I9,I10,IO,HINVG,REALK)


      IMPLICIT REAL*8(A-H,O-Z)
      DOUBLE PRECISION NU,J11,J12,J21,J22

      REAL HINVG,REALK

      DIMENSION X(1),Y(1),ZETA(5),W(5)
      DIMENSION DUM(3),F(10),DZ(10),DE(10)

      DIMENSION S(3,3),P(3,25),H(25,25)
      DIMENSION BE(3,20),G(25,20)

      DIMENSION HG(25,20),STMTX(20,20)
      DIMENSION HINVG(25,1),REALK((2*(7+I8+I9+I10)),1)

      DDX(M)=+J22*DZ(M)-J12*DE(M)
      DDY(M)=-J21*DZ(M)+J11*DE(M)

      DATA ZETA/           -.906179845938664D0,
     2 -.538469310105683D0, .000000000000000D0,
     3  .538469310105683D0, .906179845938664D0/

      DATA W/               .236926885056189D0,
     2  .478628670499366D0, .568888888888889D0,
     3  .478628670499366D0, .236926885056189D0/

      D8 =I8
      D9 =I9
      D10=I10

      NNODES=7+I8+I9+I10
      NDOF  =2*NNODES

      DO 150  IR=1,25
      DO 100 ICH=1,25
  100 H(IR,ICH)=0.0D00
      DO 125 ICG=1,20
  125 G(IR,ICG)=0.0D00
  150 CONTINUE

      DO 250 IROW=1,3
      DO 200 ICOL=1,25
```

```
200  P(IROW,ICOL)=0.0D00
     DO 225 JCOL=1,20
225 BE(IROW,JCOL)=0.0D00
250 CONTINUE

      S(1,1)=1.D0/E
      S(1,2)=-NU/E
      S(1,3)=0.0D0/E
      S(2,1)=-NU/E
      S(2,2)=1.D0/E
      S(2,3)=0.0D0/E
      S(3,1)=0.0D0/E
      S(3,2)=0.0D0/E
      S(3,3)=2.D0*(1.D0+NU)/E

     DO 500 II=1,5
     ZE=ZETA(II)
     DO 500 JJ=1,5
     ET=ZETA(JJ)

     OPZ=1.D0+ZE
     OMZ=1.D0-ZE
     OPE=1.D0+ET
     OME=1.D0-ET
     HPE=.5D0+ET
     HME=.5D0-ET
     ESQ=ET*ET
     ECU=ET*ESQ
     EQU=ET*ECU
     OMZSQ=1.D0-ZE*ZE
     OMESQ=1.D0-ESQ

     F( 8)= D8*OMZSQ*OME/2.D0
     F( 9)= D9*OMESQ*OPZ/2.D0
     F(10)=D10*OMZSQ*OPE/2.D0

     F(1)=+HPE*ET*HME*OME*OMZ/3.D0-F( 8)/2.D0
     F(2)=OPZ*OME/4.D0-(F( 8)+F( 9))/2.D0
     F(3)=OPZ*OPE/4.D0-(F( 9)+F(10))/2.D0
     F(4)=-OPE*HPE*ET*HME*OMZ/3.D0-F(10)/2.D0
     F(5)=+OPE*HPE*ET*OME*OMZ/.75D0
     F(6)=+2.D0*OPE*HPE*HME*OME*OMZ
     F(7)=-OPE*ET*HME*OME*OMZ/.75D0

     XS=0.0D00
     YS=0.0D00

     DO 300 K=1,NNODES
     XS=XS+X(K)*F(K)
```

```
      YS=YS+Y(K)*F(K)
300   CONTINUE

      XSQ=XS*XS
      XCU=XS*XSQ
      XQU=XS*XCU
      YSQ=YS*YS
      YCU=YS*YSQ
      YQU=YS*YCU

      P(1,1)=1.D00
      P(1,4)=YS
      P(1,6)=XS
      P(1,8)=XSQ
      P(1,9)=2.D0*XS*YS
      P(1,10)=YSQ
      P(1,13)=XCU
      P(1,14)=(XSQ)*(YS)
      P(1,15)=(XS)*(YSQ)
      P(1,16)=YCU
      P(1,19)=XQU
      P(1,20)=(XCU)*YS
      P(1,21)=(XSQ)*(YSQ)
      P(1,22)=XS*(YCU)
      P(1,23)=YQU

      P(2,2)=1.D00
      P(2,5)=XS
      P(2,7)=YS
      P(2,8)=YSQ
      P(2,11)=2.D0*XS*YS
      P(2,12)=XSQ
      P(2,13)=3.D0*(XS)*(YSQ)
      P(2,14)=(YCU)/3.D0
      P(2,17)=XCU
      P(2,18)=(XSQ)*YS
      P(2,19)=6.D0*(XSQ)*(YSQ)
      P(2,20)=XS*(YCU)
      P(2,21)=(YQU)/6.0D00
      P(2,24)=4.D0*(XCU)*YS
      P(2,25)=XQU

      P(3,3)=1.D00
      P(3,6)=-YS
      P(3,7)=-XS
      P(3,8)=-2.D0*XS*YS
      P(3,9)=-YSQ
      P(3,11)=-XSQ
      P(3,13)=-3.D0*(XSQ)*(YS)
```

```
      P(3,14)=-XS*(YSQ)
      P(3,15)=-(YCU)/3.D0
      P(3,18)=-(XCU)/3.D0
      P(3,19)=-4.D0*(XCU)*YS
      P(3,20)=-3.D0*(XSQ)*(YSQ)/2.D0
      P(3,21)=-2.D0*XS*(YCU)/3.D0
      P(3,22)=(YQU)/-4.D0
      P(3,24)=-XQU

      DZ( 8)= -D8*ZE*OME
      DE( 8)= -D8*OMZSQ/2.D0
      DZ( 9)= +D9*OMESQ/2.D0
      DE( 9)= -D9*OPZ*ET
      DZ(10)=-D10*ZE*OPE
      DE(10)=+D10*OMZSQ/2.D0

      DZ(1)=(EQU-ECU-((ESQ-ET)/4.D0))/(-3.D0)-DZ(8)/2.D0
      DE(1)=(4.D0*ECU-3.D0*ESQ+.25D0-ET/2.D0)*OMZ/3.D0
     -      -DE(8)/2.D0
      DZ(2)=+OME/4.D0-0.5D0*(DZ(8)+DZ(9))
      DE(2)=-OPZ/4.D0-0.5D0*(DE(8)+DE( 9))
      DZ(3)=+OPE/4.D0-0.5D0*(DZ(9)+DZ(10))
      DE(3)=+OPZ/4.D0-0.5D0*(DE(9)+DE(10))
      DZ(4)=(EQU+ECU-(ESQ+ET)/4.D0)/(-3.D0)-DZ(10)/2.D0
      DE(4)=(4.D0*ECU+3.D0*ESQ-.25D0-ET/2.D0)*OMZ/3.D0
     -      -DE(10)/2.D0
      DZ(5)=(EQU+.5D0*ECU-ESQ-ET/2.D0)/.75D0
      DE(5)=-(4.D0*ECU+1.5D0*ESQ-2.D0*ET-.5D0)*OMZ/.75D0
      DZ(6)=-2.D0*(EQU-1.25D0*ESQ+.25D0)
      DE(6)=+2.D0*(4.D0*ECU-2.5D0*ET)*OMZ
      DZ(7)=+(EQU-.5D0*ECU-ESQ+ET/2.D0)/.75D0
      DE(7)=-(4.D0*ECU-1.5D0*ESQ-2.D0*ET+.5D0)*OMZ/.75D0

      J11=0.0D00
      J12=0.0D00
      J21=0.0D00
      J22=0.0D00

      DO 350 K=1,NNODES
      J11=DZ(K)*X(K)+J11
      J12=DZ(K)*Y(K)+J12
      J21=DE(K)*X(K)+J21
      J22=DE(K)*Y(K)+J22
  350 CONTINUE

      DETJ=J11*J22-J12*J21

      WTH=W(II)*W(JJ)*DETJ*T
      DO 400 J=1,25
```

```
      DO 370 K=1,3
      DUM(K)=0.0D00
      DO 370 L=1,3
370   DUM(K)=DUM(K)+S(K,L)*P(L,J)
      DO 390 I=J,25
      HTEMP=0.0D00
      DO 380 L=1,3
380   HTEMP=HTEMP+P(L,I)*DUM(L)
390   H(I,J)=H(I,J)+HTEMP*WTH
400   CONTINUE

      DO 435 I=1,(NDOF-1),2
      ITEMP=(I+1)/2
      BE(1,I)=DDX(ITEMP)
      BE(3,I)=DDY(ITEMP)
435   CONTINUE

      DO 445 I=2,NDOF,2
      ITEMP=I/2
      BE(2,I)=DDY(ITEMP)
      BE(3,I)=DDX(ITEMP)
445   CONTINUE

      WTG=W(II)*W(JJ)*T
      DO 450 I=1,25
      DO 450 J=1,NDOF
      DO 450 K=1,3
450   G(I,J)=G(I,J)+P(K,I)*BE(K,J)*WTG

500   CONTINUE

      CALL MXINV(H,25,IERH,0)

      WRITE(6,550)IERH
550   FORMAT(1X,' INVERSION INDICATOR RETURNED
     - BY SSP(IBM) = ',I3)

      DO 625 I=1,25
      DO 625 J=1,NDOF
      HG(I,J)=0.0D00
      DO 600 K=1,25
600   HG(I,J)=HG(I,J)+H(I,K)*G(K,J)
625   HINVG(I,J)=HG(I,J)

      DO 675 I=1,NDOF
      DO 675 J=1,NDOF
      STMTX(I,J)=0.0D00
      DO 650 K=1,25
650   STMTX(I,J)=STMTX(I,J)+G(K,I)*HG(K,J)
```

```
675 REALK(I,J)=STMTX(I,J)

    IF(IO.EQ.0) GO TO 999
    WRITE(6,900)
    DO 700 KR=1,NDOF
700 WRITE(6,800)(REALK(KR,KC),KC=1,NDOF)
800 FORMAT(/,° °,10E13.5,/,° °,10E13.5)
900 FORMAT(//,° [ K ] matrix returned by § HEL710 † °//)


999 RETURN
    END
```

```
      SUBROUTINE HELSTR(XS,YS,I8,I9,I10,HINVG,DISP,STRESS)

      DIMENSION P(3,25),HINVG(25,1),PHINVG(3,20)
      DIMENSION DISP(2*(7+I8+I9+I10)),STRESS(3)

      DO 100 IROW=1,3
      DO 100 ICOL=1,25
  100 P(IROW,ICOL)=0.D0

      P(1,1)=1.D00
      P(1,4)=YS
      P(1,6)=XS
      P(1,8)=XS**2
      P(1,9)=2.D0*XS*YS
      P(1,10)=YS**2
      P(1,13)=XS**3
      P(1,14)=(XS**2)*(YS)
      P(1,15)=(XS)*(YS**2)
      P(1,16)=YS**3
      P(1,19)=XS**4
      P(1,20)=(XS**3)*YS
      P(1,21)=(XS**2)*(YS**2)
      P(1,22)=XS*(YS**3)
      P(1,23)=YS**4

      P(2,2)=1.D00
      P(2,5)=XS
      P(2,7)=YS
      P(2,8)=YS**2
      P(2,11)=2.D0*XS*YS
      P(2,12)=XS**2
      P(2,13)=3.D0*(XS)*(YS**2)
      P(2,14)=(YS**3)/3.D0
      P(2,17)=XS**3
      P(2,18)=(XS**2)*YS
      P(2,19)=6.D0*(XS**2)*(YS**2)
      P(2,20)=XS*(YS**3)
      P(2,21)=(YS**4)/6.0D00
      P(2,24)=4.D0*(XS**3)*YS
      P(2,25)=XS**4

      P(3,3)=1.D00
      P(3,6)=-YS
      P(3,7)=-XS
      P(3,8)=-2.D0*XS*YS
      P(3,9)=-YS**2
      P(3,11)=-XS**2
      P(3,13)=-3.D0*(XS**2)*(YS)
      P(3,14)=-XS*(YS**2)
```

```
      P(3,15)=-(YS**3)/3.D0
      P(3,18)=-(XS**3)/3.D0
      P(3,19)=-4.D0*(XS**3)*YS
      P(3,20)=-3.D0*(XS**2)*(YS**2)/2.D0
      P(3,21)=-2.D0*XS*(YS**3)/3.D0
      P(3,22)=(YS**4)/-4.D0
      P(3,24)=-1.D0*(XS**4)

      NNODES=7+I8+I9+I10
      NDOF  =2*NNODES

      DO 200 I=1,3
      DO 200 J=1,NDOF
      PHINVG(I,J)=0.0
      DO 200 K=1,25
      PHINVG(I,J)=P(I,K)*HINVG(K,J)+PHINVG(I,J)
200   CONTINUE
      DO 300 I=1,3
      STRESS(I)=0.0
      DO 300 K=1,NDOF
      STRESS(I)=PHINVG(I,K)*DISP(K)+STRESS(I)
300   CONTINUE
      RETURN
      END
```

B.3 ELEMENT PET4/12

The following variables are required by subroutine PET4/12:

E =Young°s modulus

NU =Poisson°s ratio

T =Element thickness

X =Vector of nodal coordinates, x

Y =Vector of nodal coordinates, y

IO =Output control variable

The stiffness matrix, REALK, is returned by subroutine PET4.

Subroutine PETSAP computes the stress vector STRESS from the following variables:

XS,YS =Coordinates of point at which stress is desired

RZ =Radius of the circular hole

DISP =Vector of nodal displacements

```
C*****************************************************************
C     KUROSH  KAFIE                          DECEMBER 1980,  M.I.T.*
C*****************************************************************
      SUBROUTINE PET4(E,NU,T,X,Y,IO,REALK)
C*****************************************************************
C     DESCRIPTION:                                                 *
C     SUBROUTINE PET4 DETERMINES THE STIFFNESS MATRIX OF A         *
C     FOUR NODE MEMBRANE ELEMENT WITH A BUILT IN CIRCULAR          *
C     TRACTION-FREE EDGE:                                          *
C                                                                  *
C     E =YOUNG'S MODULUS.                                          *
C     NU=POISSON'S RATIO.                  O 3                     *
C     T =THICKNESS.                      . .                       *
C                                      .   .                       *
C                                    .     .                       *
C                                  .       .                       *
C                          4  O            .                       *
C                               .          .                       *
C                                 .        .                       *
C                                   O. . . O                       *
C                                1           2                     *
C                                                                  *
C*****************************************************************

      IMPLICIT REAL*8(A-H,O-Z)

      REAL HINVG,REALK(8,1)
      COMMON /PET1X2/HINVG(12,8)
      DOUBLE PRECISION J,LNGT,L,NU,NUX,NUY,NUT

      DIMENSION X(1),Y(1),GS(7),GW(7),DUM(3)
      DIMENSION S(3,3),P(3,12),H(12,12)
      DIMENSION NUT(3,2),L(2,8),G(12,8)
      DIMENSION HG(12,8),STMTX(8,8)

      DATA GS/              -0.949107912342759D0,
     2 -0.741531185599394D0, -0.405845151377397D0,
     3  0.000000000000000D0,  0.405845151377397D0,
     4  0.741531185599394D0,  0.949107912342759D0/

      DATA GW/               0.129484966168870D0,
     2  0.279705391489277D0,  0.381830050505119D0,
     3  0.417959183673469D0,  0.381830050505119D0,
     4  0.279705391489277D0,  0.129484966168870D0/

      NDOF = 8
      NBETA=12

      DO 75  IR=1,NBETA
```

```
      DO 25 ICH=1,NBETA
   25 H(IR,ICH)=0.D00
      DO 50 ICG=1,NDOF
   50 G(IR,ICG)=0.D00
   75 CONTINUE

      RZ=DSQRT(X(1)**2+Y(1)**2)
      CALL ANGLE(X(2),Y(2),THETA2)
      CALL ANGLE(X(3),Y(3),THETA3)
      THETA0=(THETA3-THETA2)/2.0D00
      ALPHA =(THETA3+THETA2)/2.0D00
      C1=(X(2)*Y(3)-X(3)*Y(2))
      C2=X(2)-X(3)
      C3=Y(2)-Y(3)

      IFLAG=0

       S(1,1)=1.D0/E
       S(1,2)=-NU/E
       S(1,3)=0.0D0
       S(2,1)=-NU/E
       S(2,2)=1.D0/E
       S(2,3)=0.0D0
       S(3,1)=0.0D0
       S(3,2)=0.0D0
       S(3,3)=2.D0*(1.D0+NU)/E


      DO 300 II=1,7
      ZE=GS(II)
      DO 300 JJ=1,7
      ET=GS(JJ)

      THETA=ZE*THETA0+ALPHA
      PHI=C1/(C2*DSIN(THETA)-C3*DCOS(THETA))
      R=((PHI-RZ)/2.0D0)*ET+(PHI+RZ)/2.0D0
      J=THETA0*(((PHI-RZ)**2)*ET+PHI**2-RZ**2)/4.D0

  100 ST=DSIN(THETA)
      CT=DCOS(THETA)

      P(1,1)=2.D0*(1.D0-RZ/R)
      P(1,2)=(1.D0-(RZ**2/R**2))*CT
      P(1,3)=(1.D0-(RZ**2/R**2))*ST
      P(1,4)=3.D0*(R-(RZ**2/R))
      P(1,5)=2.D0*(R-(RZ**3/R**2))*CT
      P(1,6)=2.D0*(R-(RZ**3/R**2))*ST
      P(1,7)=4.D0*(R**2-(RZ**3/R))
      P(1,8)=3.D0*(R**2-(RZ**4/R**2))*CT
```

```
      P(1,9)=3.D0*(R**2-(RZ**4/R**2))*ST
      P(1,10)=5.D0*(R**3-(RZ**4/R))
      P(1,11)=4.D0*(R**3-(RZ**5/R**2))*CT
      P(1,12)=4.D0*(R**3-(RZ**5/R**2))*ST

      P(2,1)=2.D0
      P(2,2)=2.D0*CT
      P(2,3)=2.D0*ST
      P(2,4)=6.D0*R
      P(2,5)=6.D0*R*CT
      P(2,6)=6.D0*R*ST
      P(2,7)=12.D0*(R**2)
      P(2,8)=12.D0*(R**2)*CT
      P(2,9)=12.D0*(R**2)*ST
      P(2,10)=20.D0*(R**3)
      P(2,11)=20.D0*(R**3)*CT
      P(2,12)=20.D0*(R**3)*ST

      P(3,1)=0.D00
      P(3,2)=(1.D0-(RZ**2/R**2))*ST
      P(3,3)=((RZ**2/R**2)-1.D0)*CT
      P(3,4)=0.D00
      P(3,5)=2.D0*(R-(RZ**3/R**2))*ST
      P(3,6)=2.D0*((RZ**3/R**2)-R)*CT
      P(3,7)=0.D00
      P(3,8)=3.D0*(R**2-(RZ**4/R**2))*ST
      P(3,9)=3.D0*((RZ**4/R**2)-R**2)*CT
      P(3,10)=0.D00
      P(3,11)=4.D0*(R**3-(RZ**5/R**2))*ST
      P(3,12)=4.D0*((RZ**5/R**2)-R**3)*CT

      IF(IFLAG.EQ.1) GO TO 400

      WTH=J*GW(II)*GW(JJ)

      DO 200 KC=1,NBETA
      DO 125 NN=1,3
      DUM(NN)=0.D00
      DO 125 KR=1,3
  125 DUM(NN)=DUM(NN)+S(NN,KR)*P(KR,KC)
      DO 175 KR=KC,NBETA
      HTEMP=0.0D00
      DO 150 NN=1,3
  150 HTEMP=HTEMP+P(NN,KR)*DUM(NN)
  175 H(KR,KC)=H(KR,KC)+HTEMP*WTH
  200 CONTINUE

  300 CONTINUE
```

```
      CALL MXINV(H,NBETA,IERH,0)

      IFLAG=1

      DO 800 IX=1,3
      XA=X(IX)
      XB=X(IX+1)
      YA=Y(IX)
      YB=Y(IX+1)

      LNGT=DSQRT((XA-XB)**2+(YA-YB)**2)
      CALL ANGLE((YB-YA),(XA-XB),OMEGA)
      NUX=DCOS(OMEGA)
      NUY=DSIN(OMEGA)


      DO 700 II=1,7

      XS=GS(II)*(XB-XA)/2.0D0+(XB+XA)/2.0D0
      YS=GS(II)*(YB-YA)/2.0D0+(YB+YA)/2.0D0

350   R=DSQRT(XS**2+YS**2)
      CALL ANGLE(XS,YS,THETA)


      GO TO 100


400   NUT(1,1)=NUX*(CT**2)+NUY*CT*ST
      NUT(2,1)=NUX*(ST**2)-NUY*CT*ST
      NUT(3,1)=NUY*(CT**2-ST**2)-2.D0*NUX*CT*ST

      NUT(1,2)=NUY*(ST**2)+NUX*CT*ST
      NUT(2,2)=NUY*(CT**2)-NUX*CT*ST
      NUT(3,2)=NUX*(CT**2-ST**2)+2.D0*NUY*CT*ST

      DO 500 IROW=1,2
      DO 500 ICOL=1,8
      L(IROW,ICOL)=0.0D00
500   CONTINUE


      ENT1=(1.D0-GS(II))/2.0D0
      ENT2=(1.D0+GS(II))/2.0D0

      L(1,(2*IX-1))=ENT1
      L(1,(2*IX+1))=ENT2

      L(2,(2*IX))  =ENT1
```

```
      L(2,(2*IX+2))=ENT2

      WTG=GW(II)*LNGT/2.D0

      DO 600 KC=1,NDOF
      DO 525 NN=1,3
      DUM(NN)=0.D00
      DO 525 KR=1,2
  525 DUM(NN)=DUM(NN)+NUT(NN,KR)*L(KR,KC)

      DO 575 KR=1,NBETA
      GTEMP=0.0D00
      DO 550 NN=1,3
  550 GTEMP=GTEMP+P(NN,KR)*DUM(NN)
  575 G(KR,KC)=G(KR,KC)+GTEMP*WTG
  600 CONTINUE

  700 CONTINUE

  800 CONTINUE

      DO 850 M=1,NBETA
      DO 850 N=1,NDOF
      HG(M,N)=0.0D00
      DO 825 K=1,NBETA
  825 HG(M,N)=HG(M,N)+H(M,K)*G(K,N)
  850 HINVG(M,N)=HG(M,N)

      DO 900 M=1,NDOF
      DO 900 N=1,NDOF
      STMTX(M,N)=0.0D00
      DO 875 K=1,NBETA
  875 STMTX(M,N)=STMTX(M,N)+G(K,M)*HG(K,N)
  900 REALK(M,N)=STMTX(M,N)

      IF(IO.EQ.0) GO TO 1000
      WRITE(6,975)
      DO 925 KR=1,8
  925 WRITE(6,950)(REALK(KR,KC),KC=1,8)
  950 FORMAT(1X,8(E14.5,2X)//)
  975 FORMAT(//,' [ K ] Matrix Returned By Subroutine § PET4/12 †
     -       '//)

 1000 RETURN
      END
```

```
SUBROUTINE PETSAP(XS,YS,RZ,DISP,STRESS)
COMMON /PET1X2/HINVG(12,8)

DIMENSION DISP(1),STRESS(1)
DIMENSION P(3,12),PHINVG(3,8)

DOUBLE PRECISION XD,YD,THETAD

R=SQRT(XS**2+YS**2)

XD=XS
YD=YS
CALL ANGLE(XD,YD,THETAD)

THETA=THETAD
ST=SIN(THETA)
CT=COS(THETA)

P(1,1)=2.0*(1.0-RZ/R)
P(1,2)=(1.0-(RZ**2/R**2))*CT
P(1,3)=(1.0-(RZ**2/R**2))*ST
P(1,4)=3.0*(R-(RZ**2/R))
P(1,5)=2.0*(R-(RZ**3/R**2))*CT
P(1,6)=2.0*(R-(RZ**3/R**2))*ST
P(1,7)=4.0*(R**2-(RZ**3/R))
P(1,8)=3.0*(R**2-(RZ**4/R**2))*CT
P(1,9)=3.0*(R**2-(RZ**4/R**2))*ST
P(1,10)=5.0*(R**3-(RZ**4/R))
P(1,11)=4.0*(R**3-(RZ**5/R**2))*CT
P(1,12)=4.0*(R**3-(RZ**5/R**2))*ST

P(2,1)=2.0
P(2,2)=2.0*CT
P(2,3)=2.0*ST
P(2,4)=6.0*R
P(2,5)=6.0*R*CT
P(2,6)=6.0*R*ST
P(2,7)=12.0*(R**2)
P(2,8)=12.0*(R**2)*CT
P(2,9)=12.0*(R**2)*ST
P(2,10)=20.0*(R**3)
P(2,11)=P(2,10)*CT
P(2,12)=P(2,10)*ST

P(3,1)=0.00
P(3,2)=(1.0-(RZ**2/R**2))*ST
P(3,3)=((RZ**2/R**2)-1.0)*CT
P(3,4)=0.00
P(3,5)=2.0*(R-(RZ**3/R**2))*ST
```

```
      P(3,6)=2.0*((RZ**3/R**2)-R)*CT
      P(3,7)=0.00
      P(3,8)=3.0*(R**2-(RZ**4/R**2))*ST
      P(3,9)=3.0*((RZ**4/R**2)-R**2)*CT
      P(3,10)=0.0
      P(3,11)=4.0*(R**3-(RZ**5/R**2))*ST
      P(3,12)=4.0*((RZ**5/R**2)-R**3)*CT

      DO 100 I=1,3
      DO 100 J=1,8
      PHINVG(I,J)=0.0
      DO 100 K=1,12
      PHINVG(I,J)=P(I,K)*HINVG(K,J)+PHINVG(I,J)
  100 CONTINUE

      DO 200 I=1,3
      STRESS(I)=0.0
      DO 200 K=1,8
      STRESS(I)=PHINVG(I,K)*DISP(K)+STRESS(I)
  200 CONTINUE

      RETURN
      END
```

B.4 ELEMENT PET4X5

The following variables are required by subroutine PET4X5:

E =Young's modulus

NU =Poisson's ratio

T =Element thickness

X =Vector of nodal coordinates, x

Y =Vector of nodal coordinates, y

IO =Output control variable

The stiffness matrix, REALK, is returned by subroutine PET4.

Subroutine PETSAP computes the stress vector STRESS from the following variables:

XS,YS =Coordinates of point at which stress is desired

RZ =Radius of the circular hole

DISP =Vector of nodal displacements

```
C*****************************************************************
C     KUROSH  KAFIE                          DECEMBER 1980,  M.I.T.*
C*****************************************************************

      SUBROUTINE PET4(E,NU,T,X,Y,IO,REALK)


      IMPLICIT REAL*8(A-H,O-Z)
      REAL HINVG,REALK(8,1)
      COMMON /PET1X2/HINVG(5,8)
      DOUBLE PRECISION J,LNGT,L,NU,NUX,NUY,NUT

      DIMENSION X(1),Y(1),GS(7),GW(7),DUM(3)
      DIMENSION S(3,3),P(3,5),H(5,5)
      DIMENSION NUT(3,2),L(2,8),G(5,8)
      DIMENSION HG(5,8),STMTX(8,8)

      DATA GS/                 -0.949107912342759D0,
     2 -0.741531185599394D0, -0.405845151377397D0,
     3  0.000000000000000D0,  0.405845151377397D0,
     4  0.741531185599394D0,  0.949107912342759D0/

      DATA GW/                  0.129484966168870D0,
     2  0.279705391489277D0,  0.381830050505119D0,
     3  0.417959183673469D0,  0.381830050505119D0,
     4  0.279705391489277D0,  0.129484966168870D0/

      NDOF =8
      NBETA=5

      DO 75  IR=1,NBETA
      DO 25 ICH=1,NBETA
   25 H(IR,ICH)=0.D00
      DO 50 ICG=1,NDOF
   50 G(IR,ICG)=0.D00
   75 CONTINUE

      RZ=DSQRT(X(1)**2+Y(1)**2)
      CALL ANGLE(X(2),Y(2),THETA2)
      CALL ANGLE(X(3),Y(3),THETA3)
      THETA0=(THETA3-THETA2)/2.0D00
      ALPHA =(THETA3+THETA2)/2.0D00
      C1=(X(2)*Y(3)-X(3)*Y(2))
      C2=X(2)-X(3)
      C3=Y(2)-Y(3)

      IFLAG=0
```

```
      S(1,1)=1.D0/E
      S(1,2)=-NU/E
      S(1,3)=0.0D0
      S(2,1)=-NU/E
      S(2,2)=1.D0/E
      S(2,3)=0.0D0
      S(3,1)=0.0D0
      S(3,2)=0.0D0
      S(3,3)=2.D0*(1.D0+NU)/E


      DO 300 II=1,7
      ZE=GS(II)
      DO 300 JJ=1,7
      ET=GS(JJ)

      THETA=ZE*THETA0+ALPHA
      PHI=C1/(C2*DSIN(THETA)-C3*DCOS(THETA))
      R=((PHI-RZ)/2.0D0)*ET+(PHI+RZ)/2.0D0
      J=THETA0*(((PHI-RZ)**2)*ET+PHI**2-RZ**2)/4.D0

100   ST=DSIN(THETA)
      CT=DCOS(THETA)
      S2T=DSIN(2.D0*THETA)
      C2T=DCOS(2.D0*THETA)

      P(1,1)=(1.D0-(RZ**2/R**2))
      P(1,2)=(R-(RZ**4/R**3))*CT
      P(1,3)=(R-(RZ**4/R**3))*ST
      P(1,4)=(1.D0+3.D0*(RZ**4/R**4)-4.D0*(RZ**2/R**2))*C2T
      P(1,5)=(1.D0+3.D0*(RZ**4/R**4)-4.D0*(RZ**2/R**2))*S2T

      P(2,1)=(1.D0+(RZ**2/R**2))
      P(2,2)=(3.D0*R+(RZ**4/R**3))*CT
      P(2,3)=(3.D0*R+(RZ**4/R**3))*ST
      P(2,4)=(-1.D0-3.D0*(RZ**4/R**4))*C2T
      P(2,5)=(-1.D0-3.D0*(RZ**4/R**4))*S2T

      P(3,1)=0.0D00
      P(3,2)=(R-(RZ**4/R**3))*ST
      P(3,3)=((RZ**4/R**3)-R)*CT
      P(3,4)=(-1.D0+3.D0*(RZ**4/R**4)-2.D0*(RZ**2/R**2))*S2T
      P(3,5)=(+1.D0-3.D0*(RZ**4/R**4)+2.D0*(RZ**2/R**2))*C2T

      IF(IFLAG.EQ.1) GO TO 400

      WTH=J*GW(II)*GW(JJ)

      DO 200 KC=1,NBETA
```

```
      DO 125 NN=1,3
      DUM(NN)=0.D00
      DO 125 KR=1,3
  125 DUM(NN)=DUM(NN)+S(NN,KR)*P(KR,KC)
      DO 175 KR=KC,NBETA
      HTEMP=0.0D00
      DO 150 NN=1,3
  150 HTEMP=HTEMP+P(NN,KR)*DUM(NN)
  175 H(KR,KC)=H(KR,KC)+HTEMP*WTH
  200 CONTINUE

  300 CONTINUE

      CALL MXINV(H,NBETA,IERH,0)

      IFLAG=1

      DO 800 IX=1,3
      XA=X(IX)
      XB=X(IX+1)
      YA=Y(IX)
      YB=Y(IX+1)

      LNGT=DSQRT((XA-XB)**2+(YA-YB)**2)
      CALL ANGLE((YB-YA),(XA-XB),OMEGA)
      NUX=DCOS(OMEGA)
      NUY=DSIN(OMEGA)


      DO 700 II=1,7

      XS=GS(II)*(XB-XA)/2.0D0+(XB+XA)/2.0D0
      YS=GS(II)*(YB-YA)/2.0D0+(YB+YA)/2.0D0

  350 R=DSQRT(XS**2+YS**2)
      CALL ANGLE(XS,YS,THETA)


      GO TO 100


  400 NUT(1,1)=NUX*(CT**2)+NUY*CT*ST
      NUT(2,1)=NUX*(ST**2)-NUY*CT*ST
      NUT(3,1)=NUY*(CT**2-ST**2)-2.D0*NUX*CT*ST

      NUT(1,2)=NUY*(ST**2)+NUX*CT*ST
      NUT(2,2)=NUY*(CT**2)-NUX*CT*ST
      NUT(3,2)=NUX*(CT**2-ST**2)+2.D0*NUY*CT*ST
```

```
      DO 500 IROW=1,2
      DO 500 ICOL=1,8
      L(IROW,ICOL)=0.0D00
500   CONTINUE


      ENT1=(1.D0-GS(II))/2.0D0
      ENT2=(1.D0+GS(II))/2.0D0

      L(1,(2*IX-1))=ENT1
      L(1,(2*IX+1))=ENT2

      L(2,(2*IX))  =ENT1
      L(2,(2*IX+2))=ENT2

      WTG=GW(II)*LNGT/2.D0

      DO 600 KC=1,NDOF
      DO 525 NN=1,3
      DUM(NN)=0.D00
      DO 525 KR=1,2
525   DUM(NN)=DUM(NN)+NUT(NN,KR)*L(KR,KC)

      DO 575 KR=1,NBETA
      GTEMP=0.0D00
      DO 550 NN=1,3
550   GTEMP=GTEMP+P(NN,KR)*DUM(NN)
575   G(KR,KC)=G(KR,KC)+GTEMP*WTG
600   CONTINUE


700   CONTINUE

800   CONTINUE

      DO 850 M=1,NBETA
      DO 850 N=1,NDOF
      HG(M,N)=0.0D00
      DO 825 K=1,NBETA
825   HG(M,N)=HG(M,N)+H(M,K)*G(K,N)
850   HINVG(M,N)=HG(M,N)

      DO 900 M=1,NDOF
      DO 900 N=1,NDOF
      STMTX(M,N)=0.0D00
      DO 875 K=1,NBETA
875   STMTX(M,N)=STMTX(M,N)+G(K,M)*HG(K,N)
900   REALK(M,N)=STMTX(M,N)
```

```
      IF(IO.EQ.0) GO TO 1000
      WRITE(6,975)
      DO 925 KR=1,8
  925 WRITE(6,950)(REALK(KR,KC),KC=1,8)
  950 FORMAT(1X,8(E14.5,2X)//)
  975 FORMAT(//,' [ K ] Matrix Returned By Subroutine § PET4X5 †
           '//)

 1000 RETURN
      END
```

```
      SUBROUTINE PETSAP(XS,YS,RZ,DISP,STRESS)
      COMMON /PET1X2/HINVG(5,8)

      DIMENSION DISP(1),STRESS(1)
      DIMENSION P(3,5),PHINVG(3,8)

      DOUBLE PRECISION XD,YD,THETAD

      R=SQRT(XS**2+YS**2)

      XD=XS
      YD=YS
      CALL ANGLE(XD,YD,THETAD)

      THETA=THETAD
      ST=SIN(THETA)
      CT=COS(THETA)
      S2T=DSIN(2.D0*THETA)
      C2T=DCOS(2.D0*THETA)

      P(1,1)=(1.0-(RZ**2/R**2))
      P(1,2)=(R-(RZ**4/R**3))*CT
      P(1,3)=(R-(RZ**4/R**3))*ST
      P(1,4)=(1.0+3.0*(RZ**4/R**4)-4.0*(RZ**2/R**2))*C2T
      P(1,5)=(1.0+3.0*(RZ**4/R**4)-4.0*(RZ**2/R**2))*S2T

      P(2,1)=(1.0+(RZ**2/R**2))
      P(2,2)=(3.0*R+(RZ**4/R**3))*CT
      P(2,3)=(3.0*R+(RZ**4/R**3))*ST
      P(2,4)=(-1.0-3.0*(RZ**4/R**4))*C2T
      P(2,5)=(-1.0-3.0*(RZ**4/R**4))*S2T

      P(3,1)=0.000
      P(3,2)=(R-(RZ**4/R**3))*ST
      P(3,3)=((RZ**4/R**3)-R)*CT
      P(3,4)=(-1.0+3.0*(RZ**4/R**4)-2.0*(RZ**2/R**2))*S2T
      P(3,5)=(+1.0-3.0*(RZ**4/R**4)+2.0*(RZ**2/R**2))*C2T


      DO 100 I=1,3
      DO 100 J=1,8
      PHINVG(I,J)=0.0
      DO 100 K=1,5
      PHINVG(I,J)=P(I,K)*HINVG(K,J)+PHINVG(I,J)
  100 CONTINUE

      DO 200 I=1,3
      STRESS(I)=0.0
      DO 200 K=1,8
```

```
      STRESS(I)=PHINVG(I,K)*DISP(K)+STRESS(I)
  200 CONTINUE

      RETURN
      END
```

REFERENCES

[1] Norrie, D. H., and DeVries, G.: A Finite Element Bibliography, University of Calgary, Dept. of Mechanical Engineering, Report No. 59, June 1974, Calgary, Canada. (Also published by IFI/Plenum 1976).

[2] Zienkiewicz, O.C.: The Finite Element Method (In Engineering Sciences), McGraw-Hill, London, 1977.

[3] Pian, T. H. H., Tong, P: Basis of Finite Element Methods For Solid Continuua, International Journal for Numerical Methods in Engineering, Volume 1, 1969.

[4] Pian, T. H. H.: Derivation of Element Stiffness Matrices by Assumed Stress Distribution, AIAA Journal, Volume II, No. 78, July 1964.

[5] Pian, T. H. H.: A Historical Note About "Hybrid Elements," International Journal for Numerical Methods in Engineering, Volume 12, 1978.

[6] Tong, P., Pian, T. H. H.: A Variational Principle and the Convergence of a Finite Element Method Based on Assumed Stress Distribution, International Journal of Solids and Structures, Volume 5, 436-72, 1969.

[7] Spilker, R. L., Maskeri, S. M., Kania, E.: Plane Isoparametric Hybrid Stress Elements: Invariance and Optimal Sampling, Department of Materials Engineering, University of Chicago at Chicago Circle, Chicago, 1981.

[8] Roark, R. J., Young, W. C.: Formulas for Stress and Strain, fifth edition, McGraw-Hill, 1975.

[9] Orringer, O., French, S.E., and Weinreich, M.: User's Guide for the Finite Element Analysis Library, Aeroelastic and Structures Research Laboratory, M.I.T., 1978.

[10] Bathe, K. J., Wilson, E. L.: Numerical Methods in Finite Element Analysis, Chapter 4, Prentice Hall, 1976.

[11] Tong, P., Rossettos, J. N.: Finite Element Method (Basic Technique and Implementation), The M.I.T. Press, Cambridge, MA, 1978.

[12] Kang, D. S.: Special Elements for a Curved and Stress Free Edge by Assumed Displacement Method, Bachelor's thesis, M.I.T., 1981.

[13] Atluri, S., Rhee, H.C.: Traction Boundary Conditions in Hybrid Stress Finite Element Model, AIAA Journal, Volume 16, No. 5, May 1978.

[14] Timoshenko and Guodier: Theory of Elasticity, second edition, McGraw-Hill, 1951.

[15] Michell, J. H.: Proc. London Math. Soc., Volume 31, pp. 100, 1899.

[16] Flugge, W.: Tensor Analysis and Continuum Mechanics, Springer-Verlag, Berlin, 1972.

[17] Green, A.E., Zerna, W.: Theoretical Elasticity, second edition, Oxford University Press, Calrendon, 1968.

REPORT DOCUMENTATION PAGE

Form Approved
OMB No. 0704-0188

1. AGENCY USE ONLY (Leave blank)	2. REPORT DATE	3. REPORT TYPE AND DATES COVERED
	November 1991	Final Contractor Report

4. TITLE AND SUBTITLE

Traction Free Finite Elements With the Assumed Stress Hybrid Model

5. FUNDING NUMBERS

WU-505-63-5B
G-NAG3-33

6. AUTHOR(S)

K. Kafie

7. PERFORMING ORGANIZATION NAME(S) AND ADDRESS(ES)

Massachusetts Institute of Technology
77 Massachusetts Avenue
Cambridge, Massachusetts 02139

8. PERFORMING ORGANIZATION REPORT NUMBER

None

9. SPONSORING/MONITORING AGENCY NAMES(S) AND ADDRESS(ES)

National Aeronautics and Space Administration
Lewis Research Center
Cleveland, Ohio 44135-3191

10. SPONSORING/MONITORING AGENCY REPORT NUMBER

NASA CR-189041

11. SUPPLEMENTARY NOTES

Project Manager, C.C. Chamis, Structures Division, NASA Lewis Research Center, (216) 433-3252. Report submitted as a thesis in partial fulfillment of the requirements for the degree Master of Science to the Massachusetts Institute of Technology in June 1981.

12a. DISTRIBUTION/AVAILABILITY STATEMENT

Unclassified - Unlimited
Subject Category 39

12b. DISTRIBUTION CODE

13. ABSTRACT *(Maximum 200 words)*

An effective approach in finite element analysis of the stress field at the traction free boundary of a solid continuum was studied. Conventional displacement and Assumed Stress Hybrid finite elements were used in determination of stress concentrations around circular and elliptical holes. Specialized Hybrid elements were then developed to improve satisfaction of prescribed traction boundary conditions. Results of the stress analysis indicated that finite elements which exactly satisfy the free stress boundary conditions are most accurate and efficient in such problems. A general approach for Hybrid finite elements which incorporate traction free boundaries of arbitrary geometry was formulated.

14. SUBJECT TERMS

Continuum solid; Stress concentration; Circular holes; Elliptical holes; Free boundaries; Variable mode; Quadrilateral; Isoparametric curvilinear coordinates; Computer program; Sample cases

15. NUMBER OF PAGES

148

16. PRICE CODE

A07

17. SECURITY CLASSIFICATION OF REPORT	18. SECURITY CLASSIFICATION OF THIS PAGE	19. SECURITY CLASSIFICATION OF ABSTRACT	20. LIMITATION OF ABSTRACT
Unclassified	Unclassified	Unclassified	

NSN 7540-01-280-5500

*U.S. Government Printing Office: 1992 — 648-580

Standard Form 298 (Rev. 2-89)
Prescribed by ANSI Std. Z39-18
298-102